BNWL-1173

2 —
8-65

[redacted]

FAST FLUX TEST FACILITY
MONTHLY INFORMAL
TECHNICAL PROGRESS REPORT
AUGUST 1969

[redacted]

AEC RESEARCH &
DEVELOPMENT REPORT

J. R. Bloom 3079 3706 FROM T.O. [illegible] 1970

BNWL-1173

BATTELLE NORTHWEST
BATTELLE MEMORIAL INSTITUTE PACIFIC NORTHWEST LABORATORY
BATTELLE BOULEVARD, P. O. BOX 999, RICHLAND, WASHINGTON 99352

INFORMATION CONCERNING USE OF THIS REPORT

PATENT STATE

This document copy, since it is transmitted in advance of patent clearance, is made available in confidence solely for use in performance of work under contract with the U. S. Atomic Energy Commission. This document is not to be published nor its contents otherwise disseminated or used for purposes other than specified above before patent approval for such release or use has been secured, upon request, from the Chief, Chicago Patent Group, U. S. Atomic Energy Commission, 9800 South Cass Avenue, Argonne, Illinois.

PRELIMINARY REPORT

This report contains information of a preliminary nature prepared in the course of work under Atomic Energy Commission Contract AT(45-1)-1830. This information is subject to correction or modification upon the collection and evaluation of additional data.

LEGAL NOTICE

This report was prepared as an account of Government sponsored work. Neither the United States, nor the Commission, nor any person acting on behalf of the Commission:

A. Makes any warranty or representation, expressed or implied, with respect to the accuracy, completeness, or usefulness of the information contained in this report, or that the use of any information, apparatus, method, or process disclosed in this report may not infringe privately owned rights; or

B. Assumes any liabilities with respect to the use of, or for damages resulting from the use of any information, apparatus, method, or process disclosed in this report.

As used in the above, "person acting on behalf of the Commission" includes any employee or contractor of the Commission, or employee of such contractor, to the extent that such employee or contractor of the Commission, or employee of such contractor prepares, disseminates, or provides access to, any information pursuant to his employment or contract with the Commission, or his employment with such contractor.

PACIFIC NORTHWEST LABORATORY
RICHLAND, WASHINGTON
operated by
BATTELLE MEMORIAL INSTITUTE
for the
UNITED STATES ATOMIC ENERGY COMMISSION UNDER CONTRACT AT(45-1)-1830

ARC-ML RICHLAND, WASH.

BNWL-1173

[redacted]

FAST FLUX TEST FACILITY
MONTHLY INFORMAL TECHNICAL PROGRESS REPORT
AUGUST 1969

E. R. Astley
Project Manager

C. P. Cabell
by C. P. Cabell

September 8, 1969

BATTELLE MEMORIAL INSTITUTE
PACIFIC NORTHWEST LABORATORY
RICHLAND, WASHINGTON 99352

[redacted]

FAST FLUX TEST FACILITY
MONTHLY INFORMAL TECHNICAL PROGRESS REPORT
August 1969

ABSTRACT

This report was prepared by Battelle-Northwest under Contract No. AT(45-1)-1830 for the Atomic Energy Commission, Division of Reactor Development and Technology, to summarize technical progress made in the Fast Flux Test Facility Program during August 1969.

CONTENTS

LIST OF FIGURES

LIST OF TABLES

FAST FLUX TEST FACILITY
MONTHLY INFORMAL TECHNICAL PROGRESS REPORT
AUGUST 1969

INTRODUCTION

This issue of the FFTF Monthly Informal Technical Progress Report is organized and structured to parallel the dual responsibilities discharged by BNW as FFTF Project Manager. These dual responsibilities consist of:

(a) Management of the end-product oriented design and construction program to ensure conformance to technical requirements and to established costs and schedules.

(b) Management of the discipline-oriented technological program required for ensuring technical adequacy of the FFTF design.

A summary of progress in design and construction management work is given in Chapter I. Progress in discipline-oriented technological work is presented in Chapters II through X. These chapters generally correspond to the LMFBR Program Plan Elements. Subdivisions of the chapters, however, are based upon specific FFTF components, systems, facilities, and programs.

Within the Chapters II through X reports on specific topics show in their titles the code of the responsible FFTF organization. These codes are listed on the following page.

FFTF ORGANIZATION CODES
AS OF 8-15-69

7N00 - FFTF Division - E. R. Astley, J. C. Cochran
7N10 - Program Adm. and Control Dept. - F. J. Arrotta
7N40 - Product Assurance Dept. - R. J. Squires
7N60 - Construction Dept. - J. S. McMahon
7N70 - Fuels Dept. - E. A. Evans, W. E. Roake, T. W. Evans
7N71 - Offsite Fuels Programs - G. A. Last, B. R. Hayward, J. F. Williams
7N72 - Cladding Development - T. T. Claudson, J. C. Tverberg, J. J. Holmes, F. R. Shober
7N73 - Fuel Element Development - C. A. Burgess, R. E. Bardsley, J. W. Thornton, E. T. Weber
7N74 - Fuels Quality Assurance - H. G. Powers
7N75 - Fuels Evaluation - J. E. Hanson
7N76 - Material Control - A. W. DeMerschman
7N80 - Reactor and Plant Technology Dept. - P. L. Hofmann
7N81 - Reactor and Plant Engineering - L. M. Finch, D. Marinos, D. P. Shively, W. L. Bunch
7N82 - Safety and Systems Analysis - R. E. Peterson, D. D. Stepnewski, H. G. Johnson, R. A. Harvey, J. P. Hale, J. W. Hagen
7N83 - Nuclear and Process Technology - R. E. Heineman, W. W. Little, P. D. Cohn, R. A. Bennett, D. C. Boyd, W. R. Lewis, J. G. Bradley
7N90 - Engineering Dept. - D. L. Condotta, F. C. Grondemeyer, W. B. McDonald
7N91 - Reactor Design - S. O. Arneson, F. J. Kempf, R. C. Walker, C. A. Munro, J. M. Yatabe
7N92 - Fluid Systems - J. M. Batch, W. R. Wykoff, T. W. Withers, P. F. Shaw, R. V. Dulin
7N93 - Instrumentation Control - C. D. Swanson, C. F. R. Smith, D. C. Thompson, M. R. Wood, R. R. Cone, J. W. Mitchell
7N94 - Facilities and Site - E. M. Johnston, F. H. Shadel, C. L. Boyd, G. H. Strong
7N95 - Engr. Coordination and Planning - J. R. Carrell, K. M. Harmon, D. R. Doman, C. W. Higby, H. L. Pringle, R. L. Roske, K. G. Toyoda, H. D. Lenkersdorfer
7N96 - Metals, Materials and Codes - J. C. Tobin, M. T. Jakub, D. P. O'Keefe, J. E. Spanner, R. N. Johnson, R. H. Todd, J. E. Irvin, D. E. Mahagin, R. A. Moen, J. W. Helm, J. H. Cox

When work is actually performed for FFTF by another BNW Division, that code is also included as shown in the following tabulation:

7400 - BNW Safety and Standards Division
7A00 - Chemistry and Metallurgy Division
7C00 - Physics and Engineering
7K00 - Environmental and Life Sciences Division
7M00 - Systems and Electronics Division

I. FFTF OVERALL PROGRESS

A. PROGRAM MANAGEMENT

1. Electrical - 10

a. CSDD Status (8-18-69)

System 11 - Primary Electrical Power System	Published
System 12 - Building Electrical Power System	Published
System 15 - Communications System	Published
System 16 - Lighting System	Published

b. Progress Summary

Acceptability of 115 kV Savannah River Plant transformers and used diesel generators for FFTF installation has not been established. Tests have indicated that this equipment is in excellent condition.

2. Structures, Utilities and Containment

Systems Group 20

a. CSDD Status (8-18-69)

System 21 - Structures	Approved by DRDT
System 22 - Site Facilities	Published
System 23 - Service Piping System	Returned by DRDT for revision
System 24 - Radioactive Waste System	Published
System 25 - Heating and Ventilating System	Published
System 26 - Plant Fire Protection System	Published
System 27 - Reactor Containment System	Approved by DRDT

b. Progress Summary

The Weston Geophysical Engineers, Inc., under contract with Bechtel, are conducting seismic investigation of the site with completion scheduled for the end of August. BNW is now obtaining bids from core and well drilling contractors.

3. Reactor - 30

a. CSDD Status (8-18-69)

System 31 - Reactor Core	Submitted to DRDT
System 32 - Reactor Vessel and Shield Component	Published
System 33 - Reactor Nuclear Control Components	Submitted to DRDT
System 35 - First Core Fuel Assembly Component	Approved by DRDT

b. Progress Summary

(1) Reactor Vessel and Shield. Preliminary design work being performed by Westinghouse is devoted primarily to an evaluation of proposals received from vendors for the reactor vessel, head, and guard vessel; PSAR work; and studies pertaining to definition of reference design data.

Volume 32 of BNWL-500, FFTF Conceptual Component Design Description for the Reactor Vessel and Shield Component was issued. This document contains applicable comments received from Westinghouse and DRDT.

(2) Reactor Control Components. Interim results of the safety system independence study being performed by Westinghouse have been reviewed and discussed. It was agreed by BNW and Westinghouse that top priority should be placed on initiation

of the roller nut control rod drive mechanism tests at LMEC.

State of technology surveys on control rod accelerators, extension rod disconnects and drive line seals were prepared.
Reactor Oscillator - Westinghouse was requested to proceed immediately with the preparation of specifications for the oscillator.

(3) Core Development and Analysis. Preliminary tests with the core "inlet feature model" indicate that the current core inlet design provides adequate coolant flow distribution for all ducts. Analysis of flow loss in driver fuel channels indicates that thermocouples with slow response characteristics (i.e., those requiring two seconds to detect a 30 °F temperature increase) can provide protection against flow low rates as high as 13%/sec. This protection requires a safety system reactivity response of -75¢/sec.

Studies to reduce length of in-core components to 12 ft are in progress.

4. Fuel Handling and Radioactive Maintenance - Systems Group 40.

a. CSDD Status

System 41 - Reactor Refueling System	In AEC review
System 44 - Central Maintenance Facility	In preparation

b. Progress Summary

Fission heat generation rates were calculated for stored fuel in the vessel during operation. Rates of 13 to 105 kW were calculated for a single sub-assembly with boron steel pots and without shielding respectively.

5. Heat Transport - Systems Group 50

a. CSDD Status (8-18-69)

System 51 -	Reactor Heat Transport System	Approved by DRDT: Revision in progress

b. Progress Summary

(1) Pumps. Work has continued to obtain the pump procurement specification by September 1. Evaluation board proceedings have started so that the RFP package may be completed by October 15.

(2) Intermediate Heat Exchangers. Both Westinghouse (WARD) and Foster Wheeler (FW) have submitted interim concept selection reports in connection with their LMFBR Low Capacity IHX Design Studies. The interim reports present engineering evaluations of design alternatives and include recommendations delineating preferred basic concepts for use in pursuing design efforts. The WARD interim report has been reviewed and mutual agreement achieved on areas to be emphasized in the follow-on work.

The IHX design work being performed under contract with Babcock and Wilcox has emphasized Mean Temperature Difference (MTD) optimization, preliminary stress analysis, hydraulic studies, and mechanical design alternatives for optimizing secondary piping arrangements. Conceptual designs of both straight-tube bundle (with floating lower heat) and a helical tube bundle are proceeding in parallel. Babcock and Wilcox reports[1] that initial stress analysis calculations (based mainly on tube-sheet fatigue analysis) indicate that terminal temperature difference conditions of up to 140 °F are technically

feasible. However, Babcock and Wilcox estimates that IHX cost savings are only in the order of 10% when increasing design MTD from 75 to 95 °F. Hence, in the interest of design conservatism and stretch capability, the final Babcock and Wilcox recommendation on design MTD will likely be somewhat less than the 140 °F upper limitation.

6. Irradiation Test Facilities - Systems Group 60

a. CSDD Status

System 61 - Closed Loop System — Approved by DRDT

b. Progress Summary

A revised cost estimate for design of the 2-MW simple, unitized, modular out-of-reactor closed loop system was received from Atomics International. BNW and Westinghouse are in the process of reviewing this proposal.

A study to define expected required testing conditions for closed loops is almost complete.

7. Examination Facilities - Systems Group 70

a. CSDD Status

System 71 - Inert Gas Cell Examination Facility — Approved by DRDT

b. Progress Summary

(1) Disassembly-Reassembly Equipment. A conceptual study of disassembly-reassembly equipment for examination of FFTF core components is being

(1) *BNW Monthly Progress Letter, "FFTF IHX Exploratory Design Studies , Babcock and Wilcox Contract No. BDR-571, period from July 1, 1969 to July 31, 1969.*

provided by the General Engineering Division of ORNL. The first portion of the documentation entitled, Survey and Analysis of Remote Technology Applicable to Disassembly and Reassembly of FFTF Core Components has been completed. An addendum will identify the impact of shortened test assemblies on the disassembly-reassembly machine and facility related requirements.

(2) Decay Heat Removal System Development. The major goal of this task is to evaluate the operating conditions (e.g., flow rates, flow split and pressure drop) to control adequately the fuel cladding temperature of a discharged fuel assembly during fuel examination. The critical problem demonstrated in the FY-1969 testing program was hot zones caused by local flow stagnation points during removal of the duct from the fuel assembly. The problem was caused by interference between the combined axial positive displacement and the transverse suction flow rates during the transition period.

To prevent the hot spots and to assist in the control of foreign contaminants, the decay heat removal system was changed to provide a suction rather than positive displacement axial flow. The design of the test facility to simulate the new system has been completed and test facility modifications have been initiated.

8. Sodium and Inert Gas Receiving and Processing - Systems Group 80

a. CSDD Status

System 81 - Sodium Receiving and Processing System	Published

System 82 - Inert Gas Receiving and Processing System	Approved by DRDT
System 83 - Auxiliary Heating and Cooling System	In preparation
System 84 - Decontamination and Cleaning System	In preparation
System 85 - Chemical Analysis Facility	In preparation

b. Progress Summary

Preliminary studies indicate that radiation levels in the reactor cavity will make manned access impossible after a few months of operation. Manned access of the heat transport cells may be feasible if fission products are not present in the sodium or plated on the piping walls.

9. Instrumentation and Control - 90

a. CSDD Status

System 91 - Central Control and Data Handling System	Approved by FFTF CCB
System 92 - Reactor and Vessel Instrument System	In preparation
System 93 - Plant Instrumentation System	In preparation
System 94 - Fuel Failure Monitoring System	In preparation
System 95 - Flux Monitoring and Control System	Approved by FFTF CCB
System 96 - Radiation Monitoring System	Published

b. Progress Summary

High temperature coaxial cable (silica dielectric) demonstrated good stability in a 720 hr test at 900 °F. Design is in progress for a water mockup of the FEDAL sampling line. Vortex generators being developed to concentrate fission gas for the FEDAL System have not given satisfactory performance to date.

B. FUELS AND MATERIALS

Three PNL-1 biaxial test specimens (two prepared from adjacent sections of an irradiated fuel pin and a third from another pin) were tested at 900 °F. These specimens failed at stresses lower than predicted. The failures were characterized by intergranular cracking which originated at the inside surface of the cladding. Nonfueled but irradiated specimens tested at 900 °F revealed only transgranular failure. The presence of large carbide particles along the grain boundaries of specimens failing intergranularly is considered significant. Fuel cladding interaction may be involved.

High strain rate tests at rates of about 0.1, 1.0, and 10.0 sec^{-1} on Type 304 SS indicate that the highest strength and ductility are obtained at a strain rate of 0.1 sec^{-1} at test temperatures above 800 °F. The ultimate strength observed at a strain rate of about 10.0 sec^{-1} and 1000 °F is about 15,000 psi less than the ultimate strength at a strain rate of 0.1 sec^{-1}.

The results of creep-rupture tests in aged Type 304 and 316 SS are reported for aging temperatures ranging from 800 to 1400 °F. In general, rupture-life reductions were observed for all aged specimens.

C. PHYSICS

Development of nuclear codes for accident analyses has improved BNW capability to analyze core disruptive accidents. Planning and analysis of the critical test program at ANL has continued. The experimental program in FTR-1 on ZPPR was completed. Analyses of Phase B, Part III critical experiments was concluded.

D. SAFETY

DBA pressure and temperature transients were calculated for cavity and equipment cells. For a case with no floor cooling in the cavity, an initial cavity peak pressure of 50 psig was followed in 0.9 hr by a second peak of 16.7 psig. Addition of floor cooling reduces the secondary peak by about 6 psig. Outer containment pressures of from 4 to 6 psig are believed to result from sodium fires caused by failures of piping in the heat transfer on closed loop systems.

II. PLANT DESIGN

This Chapter presents, as Table 2-I, a current summary of principal FFTF concept characteristics and data.

TABLE 2-I. Summary of Principal Concept Characteristics and Data (7N95) as of 8/20/69

		Units	Values	Status[a]
A.	General Plant Data			
1.	Core arrangement		vertical	1
2.	Design life	years	20	1
3.	Peak flux	n/cm^2-sec	7.2×10^{15}	2
4.	Total power, initial	MW_t	400	1
5.	Reactor coolant		sodium	1
6.	Core volumn	liters	1033	2
7.	Total reactor flow	gal/min	42,240 init. 43,290 ult.	2
8.	Reactor pressure drop design maximum	psi	145	2
9.	Reactor bulk inlet temperature initial	°F	600	2
	design maximum	°F	800	1
10.	Reactor bulk outlet temperature initial core	°F	900	2
	design maximum	°F	1050	1
11.	Core temperature rise average initial	°F	300	2
	design maximum	°F	400	1
12.	Reactor cover gas		argon	1

(a) *1 - Firm requirement or definite concept characteristic.*
2 - Current reference design value.

TABLE 2-I. (contd)

		Units	Values	Status[a]
B.	Reactor Vessel			
	1. Diameter	feet	17	2
	2. Height	feet	50	2
	3. Wall thickness	inches	2	2
	4. Wall fluence, total (at 1000 °F)	nvt	2×10^{22}	2
	5. Material		304 SS	1
C.	Core Design			
	1. Number of core lattice positions		91	1
	2. Number of driver fuel subassemblies		76	2
	3. Number of closed loop positions		6	2
	4. Number of contact instrumented in-core open test positions		2	2
	5. Number of proximity instrumented open test positions		1	2
	6. Number of in-core safety rods		3	2
	7. Number of in-core control rods		3	2
	8. Number of peripheral control rods		15	2
	9. Equivalent core diameter	inches	∿48	2
	10. Active core height	inches	36	2
	11. Radial reflector material		nickel	2
	12. Reflector thickness			
	axial	inches	6	2
	radial	rows	3	2
	13. Fuel pin heat transfer area	ft^2	2980	2

TABLE 2-I. (contd)

		Units	Values	Status[a]
14.	Core coolant velocity, maximum	ft/sec	30	2
15.	Direction of coolant flow		upward	1
D.	Driver Fuel			
1.	Fuel composition		18 to 26 wt% PuO_2 74 to 82 wt% UO_2	2
2.	Cladding material		Type 316 SS	1
3.	Linear heat generation rate, average (at 90% total power)	kW/ft	7.0	2
4.	Overpower factor		1.20	2
5.	Peak linear heat generation at overpower (at 90% total power)	kW/ft	14.6	2
6.	Target burnup, average	MWd/tonneM	45,000	2
7.	Cladding heat transfer coefficient	Btu/hr-°F-ft^2	37,500	2
8.	Maximum fuel temperature (steady state)	°F	4230	2
9.	Fuel assembly length	feet	12	2
10.	Fuel geometry		Hexagonal pin cluster	1
11.	Pin diameter	inches	0.230	2
12.	Spacer wire diameter	inches	0.056	2
13.	Number of pins per assembly		217	2

TABLE 2-I. (contd)

		Units	Values	Status[a]
14.	Subassembly cross-section outside dimension (across flats)	inches	4.615	2
15.	Lattice spacing	inches	4.715	2
16.	Duct wall thickness	inches	0.140	2
E.	Physics Data			
1.	Delayed neutron fraction		0.003	2
2.	Neutron lifetime	seconds	4.0×10^{-7}	2
3.	Doppler	T(dk/dt)	-0.004	2
4.	Power density, peak	MW/liter	0.75	2
5.	Power distribution (peak/average)			
	radial		1.40	2
	axial		1.24	2
	total		1.74	2
F.	Test Facilities			
1.	Closed loops			
	- number of positions		6	2
	- location		2 adjacent to core center	2
			1 at mid-radius	2
			3 at core periphery	2
	- power handling capability	MW	4	2
	- test section outlet temperature	°F	1400 (bypass flow permitted	1

TABLE 2-I. (contd)

	Units	Values	Status[a]
- number of loops installed initially		2 general purpose loops of 2 MW capacity and up to 2 special purpose loops provided by users	2
- test section length	inches	36	2
- test section diameter	inches	2.5-3.0	1
- material (in-core tube)		316 SS	1
2. In-core open test positions			
- number with contact instrumentation		2	2
with proximity instrumentation*		1	2
- power			
- coolant flow rate			
- test assembly length		Same as driver fuel assembly	
- test assembly cross section		Same as driver fuel assembly	
- coolant		Same as driver fuel assembly.	
3. Short term irradiation facility (capability for future installation)			

* *One open test position will have superior accessibility. Driver fuel positions can be used as open test positions with limited accessibility*

TABLE 2-I. (contd)

	Units	Values	Status[a]
- type		trail cable	1
- number		1	2
- location		core periphery	2
- minimum irradiation time at constant flux	minutes	1	2
- sample length	inches	24	2
sample cross section, maximum	inches	2.5	2
G. Heat Transport System			
1. Primary loops			
- number		3	1
- primary loop material		304 SS	1
- primary loop flow (per loop) (initial)	gal/min	14,080	2
2. Primary pumps			
- number		3	1
- design pump head	feet	500	2
- available net positive suction head	feet	51	2
- design temperature	°F	1050	1
- speed control		wound rotor motor with liquid rheostat	1
- motor power			
brake	HP	1790	2
rated	HP	2500	2
3. Intermediate heat exchangers			
- number		3	1
- type		vertical shell and tube	1

TABLE 2-I. (contd)

	Units	Values	Status[a]
- LMTD			
initial	°F	85	2
ultimate	°F	99.1	2
- capacity			
initial	MW	133	2
ultimate	MW	157	2
H. Shielding			
1. Within reactor vessel			
- material		stainless steel	2
- configuration		hexagonal assemblies	2
- thickness	inches	21	2
2. Cover shield			
- material		low alloy steel	2
- thickness	feet	4	2
- coolant		argon, helium or Na	2

III. COMPONENTS

A. REACTOR CONTROL MECHANISMS (7N91 and 7C00)

1. Conceptual Studies and Component Survey

State of technology surveys on accelerators, extension rod disconnects, and drive line seals, and testing report on decelerators for the control rod development program were prepared. These reports will be issued as Draft Reports to transmit the data to the Reactor Plant Designer.

2. Roller Nut CRDM Testing at LMEC

The Test Request, preliminary test plan, preliminary inspection procedures and facility planning were reviewed at an integration meeting with LMEC, Todd Shipyards, Westinghouse, and BNW.

3. Sodium Frosting Testing

A program for acquisition of sodium frosting design data to evaluate the deposition of sodium in the annulus around the control rod drive line was submitted to the AEC for approval. It was proposed to utilize existing facilities to perform these tests.

B. FUEL DUCT DEVELOPMENT (7N96, 7A00)

1. Duct Welding Development

An automatic welding system is being developed to produce circumferential welds in the hexagonal shaped Driver Fuel Assembly duct. Purchase requests have been placed for the welding equipment. Performance testing of welding equipment prior to delivery is scheduled for October 31.

The automatic welding system will utilize the gas tungsten arc process. The system will consist of four major components: (1) welding power supply with pulsing current and function controls, (2) welding carriage with welding torch, torch motion

control, and wire feeder, (3) duct fixture with rotation control, and, (4) programmer for controlling and sequencing welding and motion operations. During the welding operation the driver fuel assembly will be in the horizontal position and will rotate under the welding torch. The equipment will be capable of making groove welds between the hexagonal duct tube and the nose piece assembly and fillet welds between the hexagonal duct tube and the end connection plate. BNW is designing and constructing the welding carriage and the rotating duct fixture, while the welding and programming equipment is being purchased.

In order to be assured that the BNW conceptual design was the best available solution to the welding problem, BNW representatives visited organizations and personnel with backgrounds and experience in welding systems to discuss processes, equipment, and concepts for producing high quality welds in hexagonal sections. The organizations visited included Thompson Electric Company, Lynn, Massachusetts; Cecil Peck Company, Cleveland, Ohio; Oak Ridge National Laboratory, Merrick Engineering Company, Nashville, Tennessee; and Sciaky Bros. Inc., Chicago. The representatives of these organizations suggested no major changes in the BNW design and agreed that the BNW system represented a sound and logical approach.

C. IN-VESSEL STORED HEAT GENERATION (7N81)

The latest conceptual design of the FTR includes in-vessel storage locations in the sodium annulus exterior to the radial shield. Calculations were made with 2DBS(R-θ) to estimate the fission heat generation in one stored fuel assembly located about 19 in. from the core barrel, within the sodium annulus. All calculations were made at full core power, and zero axial buckling was assumed throughout the configuration. Three different stored fuel zones were considered: (1) an 8 in. OD SS storage pot and a driver assembly homogenized into one material zone;

(2) an 8 in. OD SS storage pot and a driver assembly forming two distinct material zones; and (3) an 8 in. OD boron steel storage pot and a driver assembly forming two distinct material zones. In calculating the total fission heat generated, assumptions had to be made for the axial power distribution within the assembly. Two assumptions were made: (1) a flat axial distribution (the more reasonable assumption) and (2) an axial distribution similar to that in the core. The results of the calculations are summarized in Table 3.I.

TABLE 3.I. Fission Heat Generation in One Stored Fuel Assembly

	Axial Distribution	
	Flat	Core
Homogeneous	105 kW	85 kW
Heterogeneous (SS pot)	46 kW	37 kW
Heterogeneous (boron steel pot)	16 kW	13 kW

D. DUMP HEAT EXCHANGER SIMULATION (7N82)

DHX simulation has now been examined for 12-node, 6-node, and 4-node models using average coefficients, for 4-node and 6-node models using locally determined coefficients, and for a 4-node model using both average properties and average heat transfer coefficients. Comparison with the reference TAP model has been made for five cases: spatial temperature distribution for steady state with balanced coolant flows; transient behavior of coolant following a ramp change from steady-state balanced flows to moderately unbalanced flows (about 3 or 4 to 1) for both the case of high secondary-low tertiary flows and vice versa; and both cases of steady-state spatial temperature distribution for the same flow imbalances used in the aforementioned transients.

The tentative conclusions are that the use of average coefficients and properties is valid for both transient and

steady-state calculations up to moderate flow unbalances, and that four nodes give sufficient accuracy with the techniques of mixed differences which were used. The next check to be made will be the performance for greatly unbalanced flows (>10:1).

E. SURVEILLANCE AND INSPECTION

1. Maintenance and Inspection of Primary Heat Transport System Components (7N81)

Periodic inspection and maintenance will be performed on the primary system components and piping during the life of the FTR. Radioisotope contamination and induced radioactivity can be expected in the system after reactor startup. Because of this, whether inspection or maintenance can be performed by direct contact or remote means is important in establishing the needs for special tools and instruments.

Preliminary calculations indicate that: (1) radiation levels within the reactor cavity will be sufficiently high (100 to 1000 R/h) after a few months of operation at design power to make manned access to this region impossible, and (2) contact inspection and maintenance of equipment and components located in shielded HTS cells located outside the reactor cavity would be feasible throughout the facility lifetime if no fission products are contained in the sodium or deposited on the surfaces of the HTS components.

2. Inspection on Ginna Reactor (7N86)

BNW observed part of the preservice inspection of Rochester Gas and Electric Company's Robert E. Ginna Reactor. The reactor is a Westinghouse pressurized water reactor. The preservice inspection is being performed by Southwest Research Institute (SWRI).

The inspection included ultrasonic examination of the following areas of which the first five examinations were observed.

Head to flange weld - from head exterior surface

Vessel top flange weld - from flange top surface

Vessel to core support flange welds (2) - from interior surface

Vessel circumferential welds (2 elevations) - from interior surface

Head studs - from top surface

Primary coolant nozzle to vessel welds - from exterior

Primary coolant nozzle to pipe welds - from exterior

Pipe to steam generator welds - from exterior

Pipe to pump welds - from exterior

Primary pipe welds (three in each loop) - from exterior

Accumulator beltline weld - from exterior

All ultrasonic inspections were performed using a motorized bug traveling along a track. Water couplant was used either as a bubbler over the sensor face or with the sensor immersed in the water. Except for calibration difficulties most of the inspections proceeded very smoothly.

3. Ultrasonic Wheel Evaluation (7N96 - 7M00)

Evaluation of the ultrasonic wheel transducer for inspecting FFTF piping and pressure vessel welds continued this month. This unit is being evaluated in the projected FFTF environment.

The K1305 silicon rubber O-rings, the same material as the high temperature tire, were tested in various liquids at 500 °F for 20 hours. The fluids used were Voranol, Polyglycol 400, Dowtherm A and Ambliflo. The O-rings were softened and/or decomposed by all of the fluids.

COMPONENT DEVELOPMENT AND PROCUREMENT ACTIVITIES

Component	Responsible Person	Date Required	Current Status
Valves	T. W. Withers	Procurement specification required by March 1, 1970.	Design studies are in progress. Latest FFTF requirements have not been included in the studies so redirection of effort can be established.
Intermediate Heat Exchanger	L. A. Whinery	Procurement specifications required by Nov. 1, 1969.	Design studies are in progress and on schedule. Redirection of the studies to include the latest FFTF criteria has not been accomplished. Problems still exist in the areas of concept selection, tube sheet design, and pressure drop.
Dump Heat Exchanger	L. A. Whinery	Procurement specifications required by Nov. 1, 1969.	RDT has accepted the BNW development and procurement plan. AI has completed a state of technology report. Problems are expected in initiating procurement.
Primary and Secondary Pumps	W. Babcock	Specifications required by Sept. 1, 1969 at latest.	Design study completed. Failed to meet requirements in areas of NPSH, critical speed and gas entrainment. Specifications in progress with long delay in procurement evident.
Prototype Closed Loop System	M. A. Vogel/ P. F. Shaw		AI-W contracts not placed for closed loop prototype design. Rescoping effort required prior to preliminary design.
D/N Monitor for Closed Loop Systems and Reactor Systems	L. W. McClelland/ R. R. Cone	12-15-69 decision required on types of detector life testing. 2-15-71 provide technical specifications. 5-15-71 decision required on further life testing.	Evaluation of B-lined versus fission counters required for application in temperature and radiation fields. Directed toward low level detection. Order to purchase fission counters out for comment. Delivery due Dec. 1, 1969. Testing in progress.

COMPONENT DEVELOPMENT AND PROCUREMENT ACTIVITIES (cont.)

Component	Responsible Person	Date Required	Current Status
FEDAL Multiple Line Connectors	S.O. Arneson/ J. M. Batch		Development is part of 189-13290 LMFBR Component Development FFTF Fuel Handling System 41 at AI. Specific activities not defined in AI 189 for FEDAL. This component has been included in instrument tree design.
FEDAL Gas Disengager (ANL)	L.J. Koch/ R.A. Jaross (ANL) M. J. Rieb (BNW)	10-1-69. First sodium tests complete (bubble size experiments). 3-1-70. Second tests complete. 7-1-70. Prototype design complete. 1-1-71. Procurement of prototypes complete.	Fabrication of W design in progress. ANL to test and develop prototype.
FEDAL flowmeter for gas disengager	R.A.Jaross (ANL) M.J. Rieb (BNW)		Assumed to fall out of ANL program (41903-36 Detail A) for in-core flowmeters for driver fuel and open loops. Since the disengager and flowmeter are both ANL tasks, it will require ANL interdepartment cooperation.
FEDAL Cover Gas Radiation Detectors for Reactor and Closed Loop	C.D. Swanson/ J. M. Batch	12-1-69. Procurement complete (GM tubes). 7-1-70. Report recommending acceptance or rejection of tubes. 1-1-71. Purchase specs complete. 7-1-72. Testing complete.	Concept not firm. Testing of following concepts required: 1) photomultiplier tube combination with adsorption bed. 2) charged wire detector 3) gas chromatograph. Source of funding and test authorization not sufficient to test all concepts.
FEDAL Sodium Aerosol Filters	C. D. Swanson		No formal development program in progress. This component has just become evident from W conceptual design work as part of the gas detection system.

COMPONENT DEVELOPMENT AND PROCUREMENT ACTIVITIES (cont.)

Component	Responsible Person	Date Required	Current Status
FEDAL Prototype Sampling Line	J. M. Batch/ J. W. Bartlett	9-1-69. Design complete. 5-1-70. Fabrication and installation complete. 11-15-70. Testing complete (experimental model) 1-1-72. Prototype testing complete	Planning for prototype design and testing in water with follow-on sodium tests for study of bubble entrainment. Work package to RDT for approval. Work plan in preparation by Labs, but overdue.
FEDAL Vortex Generator and Pickup Tube	J.M. Yatabe	9-15-69. First device delivered for sodium testing. 10-15-69. First water tests complete. 2-15-70. Tests on mixing complete.	Early tests on BNW design. W design in process of drafting and fabrication. Vortex generator not performing as expected. Not concentrating bubbles as much as required. Sodium tests planned for early FY-1970. W design presently more of a paper study than a fabrication design.
Closed Loop DHX	M. Vogel/ J. M. Batch		W using AI under letter contract to prepare specs for main HTS. The same route is expected to be utilized for the closed loop DHX.
Closed Loop Pumps	M.Vogel/ J.M. Batch	3-70. Spec prepared.	BNW has RDT authorization to place development contract for closed loop pumps. W assisted by LMEC preparing specs. Derating closed loop system by RDT-BNW June 23-24 will result in redefinition of concept with potential procurement delay. W evaluating linear induction e.m. pump for closed loop application.
Closed Loop Tube	J.W. Kolb/ S.O. Arneson		RFP in preparation for prototype tube fabrication contract. W performing design modifications as input to tube fabrication. Development of welding, and cutting for specimen removal in progress. Development of mechanical seals and mechanical latch for top face hardware, closed loop tube.

IV. INSTRUMENTATION AND CONTROL

A. SENSOR DEVELOPMENT

1. Pressure Sensors for Sodium Service (7N93 - 7C00)

Tests of the Consolidated Electrodynamics Corp. transducer 4-361-001-SN2260 (rated at 600 °F and 250 psi) is continuing at 725 °F. Variation in the pressure reading from this transducer was traced to a faulty pressure regulator controlling the sodium pot pressure.

2. In-Reactor Coolant Thermocouples (7N93 - 7A00 - 7M00)

The irradiation of 54 chromel-alumel thermocouples in capsules BT-3 and BT-4 at EBR-II has been completed. These are 1/16 in. OD stainless steel sheathed thermocouples. Half of them have grounded junctions; the other half are ungrounded. These thermocouples were exposed to a fluence of about 3×10^{21} nvt (fast flux) and a temperature of about 1000 °F. They are now in transit to BNW for post irradiation testing which will include measurements of calibration, time response, wire resistivity and insulator resistivity.

Development efforts during the reporting period were concentrated on preparations for these post irradiation tests.

B. LOW LEVEL NEUTRON FLUX INSTRUMENTATION

1. Detector Specifications (7N93 - 7M00)

The new detector specification (B-67398) titled Tentative Technical Specifications for FFTF Neutron Fission Counter has been completed and sent to BNW Purchasing. Compared to detectors for conventional thermal reactors, the FFTF requires higher sensitivity, guarded detectors with significantly improved capability for tolerance of combined temperature (900 °F) and gamma (10^6 R/hr) environments, and long lengths of cable (∿45 ft) also subjected to high gamma and temperature levels.

2. Coaxial Cable Tests (7N93 - 7M00)

Engineering developmental testing concluded a relatively long term (720 hr) temperature examination of high-temperature coaxial cable (silica dielectric) that demonstrated good stability. The cable, heated to 900 °F, transmitted signal pulses without measurable loss throughout the test. During the test, the cable capacitance remained constant at 234 pF, while the insulation resistance held within the range of 2 to 4×10^9 ohms.

C. FFTF CONTROL ROOM MOCKUP (7N93 - 7M00)

Work on the Philco-Ford (D-30) display system continues. One of the vendor's field engineers inspected the unit and corrected problems also. Experiments have been completed on background overlay techniques utilizing the D-30 display system. As a result, the display system now has the following capabilities:

- Built-in symbol generation
- Overlay of both positive and negative images, utilizing a slide projector and a video camera
- Image overlay using an edge-lit, engraved plastic mask superimposed on the display screen.

V. SODIUM TECHNOLOGY

A. RADIOACTIVE TRANSPORT (7A00)

Post-test examination of surfaces from the dismantled radioisotope transport loop is underway. Preliminary examination revealed up to two mils of deposited material in the surge tank, and intergranular penetration above the liquid level in the surge tank. Other examinations (e.g., scanning electron microscope, X-ray fluorescense) will be made to characterize the surfaces and deposits.

B. SAMPLING AND ANALYSIS OF RADIOACTIVE SODIUM (7A00)

1. Remote Sampler Development

The objective of this activity is to develop and proof test remotely operable samplers for the highly radioactive sodium from the FFTF.

By-pass sampler alterations are waiting completion of the X-ray tests of the welds necessary before installation of the pneumatic valves in the lower loop. An operating procedure and a job hazard breakdown have been written and are now being reviewed by Development Engineering Operations of the Physics and Engineering Department.

A new die for crimp sealing of removable section samples has been fabricated and tested. It provided a small area of extreme pressure through the use of a 1/8 in. high ridge 0.1 in. wide across its face. The new die repeatedly sealed empty annealed nickel tubing. However, it did not produce helium-tight seals after the tubing was filled with sodium.

2. Selection and Testing of In-Line Sodium Analysis Instruments

a. Oxygen Meter

Meter responses resulting from cold trap temperature changes were reported by GE for a UNC oxygen meter. Their values

vary considerably from the range of responses measured at BNW during Na_2O additions to the Sodium Purification Loop. Attempts to duplicate the GE responses on the BNW loop were unsuccessful. The Sodium Purification Loop cold trap was operated at 380 °F for six days and the meter response followed the previous curve measured during Na_2O additions. Cold trap temperatures greater than 380 °F could not be produced with the present heating and flow rates available.

b. Carbon Meter

A small signal response noted during the addition of sodium carbide to the Sodium Purification Loop did not result from any significant increase in the carbide content of the loop sodium. Analytical results show that most of the sodium carbide did not dissolve, and remained in the addition tube.

The carbon meter showed no change in response over a several-week period during which methane in the cover gas was reacting with sodium in the loop surge tank. (See next item)

3. Evaluation of Techniques for the Controlled Addition of Impurities to Sodium

A sodium carbide addition attempt described previously was apparently unsuccessful. Although no quantitative measure of carbide remaining in the addition tube could be made, large amounts were visible in the addition tube after it plugged. No carbide or total carbon increase was detected in sodium samples taken from two hours to several days after the addition attempt.

The argon cover gas in the Sodium Purification Loop was replaced by a 1000 ppm CH_4-argon mixture. After pressurization to 3 psi, the methane and hydrogen were monitored in the loop cover gas using a gas chromatograph. The methane reacted slowly with the sodium, resulting in an increase in the hydrogen level. No change in carbon content in the sodium was detected either by the on-line carbon meter or by wet chemical analysis.

C. COVER GAS STUDIES

1. Cover Gas Impurity Reactions Over Sodium

Reaction rates between sodium and carbon dioxide were measured during the report period. At 150 °C (302 °F) the reaction proceeded rapidly as long as the sodium surface remained free from reaction products. As the reaction products accumulated on the molten sodium surface the reaction rate decreased and the reaction finally ceased. The length of time required for this to occur was found to decrease with temperature; at 250 °C (482 °F) the reaction proceeds indefinitely at a slow rate. Agitation of the sodium surface increases the reaction rate.

These investigations indicate that carbon dioxide will not exist in significant concentrations in the argon cover gas over an agitated sodium pool such as that in the FFTF. If CO_2 is detected it will indicate that the sodium surface is covered with a reaction product and that very substantial contamination has occurred.

2. Selection and Testing of Cover Gas Instruments and Sampling Systems

The objective of this activity is to provide proven sampling and analysis equipment and technology for the cyclic on-line monitoring of impurities, including fission gases, in the FFTF sodium cover gas.

Examination of the theory of condensation and vapor removal based on a combination of mass transfer and nucleation thermodynamics has been completed and a vapor trap design equation has been formulated. Using the results of this study, a prototype trap has been designed and fabricated to handle two liters per minute of gas at an inlet temperature of 1400 °F and a desired exit sodium vapor concentration of 0.05 pp. The design required 15.5 stages with a stage height

of 3.1 cm for an over-all length of 19 in. in a 2.1 in. diameter section. The trap will be tested to verify the design performance during the next report period.

Preliminary calculations have been completed of the rate of diffusion of xenon through argon in an effort to determine whether or not mixing will be required to obtain valid samples of the FFTF cover gas. The calculations indicate that rapid response to the introduction of xenon into a large gas space cannot be achieved by diffusion mixing alone.

D. EVALUATION OF CARBON STEELS FOR SODIUM SERVICE (7N96)

Carbon steel has been considered for some applications in the Sodium Receiving and Processing System. A study is being conducted to identify the limiting conditions for its use, the potential problems associated with its use, and the estimated cost saving resulting from its use in place of the general reference alloy, Type 304 SS. Preliminary findings of this study are described below.

Graphitization, surface oxidation, potential nitriding of the surface (in a nitrogen cover gas) and diffusion bonding to itself limit the long-term application of this family of alloys to temperatures below 775 to 850 °F. From the standpoint of mechanical design, the allowable stress values are quite comparable to those for low alloy and austenitic stainless steels up to 700 °F, after which the allowables for carbon steel drop sharply. Fatigue design allowables are identical for carbon steel at 700 °F and austenitic stainless steel at 800 °F. The thermal properties of the carbon steels are significantly better than those of the austenitic stainless steel, i.e. thermal conductivity is higher by a factor of 2 to 3.

Although no precise corrosion models are available, carbon steel has been used successfully for long periods of time in contact with sodium at temperatures of 600 °F. In a mixed alloy

system such as one with carbon steel and austenitic stainless steel, predicting corrosion behavior becomes more difficult. In addition, chemical cleaning of mixed alloy systems is a serious problem leaving in-service cleaning with sodium as about the only alternative known at this time.

Carbon steel is readily weldable, generally not requiring the pre or postweld heat treatment associated with the low alloy steels such as 2 1/4 Cr-1 Mo. From the standpoint of cost, mill products of carbon steel are 1/10 to 1/7 the cost of comparable stainless steel products, while fabricated components range from one third to one half the cost of stainless steel products.

E. FEDAL SYSTEM DEVELOPMENT (7N92)

1. Prototype Sampling System Development (7A00)

Plans are now proceeding with the design requirements and work plans for fabrication and operation of the water mockup of the FEDAL sampling line. The loop will be operated in the 324 Building and testing will be limited to one design. Performance characteristics will be assessed with and without the use of a jet pump in the sample line and without the mating of the vortex generator and the sample line. Bubbles will be injected into the sample line inlet individually and in streams to assess bubble transport characteristics in the line. Air and, possibly, radioactive inert gases will be used.

A literature search has been conducted on methods of generating gas bubbles of varying sizes from 50 microns to 10 cm^3 in diameter. The search revealed that many authors have attempted to study the factors influencing bubble size on a simple scale, but from the diversity of their conclusions it is obvious that this problem is more complex than has been generally assumed. While streams of bubbles within a given size range are rather easy to generate, individual bubbles in the

100 micron range are considerably harder to obtain. Preliminary experimentation may be necessary before a satisfactory device is found for the water mockup loop. This device should generate suitable bubble volumes with a ± 15% accuracy.

2. In-Core Gas Concentrator Development FS-C

To locate fuel assemblies with failed cladding, sodium will be sampled from each individual fuel assembly and analyzed for fission product gas. To ensure that the sample collected has sufficient fission product gas concentration, a vortex generator has been placed in each fuel assembly instrument package to concentrate gas bubbles to the inlet of the sampling tube leading to the out-of-vessel detection cell.

The vortex generators have been tested in water; first, with nine blades, with a 45-degree discharge angle on a 1.5-in. diameter hub; and second with eight blades with a 50-degree angle on a 2-in. hub. Using hollow plastic microspheres to simulate gas bubbles (a conservative simulation with respect to separation caused by their higher density) separation efficiencies were evaluated. In all cases to date separation efficiencies have been very low, on the order of one percent of the total injected quantity. Measurement of velocity profiles to verify analytical methods to predict performance was made and verified the models used. Overall pressure drop of the devices at 450 gpm (water) was low, remaining below two psi.

Gas Release Studies - Tentative agreement was reached with Argonne National Laboratory to evaluate experimentally gas release from small cladding breaks (approximately 0.001 in.) to provide their requirements in terms of bubble size for the vortex generator development. A complete description of the desired bubble release tests involving high-speed photographic studies of bubbles released from small defects on a single pin has been transmitted to ANL for their comment and to provide information required in the test apparatus design.

F. SODIUM TEST FACILITIES MANAGEMENT (7N95)

1. Test Facilities Planning

Construction work is progressing on the building for FFTF Sodium Facilities. All of the concrete floor slabs, foundations, and equipment pads have been poured. All underground piping and most of the conduit has been completed. The structural steel for the 100 ft. by 60 ft. ARMCO building has been erected and the building wall panels and insulation on the building walls and about one half of the roof have been put in place. The concrete block walls for the personnel area have been completed. The two 750 kVA transformers (13.8 kV to 0.48 kV) have been moved to the job site.

Design work by Vitro Engineering is progressing on the LMFBR Core Segment Development Facility and is now estimated at 50% complete.

The design of the Fast Reactor Thermal Engineering Facility is proceeding under the direction of BNW. The revised quality assurance plan has been prepared and supplemented with QA procedures and requirements. Requests for proposal for the test section dc power supply were issued and expressions of interest were received from Allis-Chalmers, Westinghouse, General Electric and I.T.E. All vendors requested an extension of time to prepare and submit proposals. August 11 had been set as the date for bids, but two companies in their bids requested a further time delay to submit prices. Cost comparison and configuration studies are being performed on three basic segments of FRTEF design to establish preferred equipment location and type. These include:

- Location of process equipment structure inside the 3718 Building versus outside Building.
- Use of an EM pump versus the CANEL Project excess mechanical pump.

- Use of propane versus natural gas fuel for the preheat of the air cooled heat dump.

BNW and the HTSF A/E are continuing to update the preliminary design criteria to final design criteria. The scheduled submittal date for review of final design criteria was August 25.

The preliminary project proposal for the PCLDI has been submitted to RL for approval. Final negotiations with Westinghouse for the prototype loop design are in progress. It is expected that preliminary design will start in September.

2. Sodium Facilities Operation

The objectives of this section and description of equipment were given in BNWL-915[1] and BNWL-1062.[2] The status of the sodium facilities is given in the tabulation below:

Small Component Evaluation Loop	Failure of one field coil on the primary pump shut this loop down from test conditions 19.5 gpm ∿31 fps 1150 °F). An examination of the coil revealed that it had shorted to ground, which in turn caused one main fuse to fail and the loop to scram (drain) from loss of sodium flow. The pump field buss and coils were removed and replaced with two new coils obtained from excess CANEL equipment. Following reinstallation, resistance and megger checks were made on the new coils as well as the two remaining field and transformer coils. Further checks were made of lead-in wires and capacitors to document coil resistances and to verify that no grounds were present in the circuit, and the loop was preheated

1. *BNWL-915. FFTF Test Facility Monthly Informal Technical Progress Report. October 1968. Battelle-Northwest, Richland, Washington.*
2. *BNWL-1062. FFTF Test Facility Monthly Informal Technical Progress Report. April 1969. Battelle-Northwest, Richland, Washington.*

and filled to check pump performance. During this check the pump would not meet its original performance characteristics. The maximum flow obtainable was one half the previous capability. The loop was drained and radiographs were taken of the test assembly and inlet to the pump throat. The radiographs verified that the test assembly was intact and that there were no obstructions at the inlet to the pump throat. Both sets (upper and lower) of field coils were than removed from the pump and the transformer buss braze joint was found to be severely cracked at the suction end of the throat. A new pump throat is on order.

Small Heat Transfer Loop

The first 7-pin cluster was installed in this loop during the last week in June. The loop was preheated and charged on 6-30-69. Testing began on 7-1-69, and was completed on 7-2-69. For this test, pin power was held at $\sim$30 kW while cycling at ΔT across the cluster. Following the test, the cluster was removed from the loop, sealed and returned to test sponsors for visual examination and repair of test thermocouples. Initiation of a program to obtain a calibrated flow meter for this meter for this facility began with loop testing of a new magnet on 7-21-69. For this test the new magnet was installed in the loop in series with the existing flowmeter. The loop was started up and the output of both magnets recorded at different flows and temperatures to 1200 °F. The new magnet will be removed and shipped to LMEC for calibration.

Static Sodium Pots

Cycling of pressures and temperatures in static pot No. 3 continued throughout this report period. A new test pressure transducer was installed in pot No. 4 on 7-8-69. Testing on this instrument began shortly after installation and is continuing. Installation of a new transducer in static pot No. 1 was completed on 7-15-69. Testing will begin on this transducer when test parameters have been finalized.

Sodium Purification Loop	This loop has operated continuously throughout this report period. A gas chromatograph was connected to the expansion tank cover gas to monitor controlled additions of impurities to the cover gas. The carbon meter and oxygen meter also were operated continuously throughout this period.
Fission Product Screening Loop	Following installation of additional bracing on the main flowmeter and repair of several trace heaters, this facility was started up on 7-11-69 for recheck of calibration on this magnet. During this run (7-14-69), the primary pump throat slipped down slightly and came in contact with one field conductor of the pump. This created a short and the conductor failed. The pump throat was not damaged. During replacement of the conductor and installation of supports to prevent pump throat movement, all sodium was drained from storage tanks and the system recharged with purified sodium. Following recharging of the feed tank the loop was started up on 7-25-69 and flowmeter data obtained up to 1100 °F. The loop is presently shut down for installation of six used bellows seal valves (from the radioisotope loop) in the three test legs. These candidate valves have been cleaned by different processes and will again be exposed (for 400 hr) to 1200 °F sodium to evaluate the effect of these cleaning processes on bellows life.
Mechanical Properties Loop	Test section fabrication continued this month. A preliminary design for modifications required for unattended operation has been initiated.

VI. CORE DESIGN

A. FUEL ASSEMBLY DESIGN STUDIES

BNW and Westinghouse have both generated methods proposed to reduce the length of the fuel assembly to 12 feet. No decision on the optimum method has been made to date.

1. BNW Core Assembly Length Studies (7N81)

Study of the defined technical bases noted in last month's progress report[1] resulted in a parametric analysis of the length increments involved with the core components.

Based on this study, it appears that the length-controlling components are the driver fuel assembly and the safety/control rod poison assembly. The controlling component depends on the assumptions made.

As with any trade-off study, optimizing a given parameter, (in this case the length) usually results in penalties to other parameters. Table 6.I summarizes the methods investigated for shortening the fuel assembly length, and points out the associated penalties and the uncertainties. The lengths noted in Table 6.I are minimums for each increment and can not be combined arbitrarily.

In studying the incremental lengths for the control rods, a first assumption must be made concerning the need for rod followers. If a full-length follower is needed, reduction in the below-core length is limited to a few inches since a length equal to the full length of the active core must be available below the core when the rod is at the full-in position.

(1) *FFTF Monthly Informal Technical Progress Report, BNWL-1164. July 1969. Battelle-Northwest, Richland, Washington.*

TABLE 6.I. Fuel Subassembly Length Increment Summary

Increment	Method of Shortening	Penalty	Absolute Minimum	Uncertainties
Inlet				
(a) Hydraulic Balanced	Increase inlet velocity	Erosion and cavitation	17 inches	
(b) No balance	Eliminate balance feature	Develop another holddown method	6 inches	Capability to design and develop an alternate holddown system
Below Core				
(a) 10 year life	Add shielding	Additional pressure drop and increased cost	22 inches (based on 500 °F inlet at tubesheet and SS pin)	Effect of streaming and damage to the receptacle
Core and Upper Reflector	None	None	42.5 in. (includes insulator pellet and reflector)	
Plenum	Reduce burnup	Reduced fuel life	36 (BU = 60,000)	Inability to achieve plant availability goal.
Upper Hardware	None	None	1.5 in.	
IVHM and Probe	Eliminate pre-position	Possibility of bridging during clamping	8 in.	Capability to reassemble distorted core from the shutdown "open" configuration.

A possible balanced design might be obtained by using below-core plenums in the rods with a reduced volume fraction of metal in the follower. Length increments with these assumptions are given in Table 6.II.

It should be noted that the effect on instrument life of removing two feet above the core has not been considered. Figure 6.1 shows the driver fuel assembly configuration based on this study.

2. BNW Below Core Shield Thickness Studies (7N81)

Reduction in fuel assembly length may be achieved by reducing the below-core shield thickness. Calculations were made for three shield compositions to determine the necessary shield thickness to satisfy a fluence limit of 3.5×10^{21} nvt at the grid plate. Where appropriate, adjustments were made on the calculations to account for possible streaming of neutrons through the shield pin arrays. The results of the calculations are summarized in the following tabulation.

Shield Compositions and Thicknesses

Composition (vol%)			Shield Thickness (in.)	Core to Grid Plate Distance (in.)
Na	SS	B_4C		
87.4	12.6	---	14	61.2
43.0	57.0	---	7	54.2
43.0	20.0	37.0	5	52.2

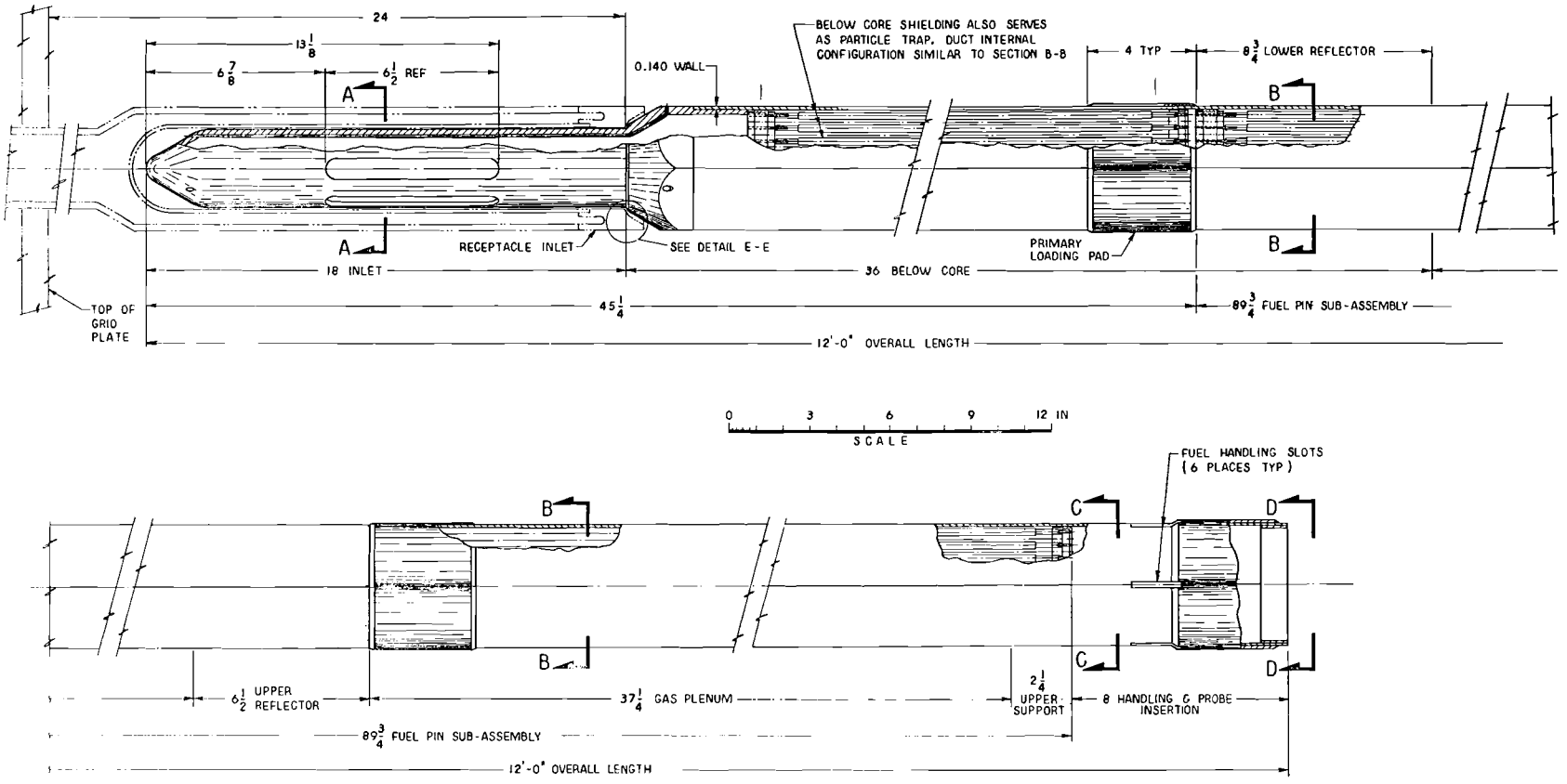

SK-3-14718

FIGURE 6.1. Twelve-Foot Driver Fuel Assembly

TABLE 6.II. Recommended Fuel Length

Increment	Present Length (in.)	Reduction (in.)	New Length (in.)	Penalty
Inlet	18	0	18	None
Below Core	42	6	36	20.75 SS shield ΔP increased by 12 psi. Clamping load up 140%.
Core	36	0	36	None
Reflector	6.5	0	6.5	None
Plenum	40.5	-	37.25	Peak burnup reduced to about 72,000 MWd/T
Upper Support	2.25	0	2.25	None
Handling & Probe Insertion	8.0	0	8.0	None
Plenum Contingency	14.75	14.75	0	Potential for advanced unvented fuels decreased

3. Ward Core Assembly Length Studies (7N91)

A fuel element design review was held during the reporting period. Westinghouse, ARD (WARD) has examined the problem of reducing the length of the fuel assembly to twelve feet. The recommended fuel assembly consists of the following zones:

	Measurement (in.)
Fuel handling and sealing of instrument assembly	6
Fission gas plenum	48
Reflector	6
Fuel	36
Reflector	6 to 8
Shield	22 to 24
Nozzle	18

The principal problem arising from this arrangement is the high fluence to the core support structure. The design criterion being utilized by WARD is a life of 10 years for the core support structure at a temperature of 500 °F with an end-of-life residual 10% total elongation in the support plate and 5% total elongation in the fuel receptacles. The criteria lead to a total fluence on the support plate of 2.7×10^{21} and 4.0×10^{21} at the receptacles. If a pin type shield (38.5% Na and 61.5% SS) is used, a length of 18 in. is required to protect the grid plate and 32 in. to protect the receptacle. Evaluation of alternative shield configurations is being pursued.

WARD is examining a core support structure consisting of two 1/2 inch thick plates separated by a space of $\sim$4 feet and reinforced by a series of horizontal plates. Receptacles for the fuel assembly protrude approximately 8 in. above the upper plate and extend to the lower plates.

Removable Driver Fuel Instrument Assembly (7N91-7C00)

A mockup simulation of the Westinghouse Concept V-B Driver Fuel Instrument Assembly and a curved section of a guide tube has been fabricated, and is currently undergoing testing. The objective of this test is to show that the instrument package can be readily inserted and withdrawn in a curved guide tube of this design. The mockup consists of the lower section of the instrument assembly, including a dummy flow meter, five thermocouples, five ball and socket joint sections containing eight thermocouple leads. The guide tube was made up from 2-in. Schedule 40 pipe with one reverse bend extending into a 90 degree bent section. The bend radius for both sections is 36 inches. All the fabricated parts were made from Type 304 SS. Testing is being conducted in air at ambient conditions. Preliminary results have been favorable; the insertion and removal forces on the instrument assembly are very small.

B. FUEL ASSEMBLY PERFORMANCE TESTING

1. Heat Transfer Test of 7-Pin Bundle (7N91-7C00)

The purpose of this work in FY 1970 is to perform sodium heat transfer testing with multi-pin models of FFTF fuel assemblies to determine local cladding temperature profiles in normal and structurally destorted FFTF fuel assemblies. The preliminary 7-pin bundle test, to evaluate the temperature difference between edge and central coolant channels and the potential hot spot under a wire wrap spacer, was completed. While several thermocouples (mainly cladding thermocouples) failed to operate during the test, sufficient information was obtained to provide the following conclusions:

- The fuel thermal analysis model, COBRA, predicted the average coolant temperature differences over the range of Pellet Number range of the test with a mixing coefficient of 0.0068. Further water mixing tests are required to verify this value of the mixing coefficient.

- Temperature differences existed between the outer subchannels themselves and the inner channels themselves, at a single axial position. This is postulated to be caused by forced diversion of coolant and possibly by tolerance buildup.
- Initial results from limited data indicate that excellent cooling occurred at the region under the wire wrap spacer and that the potential cladding hot spot directly under the spacer may not exist. Further testing will be required to verify this finding.

The first test assembly is undergoing modification to prevent the thermocouple shorting problem that occured in the first test. A retest to verify and extend the test results is planned for the next reporting period.

2. 7-Pin Loose Wire Test (7N91-7C00)

The 7-pin loose wire test assembly is for a specific test to evaluate the potential for excessive mechanical wear caused by movement of loose or broken wire wrap spacers. The test assembly had been exposed to flowing sodium (flow rate 30 ft/sec at 1150 °F) for 1000 hr when a failure in the pump of the SCEL caused a shutdown. To complete this test with a minimum of delay the 7-pin test assembly will be transferred to HTL-I for continuation of the life test between heat transfer testing.

3. 7-Pin and 37-Pin Bundle Coolant Mixing and Flow Distribution Tests (7N91-7C00)

Facility modification and test assembly design are 40% completed for the 7-pin and 37-pin mixing test assemblies to provide mixing data to permit analytical verification of the 7-pin heated test results in sodium and subsequently the extrapolation of these data to the conditions of the FFTF fuel assembly.

4. Mark II Full Size Test Assembly (7N73-7C00)

The Mark II test assembly is a full-sized assembly model to be tested for 9000 hours at condition of maximum reactor flow, cladding surface temperature and coolant purity to provide a verification of the mechanical design and evaluate the effect of potential long-term failure modes, (e.g., vibration-induced fretting or erosion). The fabrication of the test assembly is being delayed to permit the resolution of specific design changes. These include: Wire wrap diameter, bottom and top grid design and end cap design.

C. RADIAL RESTRAINT DESIGN

BNW-Westinghouse Reviews (7N91)

Technical information meetings were conducted with Westinghouse design personnel to determine the status of the Westinghouse design effort and to exchange technical data on the various aspects of core restraint. Subjects discussed included:

- Radial restraint requirements
- Anlytical techniques for predicting motion
- Restraint testing program
- Restraint devices
- Interfaces with core restraint

This meeting served to promote understanding of the core restraint technical problems, but it did not result in a recommended core restraint scheme.

D. IRRADIATION TEST FACILITIES DEVELOPMENT

1. FFTF Closed Loop Test Characteristics (7N81)

A study, FFTF Closed Loop Test Characteristics, is near completion. It characterizes the CL test capability over a test diameter range of 3.0 to 2.5 in. and less for a typical

test bundle length of 72 in. and an assumed ΔP of 90 psi for spirally wrapped wire spacers. The bundles are 61-, 37- and 19-pins on triangular array with pitch-to-pin diameter ratios of 1.1 to 1.3. Coolant temperature rises of 200, 300 and 400 °F are examined.

The test capability is characterized by a series of curves covering parameters of flow, velocity, test power, linear power, cladding heat flux and fertile-to-fissile ratio for a flux of 7×10^{15} nv.

The parameters believed most likely to set the maximum test conditions are identified as follows:

- 20 kW/ft for Pu-U oxide fuels gas bonded
- 40 kW/ft for Pu-U carbide fuels gas bonded
- 55-60 kW/ft for Pu-U carbide fuels sodium bonded
- Sodium coolant velocity of 50 fps
- 4 MW power assumed as maximum system heat removal capability

Table 6.III summarizes maxima of important parameters as derived for the test diameters of 2.5 and 3.0 inches. The boxed values appear to be unacceptable. Table 6.IV is a tabulated commentary to supplement Table 6.III.

The parametric curves of this study are a preliminary characterization of the FFTF closed loop test capability. It is concluded that test diameters between 2.5 and 3.0 inches are satisfactory for the testing of fuels at the most severe conditions anticipated in fast breeder power reactors.

2. Closed Loop Weld Closure Studies (7N91, 7N92, 7C00)

Primary objectives of this task are to demonstrate the feasibility of employing remote-controlled mechanically-driven tungsten arc welding as a means of making a final reliable closure seal between the closed loop nozzle plug and reactor top face spool piece.

TABLE 6.III. Maximum Characteristic at P/d = 1.3

ΔT, °F	Test Diameter No. of Pins	2.5			3.0		
		61*	37	19	61	37	19
	Power, MW	1.9	2.9	3.6	4.2	4.8	5.6
400	Linear, kW,ft	11	27	62	23	46	98
	Heat Flux, $\frac{10^6 \text{ Btu}}{\text{hr-ft}^2}$	0.7	1.47	2.5	1.3	1.95	3.2
	Power, MW	1.5	2.2	2.7	3.2	3.6	4.3
300	Linear,kW/ft	8	19	47	17	32	74
	Heat Flux, $\frac{10^6 \text{ Btu}}{\text{hr-ft}^2}$	0.53	1.1	1.9	1.0	1.47	2.4
	Power, MW	1.0	1.5	1.8	2.1	2.5	2.8
200	Linear, kW/ft	5.2	14	31	11.5	22	48
	Heat Flux, $\frac{10^6 \text{ Btu}}{\text{hr-ft}^2}$	0.35	0.75	1.3	0.65	1.0	1.6
	Pin Diameter,in.	0.20*	0.236	0.325	0.226	0.289	0.387
All	Flow, gpm	130	200	240	285	330	375
	Velocity,fps	32.5	42	49	41	49	57

* *Assume d_p = 0.20-inches is minimum; p/d = 1.2*

Photos of the sodium contaminated weld joint, which was reported on in the last report period, are included in this report. Figure 6.2 is a top view of the simulated closed loop weld test specimen showing extent of sodium contamination. Figure 6.3 is a view of the area where the welding arc was fired and maintained for a short period. Note the large ball-shaped area at the end of the torch electrode. This condition

TABLE 6.IV. Tabulated Commentary to Supplement Table 6.III

Test Diameter inches	2.5			3.0		
T, °F / No. of Pins	61	37	19	61	37	19
400	Moderate power Oxide Fuel tests 11 kW/ft	Moderate power Gas-bonded carbide fuel test 27 kW/ft 1.47×10^6 q/A	More than enough power for Na-bonded carbide fuels 62 kW/ft 2.5×10^6 q/A Excluded	More than enough power for oxide fuels. Low power for gas-bonded carbide fuels. 23 kW/ft	More than enough power gas-bonded carbide fuels. Moderate power for Na-bonded carbide fuels 46 kW/ft	Excluded - Linear power = 98 kW/ft & 3.2×10^6 q/A too high
300	Moderate power oxide fuels 8 kW/ft	Maximum power for oxide fuels 19 kW/ft	More than enough for gas-bonded carbide fuels, Good for moderate power Na-bonded carbides 47 kW/ft 1.9×10^6 q/A	Good for oxide power range to 17 kW/ft	Moderate power for gas-bonded carbide fuels 32 kW/ft 1.47×10^6 q/A	Excluded - Linear power = 74 kW/ft & 2.4 q/A too high
200	Low power oxide fuels	Good for oxide fuels to 14 kW/ft	Moderate power gas-bonded carbide fuels	Moderate power oxide fuels to 11.5 kW/ft	Maximum power oxide fuels and lower power gas-bonded carbides 22 kW/ft	Moderate to high power-Na-bonded carbide fuels 48 kW/ft 1.6×10^6 q/A but see velocity
Velocity Comment	32.5 fps	Limit of 42 fps Probably OK	Limit of 49 fps requires flow tests	41 fps limit probably OK	Limit of 49 fps requires flow tests	Limit of 57 fps excluded as too high. Troubles are sure.
Max. pin dia at p/d = 1.1	0.22 inch	0.283	0.395	0.27	0.35	0.49; few prospects this large

Neg 0692819-2

FIGURE 6.2. Sodium Contaminated Weld Joint

Neg 0692818-4

FIGURE 6.3. Area Where Welding Arc Was Fired

is caused by the intense arc heat vaporizing the sodium. Some of the vapors are trapped under the weld puddle, until finally, sufficient pressure is created which literally "blows" molten metal out of the puddle and onto the electrode. Figure 6.4 shows the extent of sodium vapor accumulated on the upper edge of the spool section. As noted in the last monthly FFTF Technical Progress Report (July), weld joint inspection and cleaning methods are definitely required and must be established to prevent sodium vapor problems on the reactor.

Quality Assurance "Fabrication Control" forms have been established, and will be utilized during fabrication of simulated weld test specimens.

Fabrication has been completed on the weld head assembly.

Six each Type 304 and 316 SS simulated closed loop weld test assemblies were fabricated and shipped to Thomson Electric Welder Company, Lynn, Massachusetts, for their evaluation of the PIGME welding process.

A Woodruff key cutter, modified for side cutting, has been shop tested on stainless steel weld samples. This circular cutter produces a fine chip and there was no visible evidence of wear after one hour and forty-five minutes of operation.

Fabrication on the four-tooth trepanning test module assembly, based on the Do All Company cutter design, has been completed. Preparations are under way for testing this assembly on samples welded by remote application. This cutting technique employs a pulsed feed to eliminate the possibility of long machined stringers clogging the vacuum exhaust passages. Also nearing completion is the side mill cutter test module. This assembly can accommodate four cutters and will be equipped with a vacuum system to remove the chips from the joint area.

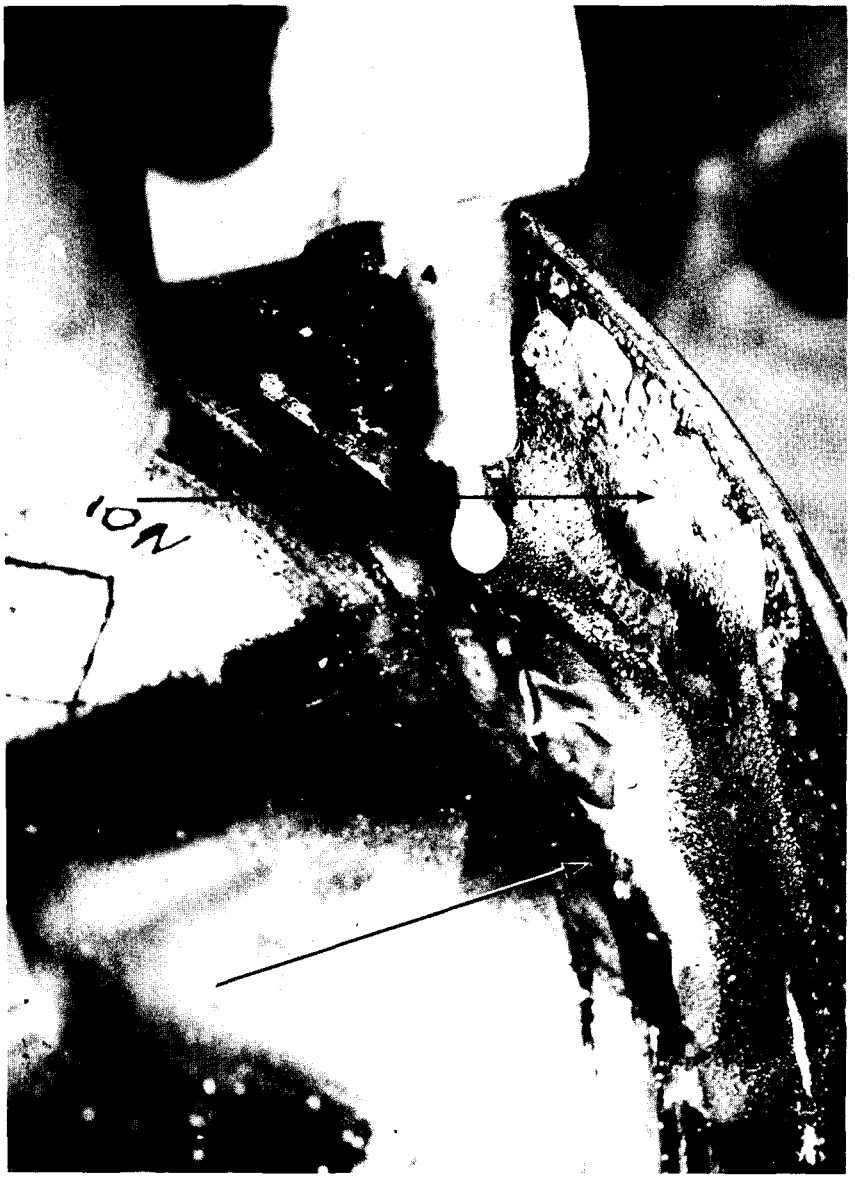

Neg 0692818

FIGURE 6.4. Sodium Vapor Contamination at Upper Edge of Spool Section.

Closed Loop Mechanical Seal Closure Program (7N91 and 7C00)

The objectives of this task are to: (a) provide experimental test data verifying the principle of operation of a creep compensating connection assembly, (b) provide experimental test data for each of six specified seal concepts being considered for FFTF closed loop nozzle closure application, and (c) establish a reference clamping device design and seal(s) for subsequent reliability testing.

a. Creep Compensated Connector Nozzle

Fabrication of the nozzle has been completed. The components were transferred to Building 314 for assembly and testing. The nozzle was assembled utilizing the NDA 4-point seal module to make a completed assembly. The seal module, without a seal, was used for latching tests. Initial actuation of the connector showed that the latch fingers had grooved the latch actuating shoulder which indicated the timing for engagement of the latch was not correct. Work is underway to correct this problem.

b. Nickel Seals

Material for the nickel seals was received from the vendor and three seals fabricated (Reference, SK-3-15141). A check analysis on the material, performed by an independent laboratory, confirmed the vendor's analysis showing that the material meets purchase specifications. Ultrasonic testing also showed the material to be free from defects as specified.

A seal test module was fabricated (Reference, SK-3-15141). Each of the three seals was compressed in the module by means of a Baldwin compression testing machine. Preliminary conclusions drawn from these test results are: (1) seal loadings somewhat greater than anticipated may be required to produce adequate penetration of the threads in this material; and (2) the thread form as fabricated does not conform to the standard

form used for calculations. This is responsible for the lack of "fill" in the roots even when adequate penetration is achieved. A load of 200,000 lb produces a penetration of about 0.007 in., which is nearly twice the calculated amount of penetration which should produce complete fill.

c. Belleville Spring Stack

Fabrication of the Belleville springs was completed by Tech Shops and the material was heat treated. A check of material hardness showed that it was not within specification. The material was annealed and rehardened with subsequent recheck of material showing the hardness within specification. The springs were subjected to compression testing and a load-deflection curve was determined for each spring. In addition, load-deflection characteristics of the spring stack used in the creep compensated connector were determined.

The individual spring and spring stack curves agree with calculated values within 5%.

E. FLOW TESTS - PIPED VESSEL INLET ARRANGEMENT (7N95-7C00)

The one-third size hydraulic model of the FFTF piped inlet arrangement was operated with the Concept V-A inlet arrangement and a new basket which was fabricated from 1/2 inch thick material and with 1/2 inch holes. Flow distribution data were obtained for the test program and reduced using the computer program, with results which may be summarized as follows:

- A small natural vortex much smaller than that produced with the original inlet basket forms within the basket during all tests.
- A vortex forms within the ellipsoidal enclosure and is dependent upon the angle of the inlet downcomer.
- Flow through the individual ducts is quite uniform.

Demonstration tests have been run using the inlet plenum feature model to evaluate qualitatively the movement and breakup of gaseous bubbles injected in the system. Passage of large coherent bubbles through the central regions of the FFTF would have severe effects upon reactivity because of the central positive void coefficient. These tests were initiated to investigate the tendency for bubbles, if they should exist, to concentrate toward the core central region within the basket before passage through the core.

In all cases where the air was introduced through the downcomer, the observed voids appeared as small (1/8 to 1/4 in. diameter) bubbles. The bubbles were swept with the coolant without visible tendencies for concentration toward the core center. With the nozzles angled toward the tangential direction, the tangential velocity outside the basket quickly distributed the void around the basket. Even with the nozzle perpendicular to the basket, the bubbles appeared to first enter the reflector regions and then the core regions. In general, the tests have shown that the present inlet configuration does not tend to concentrate bubbles at the core center.

F. HYDRAULIC CORE MOCKUP (HCM) CONSTRUCTION (7N95)

Contract award on the 1/2 scale model was held up pending receipt of the Defense Contract Audit Agency audit of Atkins and Merrill, Inc. This audit took longer than anticipated. Audit information was received and has been evaluated. Simultaneously, means of achieving cost savings with regards to the model are being explored and will be finalized prior to contract award.

Westinghouse suggestions on design of the 1/2 scale model for vibration testing were received and are being evaluated, particularly in regards to the impact on model fabrication.

Reactor concept changes continue to impact design schedule and costs, and the construction schedule. Some recent decisions and studies in progress which are causing piping design changes include such decision as the use of three primary loops instead of six, proper vessel height, and nozzle elevation.

G. CHANNEL INSTRUMENTATION REQUIREMENTS ANALYSIS (7N82)

Use of an automatic power setback action to prevent coolant boiling induced by channel flow loss was investigated for various safety rod insertion rates. Protection against flow loss ratio as high as 13% per second is afforded by a safety system reactivity response of -75¢/sec when the system trip action is initiated by detection of a 30 °F temperature increase in a 2.0 second time constant thermocouple. Low rate setbacks, such as -10¢/sec (which provide a power reduction of only about 5%/sec), are able to protect against proportionately low-flow loss rates.

Some flow loss-temperature transient studies of test loop behavior have also been completed. Initial results have been obtained for the model of a sodium-bonded, full length carbide fuel test assumed to have a lineal heat rating of 43.5 kW/ft. Channel sodium flow rate is set initially at a value which establishes a temperature rise across the test, equal to that in a hottest driver channel.

The consequently increased flow velocity reduces the time of transit of abnormal coolant temperature conditions to thermocouple positions and makes a quickly responding thermocouple more effective at initiating scram. Thus, an instantly responding TC is able to provide protection against an 85%/second flow loss rate when set to trip at +30 °F whereas the same TC disposition in a driver channel furnishes protection against a flow loss rate of 30%/second.

H. HOT CHANNEL FACTOR APPLICATION (7N82)

Hot channel factors (HCF) must be applied to average temperatures calculated in the reactor model to obtain maximum temperatures for safety evaluations. Two hot channel temperatures of interest are maximum core outlet coolant temperature, and maximum cladding inner surface temperature. Hot channel factors have been established and are given in BNWL-1064.[1]

Incorporation of these factors in the system models results in a larger enthalpy rise factor than had previously been used. This change in addition to system engineering changes will require some reevaluation of peak cladding temperatures associated with given transients.

---

1. *E. G. Stevens, et. al., FFTF Fuel Pin and Subassembly Conceptual Design Methods and Data, BNWL-1064, Battelle-Northwest, Richland, Washington, May 15, 1969.*

VII. FUELS AND MATERIALS

A. MECHANICAL PROPERTIES OF STRUCTURAL MATERIALS (7N96-7A00)

1. Uniaxial Creep

Work is in progress to evaluate the effects of aging on rupture-life and creep rates of Types 304 and 316 stainless steel.

The specimens were aged 3045 hr at temperatures ranging from 800 to 1400 °F. Figures 7.1 and 7.2 show the results of these tests. As indicated by the dashed line, there appears to be a maximum stress level and above this point the specimen will break on loading. This maximum stress appears to decrease as the aging temperature of the specimens increases. Metallography has shown that carbide formation is more predominant at the higher aging temperatures. This can be seen from Figure 7.3, which contains micrographs of Type 316 SS aged at 800, 1100, and 1400 °F.

Deviation of short time results from the control curve (for solution-treated control specimen) is more noticeable after 1400 °F aging than in any other temperature investigated thus far. Another interesting result is that Type 316 SS specimens aged at 900 °F exhibited longer rupture lives than the control specimens at stresses above 50,000 psi. Those specimens aged at 1400 °F also exhibited an increase in creep rate when compared to control specimens. This is shown in Figures 7.4 and 7.5. Tests are now in progress to determine at what temperature this departure from solution-treated control specimens begins. From the existing data, it appears that at all test temperatures, for both Types 304 and 316 SS, the rupture life of the aged specimens may be the same as that for the control specimens at low stresses. Differences in creep rate are expected to continue at low stresses.

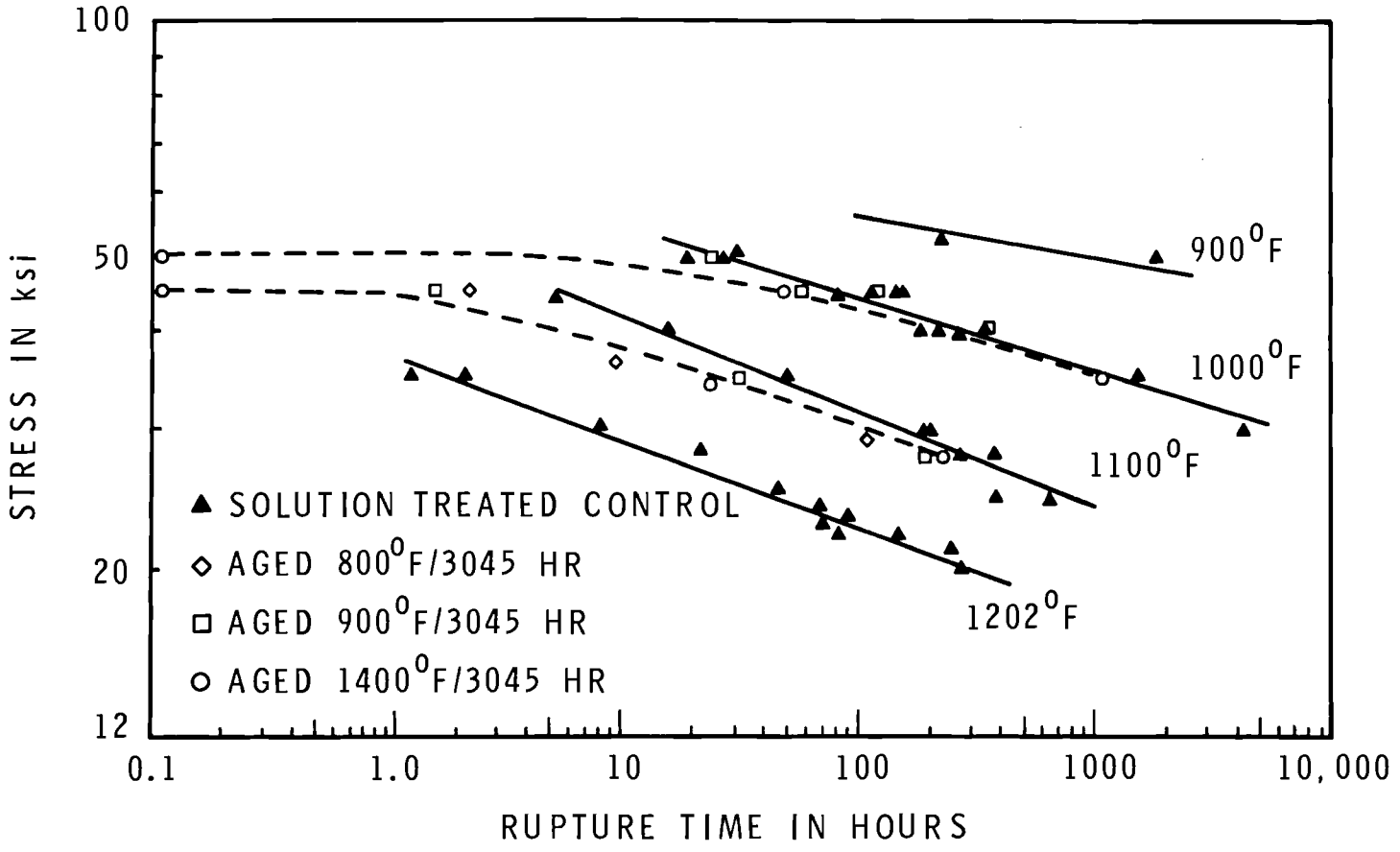

FIGURE 7.1. Effect of Aging on the Creep-Rupture Properties of AISI Type 304 SS

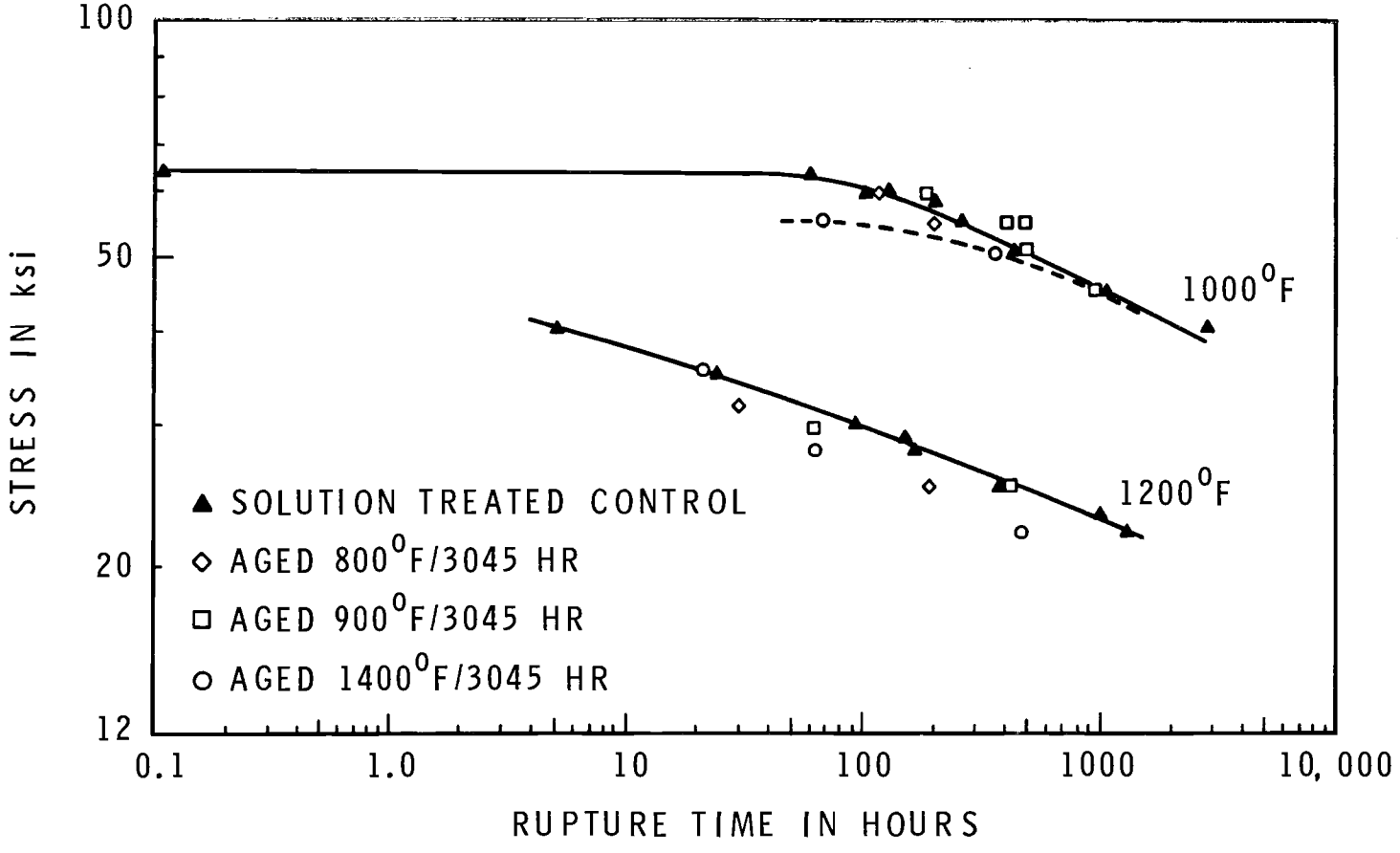

FIGURE 7.2. *Effect of Aging on the Creep-Rupture Properties of AISI Type 316 SS*

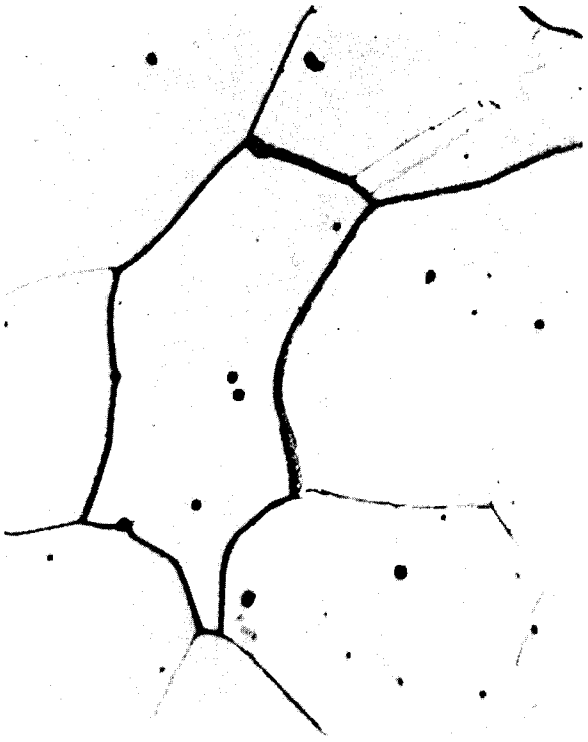

469 - 973C - 1000X
Aged 800 °F

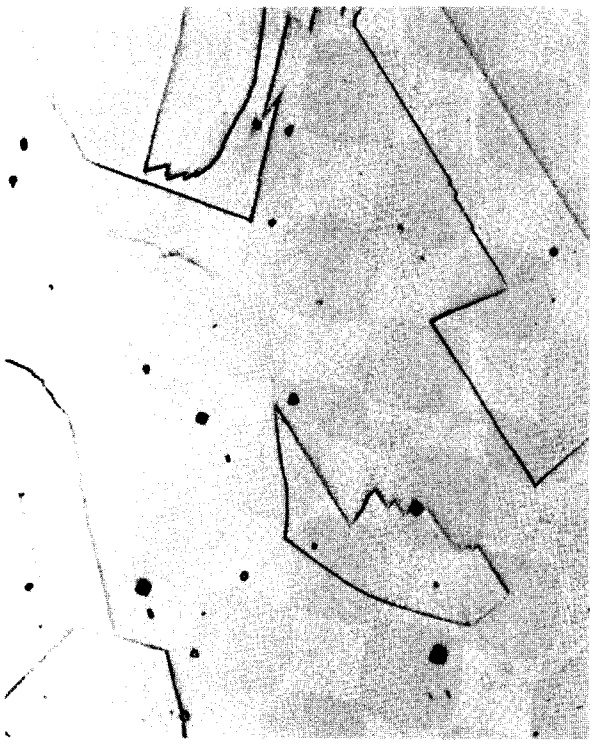

469 - 978C - 1000X
Aged 1100 °F

469 - 995C - 1000X
Aged 1400 °F

FIGURE 7.3. Type 316 SS CANEL Heat S. T. + Specified Aging/3045 Hr

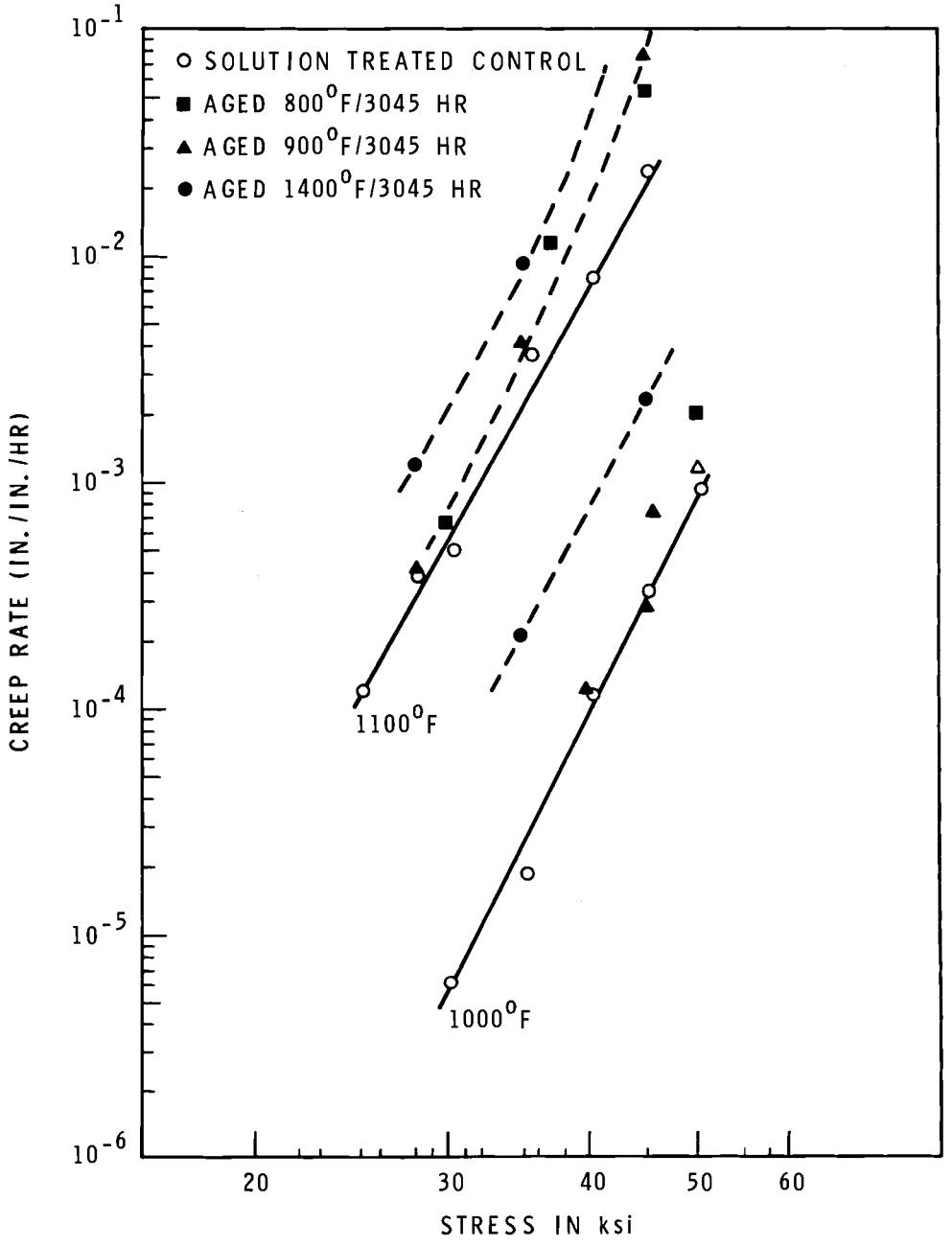

FIGURE 7.4. Effect of Aging on the Creep Rate of AISI Type 304 SS

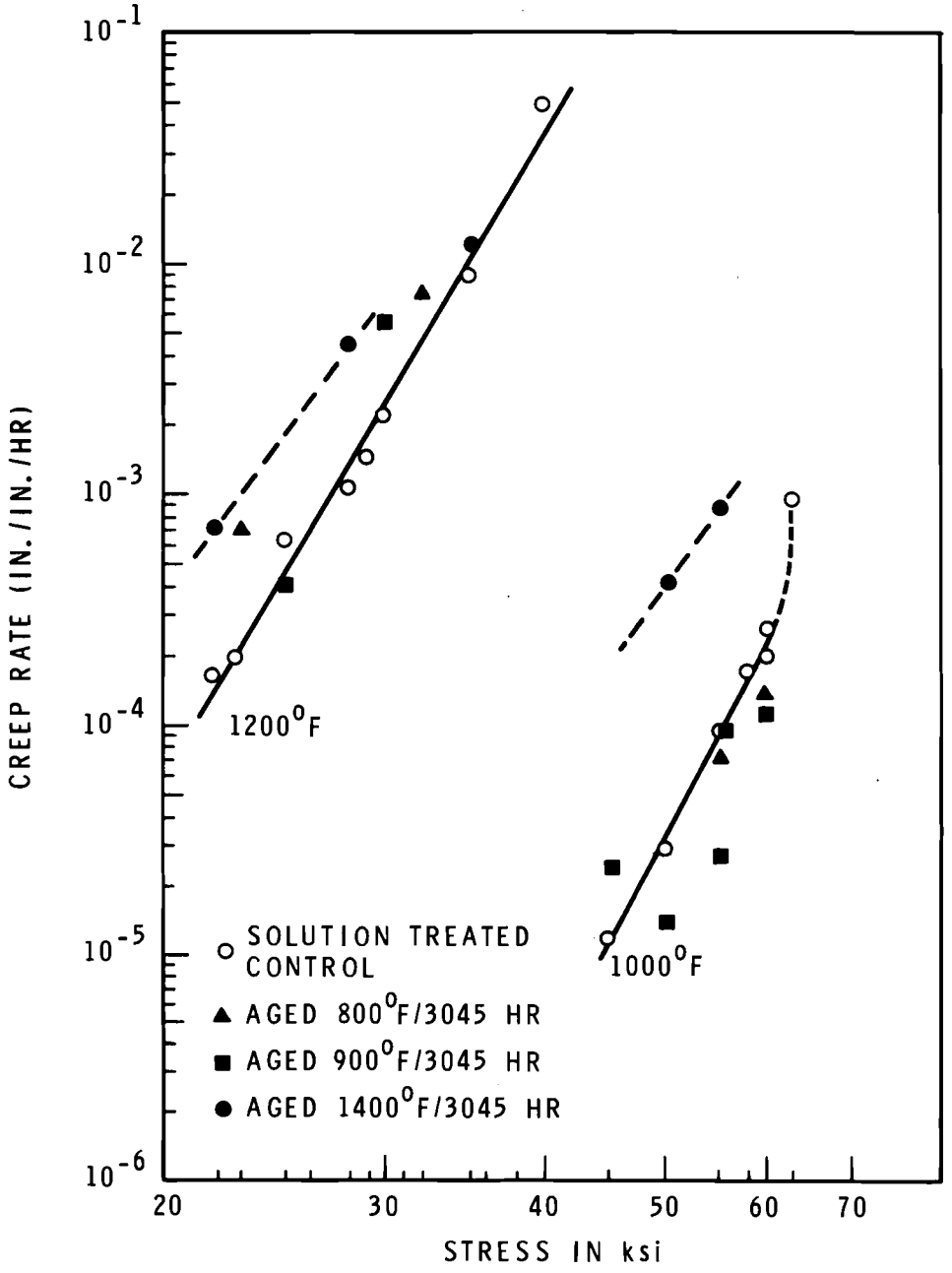

FIGURE 7.5. Effect of Aging on the Creep Rate of AISI Type 316 SS

The plot which correlates stress-rupture data using the theta parameter $\left[\theta = t_r \exp(-\Delta H/RT)\right]$ is shown in Figure 7.6. The objective of this part of the creep-rupture program is to provide information on the behavior of irradiated AISI Type 304 SS at relatively low stresses (below 25,000 psi) for relatively long periods of time ($\sim$100,000 hours).

Both the solution-treated control specimens and the specimens irradiated at 900 °F at a fluence of $\sim 1 \times 10^{22}$ n/cm^2 fit in a linear plot for the stresses and temperatures investigated. From previous data,[1] it appears the curves may bend down at lower stresses.

Creep-rupture tests have been made on welded specimens. There are four weld processes to be investigated in the future and these are sub-arc, stick-electrode, TIG and MIG. From results obtained thus far, it appears the stick-electrode type weld will produce specimens with a longer rupture life at a given stress than any of the other three processes.

Transient strain has been determined for Type 316 SS. The purpose of this phase of the program was to provide a means whereby transient strain of irradiated (900 °F - $\sim 1 \times 10^{22}$ n/cm^2) AISI Type 316 SS could be obtained as a function of initial stress. Transient strain is defined here as being the value of strain obtained when the second stage of the creep curve is extrapolated to zero time. The data were obtained for test temperatures ranging from 1000 to 1400 °F and are shown in Figure 7.7. The data show that the irradiated specimens had a substantial reduction in transient strain at the higher stresses.

---

1. *E. R. Gilbert and N. E. Harding, "In-Reactor Creep of Structural Materials for Nuclear Applications", BNWL-SA-1458. Paper presented and to be published in the proceedings of ASTM Symposium on Effects of Radiation on Structural Metals, held in San Francisco, California, June 26-28, 1968.*

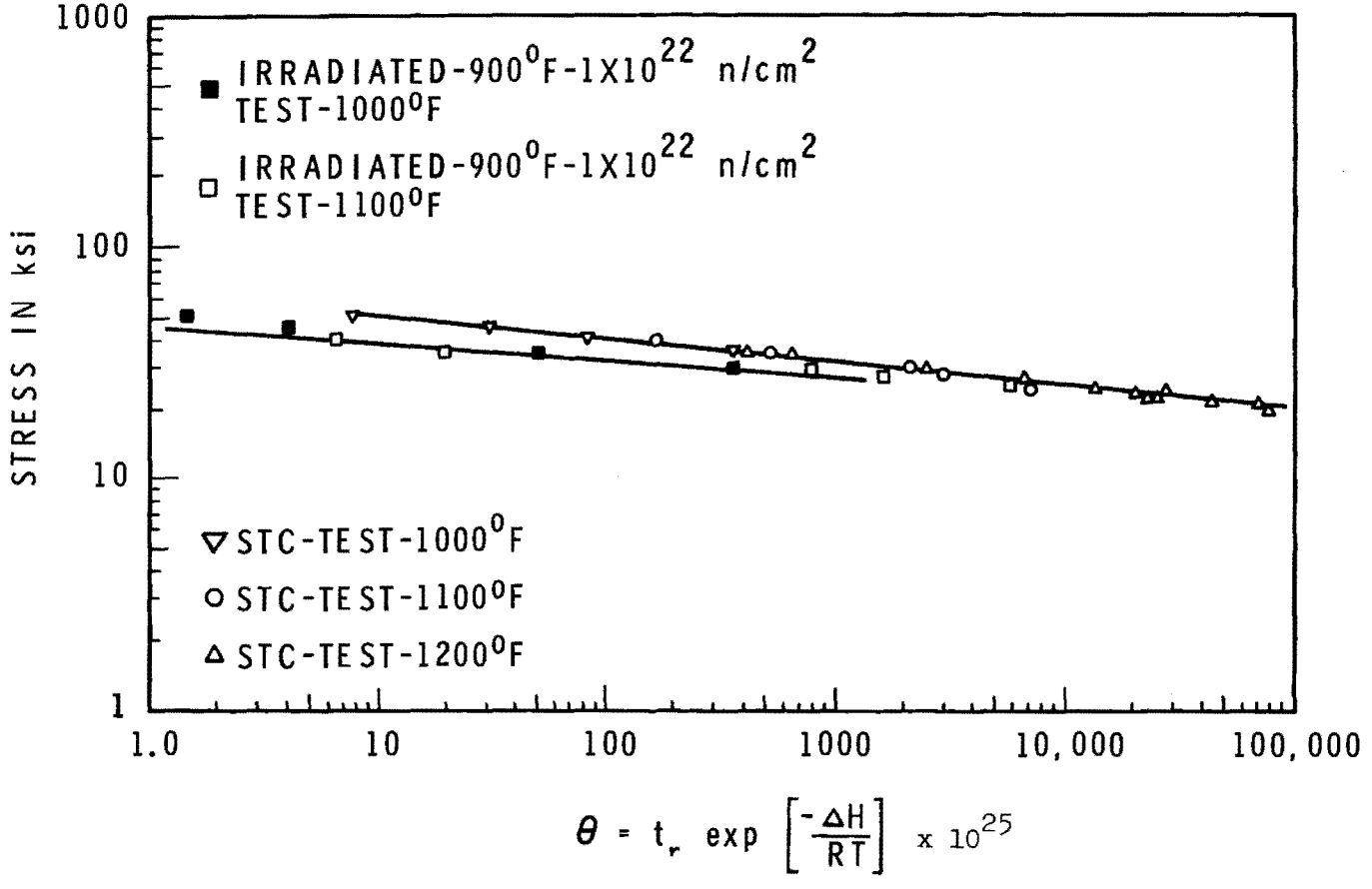

FIGURE 7.6. *"Theta Parameter" Plot of Creep-Rupture Test of Type 304 SS*

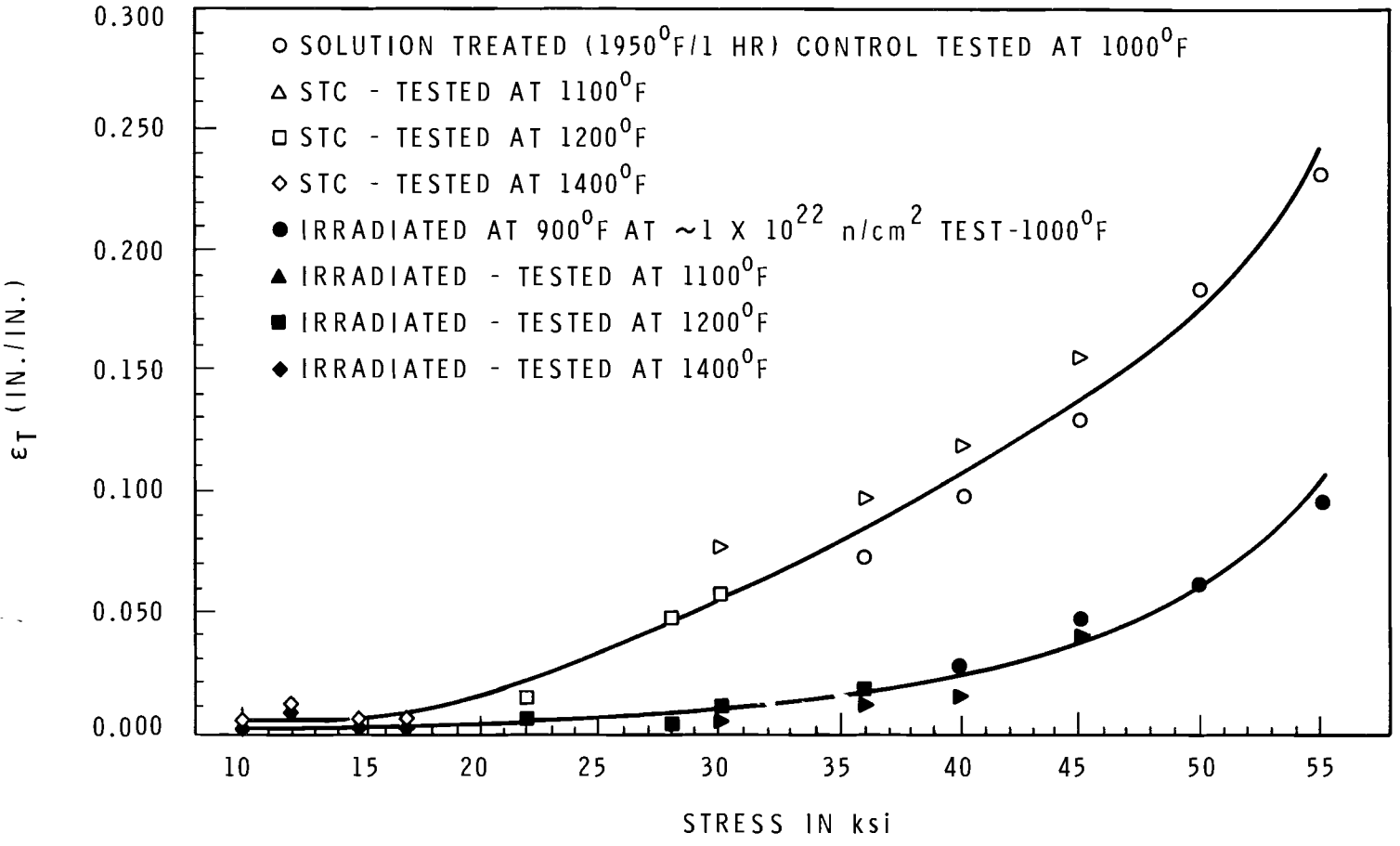

FIGURE 7.7. *Effect of Irradiation on Transient Strain in AISI Type 316 SS*

2. High Strain Rate Effects (7N96-7A00)

The objective of the high strain rate studies is to evaluate the effects of high strain rates on the mechanical properties of LMFBR materials which are expected to be used in the FTR vessel and core components. The results of this program will provide information on the behavior of the vessel during impact from within and on the behavior of core components during thermal transients and other conditions of rapid loading.

During the past month, several high strain rate tests were completed on the Krafft-Hahn dynamic loader. Tests were performed at strain rates of 0.1, 1, and 10 sec^{-1} at temperatures from room temperature to 1600 °F in air. The preliminary results are presented in Figures 7.8 and 7.9.

In comparing the data in Figure 7.8 and Figure 7.9 obtained on 304 SS at strain rates of about 0.1, 1.0, and 10 sec^{-1} to that obtained by Lovell and Ward at a strain rate of 0.00003 sec^{-1}, it becomes apparent that the rate of straining significantly affects the mechanical properties of Type 304 SS at elevated temperatures. In Figure 7.8, it is apparent that the highest ultimate and yield strength are obtained at a strain rate of about 0.1 sec^{-1}. The values obtained at a strain rate of 1.0 sec^{-1} appear to parallel those obtained at a strain rate of 0.1 sec^{-1}, but the ultimate and yield strengths at the higher rate are much lower at all test temperatures.

Since tests at a strain rate of about 10 sec^{-1} have only been completed at a test temperature of 1000 °F, it cannot be said with certainty what effect this increase in strain rate will have on the ultimate and yield strength at other test temperatures of interest.

Since the energy required to cause plastic flow and subsequent failure in the FTR vessel under conditions of rapid loading is of interest, an estimate of the effect of strain

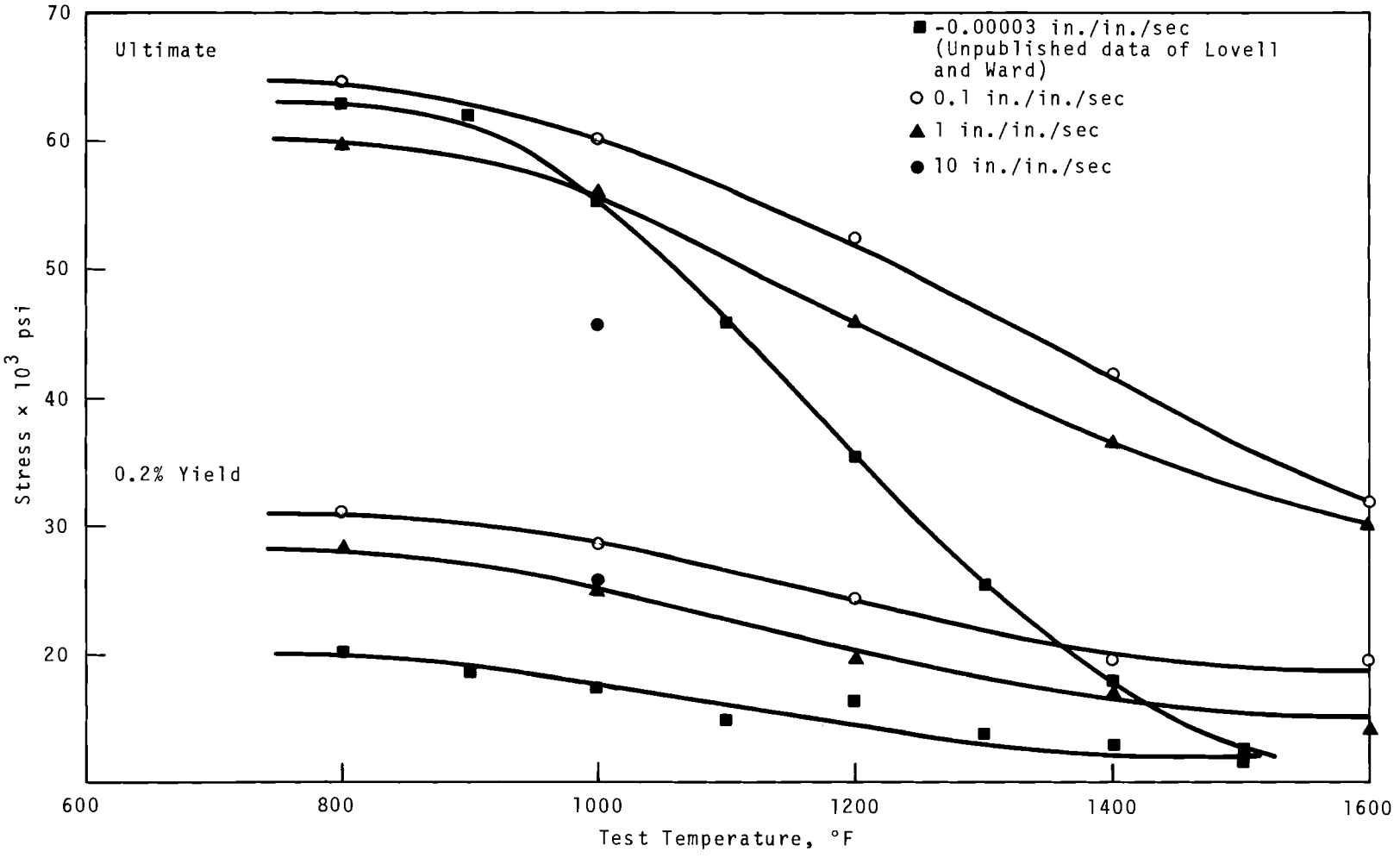

FIGURE 7.8. The Strength of Annealed Type 304 SS

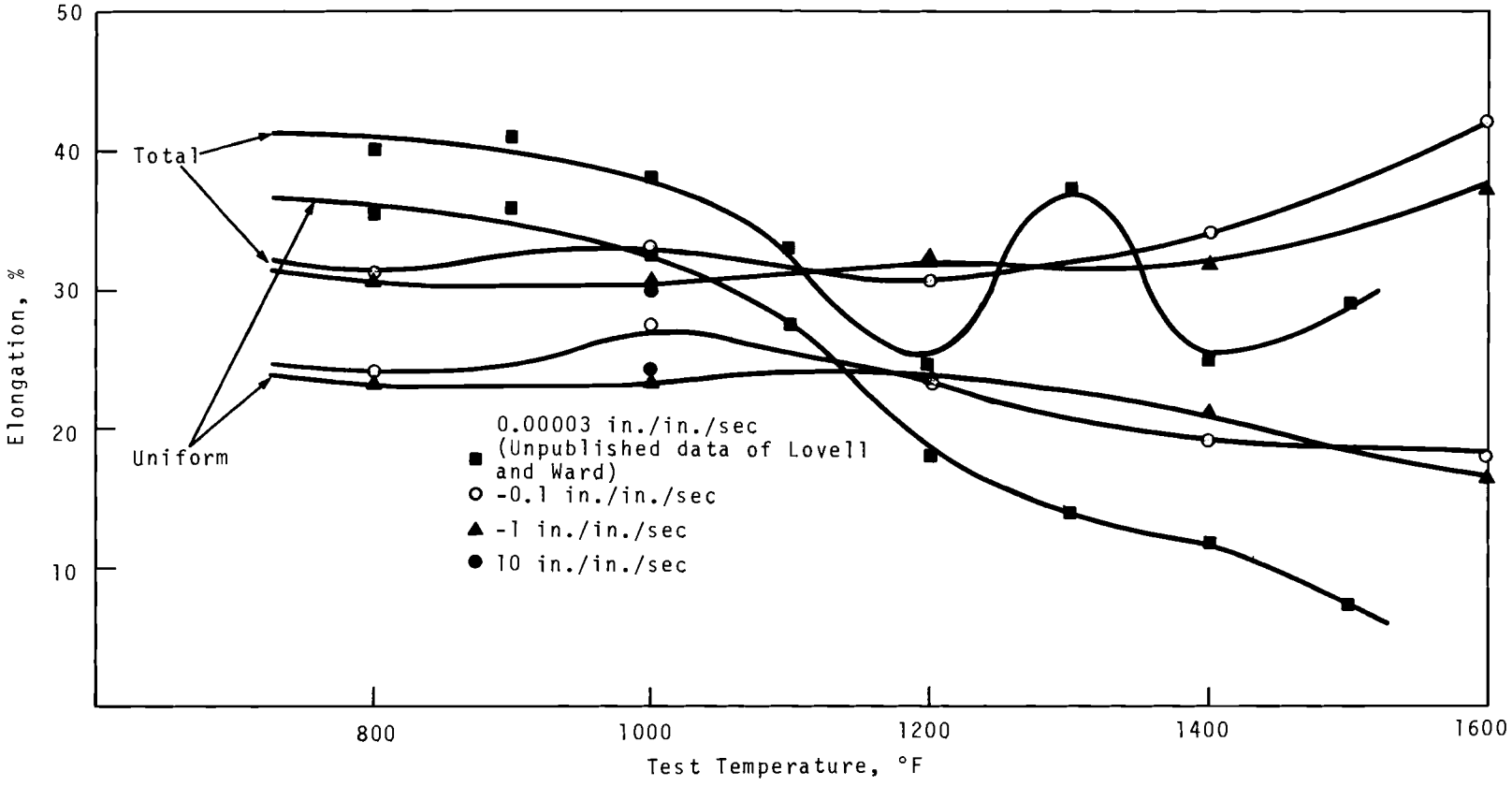

FIGURE 7.9. The Ductility of Annealed Type 304 SS

rate of this energy can be obtained by determining the area under a stress-strain curve. Since the stress-strain curves were available at four strain rates (0.00003, 0.1, 1.0, and 10.0 sec^{-1}) at a test temperature of 1000 °F, a rough approximation of the area under each curve was made by multiplying the ultimate strength times the total elongation. The numbers obtained are as follows:

Strain Rate, sec^{-1}	Area (Approximate), $\times 10^3$ in.-lb
0.00003	2110
0.1	2000
1.0	1705
10.0	1370

These values indicate that the energy required to cause deformation and failure in the vessel at a strain rate of 10 sec^{-1} would be about 65% of the energy required at a rate of 0.00003 sec^{-1}.

B. FUELS TESTING

1. PNL-1 Biaxial Test Specimen Failures (7N70)

Three PNL-1 biaxial test specimens, two prepared from adjacent sections of an irradiated fuel pin and a third from another pin, were tested at 900 °F. These specimens failed at stresses lower than predicted. The failures were characterized by intergranular cracking which originated at the inside surface of the cladding. Nonfueled but irradiated specimens tested at 900 °F revealed only transgranular failure. The presence of large carbide particles along the grain boundaries of specimens failing intergranularly is considered significant. Fuel cladding interaction may be involved.

2. Other Irradiation Testing of Fuels (7N70)

PNL-2, a 19-pin encapsulated subassembly, continues to operate satisfactorily in EBR-II after an exposure of 43,000 MWd/tonneM.

Three experimental subassemblies, each with 37 unencapsulated pins, continue to operate in EBR-II. The exposures for PNL-3, 4 and 5 are 9,500, 11,000 and 19,500 MWd/tonneM, respectively. Calculations with newly updated stainless steel swelling equations indicate that after 30,000 MWd/tonneM, subassembly PNL-3 will develop an interference fit between the hexagonal tube and the fuel pin bundle and that the clearance between adjacent hexagonal tubes will be reduced from the initial 0.030 in. gap to 0.008 in.

Two capsules, BNW-1-10 and 12, continue irradiation in the ETR toward a goal exposure of 100,000 MWd/tonneM. Their estimated exposures are now 65,000 MWd/tonneM.

Procedures for the first reencapsulation of fuel for an EBR-II/TREAT test are being finalized, and the PNL-1-1 test is scheduled for late September.

3. EBR-II Driver Fuel Examination (7N70)

Examinations of an additional irradiated pin and three additional nonirradiated pins of EBR-II driver fuel (U+5Fs) confirmed that the length decrease experienced by the centrifugally bonded pins is an irradiation growth phenomenon brought on by the presence of textured alpha uranium.

4. Tests at CCTL (7N70)

Several pins from the CCTL, 217-pin subassembly which was in 1060 °F, flowing sodium for 3600 hours, were sectioned for cladding and wire wrap examination. There is no evidence of appreciable surface corrosion or erosion on any of the samples.

5. Irradiation of Hypostoichiometric UO_2-PuO_2 Fuel (7N70)

The status of the BNW-1 series of capsules is summarized in Table 7.I. Two capsules continue their irradiation toward a goal of 100,000 MWd/tonneM. Four are being examined in the BNW Radiometallurgical facilities and examination of six are essentially completed.

a. Compilation of Fabrication and Irradiation Histories

A complete fabrication history is being assembled for each of the BNW-1 experiments. This is to include analyses of the fuel from the powder stages through to the fuel pin, the processes involved, certification of capsule components, complete assembly details and all preirradiation measurements.

Irradiation histories are also being compiled for each experiment. Plots of temperature versus time are being studied to correlate the thermocouple readings to temperatures obtained from the TIGER V computer program analyses.

b. Gamma Scanning on Irradiated Pins

Axial gamma scans for gross activity and for $^{95}Zr/^{95}Nb$ have shown several activity peaks on BNW-1-1, 1-2, 1-3 and 1-5. Spectra data collected along the length of the fuel pins including several directly on the activity peaks are being analyzed with a computer program GSSLRN (Guassian-Learn) to determine the major gamma emitting isotopes present. The activity peaks on the gross gamma scans corresponds to axial positions on the fuel pin neutron radiographs where high density material (presumably fission product ingots) can be seen in the central voids of the fuel. Preliminary analysis from the BNW-1-1 spectra data on the computer program indicates that the fission product ruthenium is the major contributor to the activity peaks along the fuel except for one approximately one mil from the top of the fuel column. The

TABLE 7.I. Summary Status of Irradiation Experiments Conducted Under Task FP-6

TABLE 7.I Summary Status of Irradiation Experiments Conducted Under Task FP-6

Test Designation	Description[1] Fuel Form	O/M	Facility	Goal Exposure MWd/tonneM	Actual Exposure MWd/tonneM	Discharge Date	Status
BNW 1-1	Solid	1.93	MTR	100,000	(Est)120,000	2-69	Being Exam. at BNW
BNW 1-2	Solid	1.93	ETR	50,000	(Est) 70,000	2-69	Being Exam. at BNW
BNW 1-3	Solid	1.96	MTR	100,000	(Est)150,000	2-69	Being Exam. at BNW
BNW 1-4	Solid	1.96	MTR	50,000	71,000	6-68	Exam. Completed at BNW
BNW 1-5	Solid	2.00	MTR	100,000	(Est)160,000	2-69	Being Exam. at BNW
BNW 1-6	Solid	2.00	MTR	50,000	85,200	10-68	Exam. Completed at BNW
BNW 1-7	Annular	1.93	MTR	50,000	<1,000		Lead Tube Failed. Exam. at BNW
BNW 1-8	Annular	1.93	MTR	100,000	29,000	1-68	Failed. Exam. at BNW
BNW 1-9	Annular	1.96	MTR	50,000	81,000	6-68	Exam. Completed at LASL
BNW 1-10	Annular	1.96	ETR	100,000	(Est) 65,000	(Est)2-70	Discharged 2-69 for Interim Exam. Recharged 5/69
BNW 1-11	Annular	2.00	MTR	50,000	87,400	8-68	Exam. Completed at LASL
BNW 1-12	Annular	2.00	ETR	100,000	(Est) 65,000	(Est)2-70	Discharged 2-69 for Interim Exam. Recharged 5/69

(1)

Fuel

25% PuO_2 - 75% UO_2
Pellets 0.212 in. OD (0.052 in. ID for annular pellets)
Smeared density - 87.5% TD
Pellet density - solid pellet 93% TD, annular pellet 95% TD
Fuel column length 13.5 in.

Cladding

OD - 0.250 in.
Wall thickness - 0.016 in.
Type 304 SS

spectra analysis indicates that cesium is the major activity contributor of this position. There is an indication that Cs has migrated more generally to the top of the fuel pin and even into the plenum region. Analysis of the gamma scan data and spectra is continuing.

C. CARBIDE STABILIZATION IN STAINLESS STEEL (7N72)

A stabilizing treatment presented in Table 7.II, designed to precipitate carbides on intragrain slip planes rather than on grain boundaries, was given to several specimens of Type 316 SS sheet. The as-treated microstructure, Figure 7.10, shows carbide occurring in about an equal amount on both slip planes and grain boundaries. Examination of TIG welds in treated material discloses increased re-solution of carbides with increasing proximity to the weld bead as illustrated in Figures 7.11, 7.12, 7.13 and 7.14. The usual sensitized structure, consisting of a heavy carbide network in the grain boundaries, did not develop in the heat-affected zone. Further work will determine the resistance of the stabilized structure and the heat affected zone to intergranular attack in hot HNO_3.

TABLE 7.II. Heat Treatment for Stabilizing Type 316 SS

Solution Anneal, 2000 °F, 15 minutes
Cold Work, 25% Reduction of Area
Precipitation Treatment - 900 °F, 24 hr
1300 °F, 216 hr

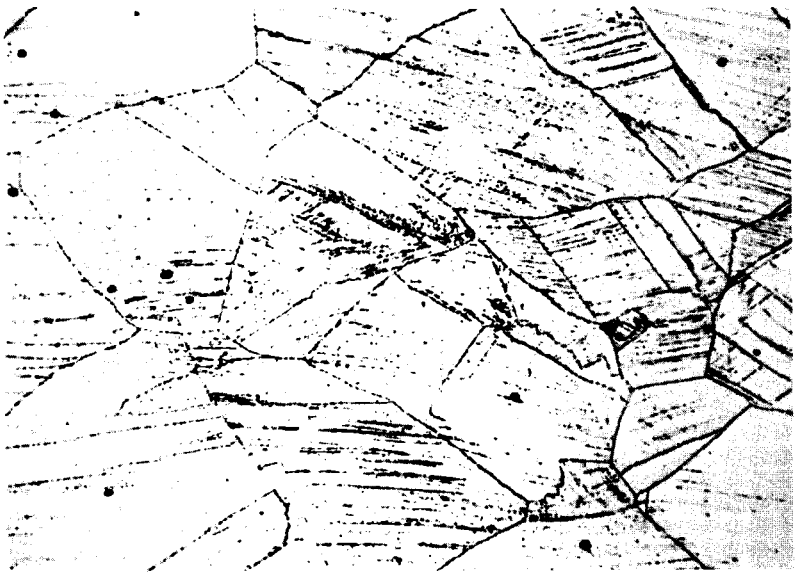

469-713 500X

FIGURE 7.10. Stabilized Grain Structure in Type 316 SS

469-714 F 500X

FIGURE 7.11. Stabilized Type 316 SS 0.085 in. Sheet Followed by TIG Welding with Addition of Weld Filler. (Note the presence of prior austenitic grain boundaries.)

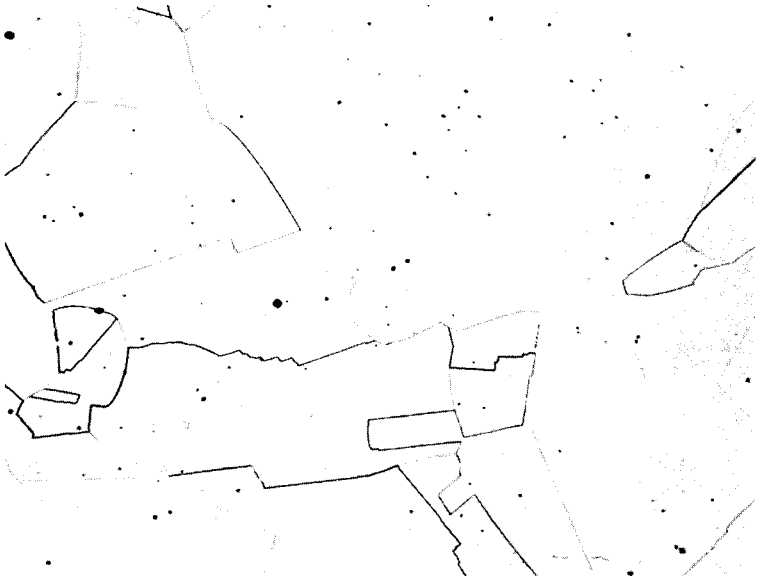

469-714 E 500X

FIGURE 7.12. Stabilized Type 316 SS in the Heat Affected Zone Approximately 0.050 in. from the TIG Weld Bead. (Again note the prior structure.)

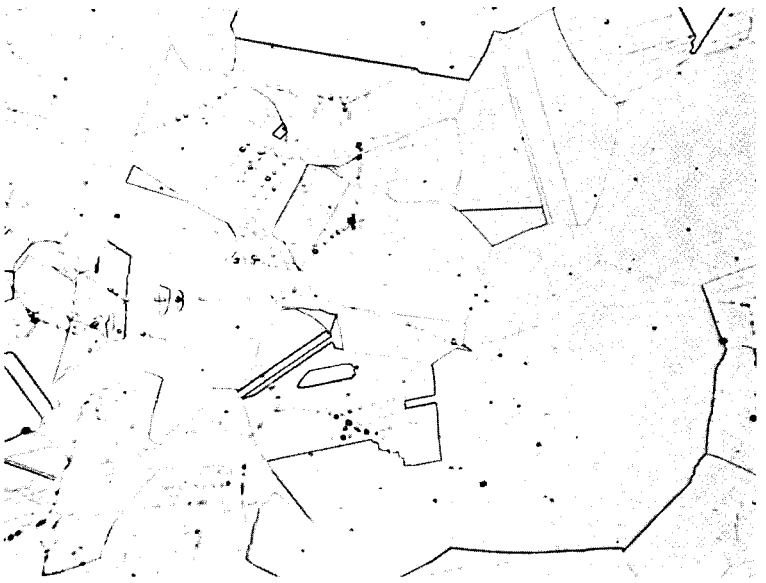

469-714 D 500X

FIGURE 7.13. The Same Conditions as Figure 7.12 Except Approximately 0.125 in. from Weld Bead.

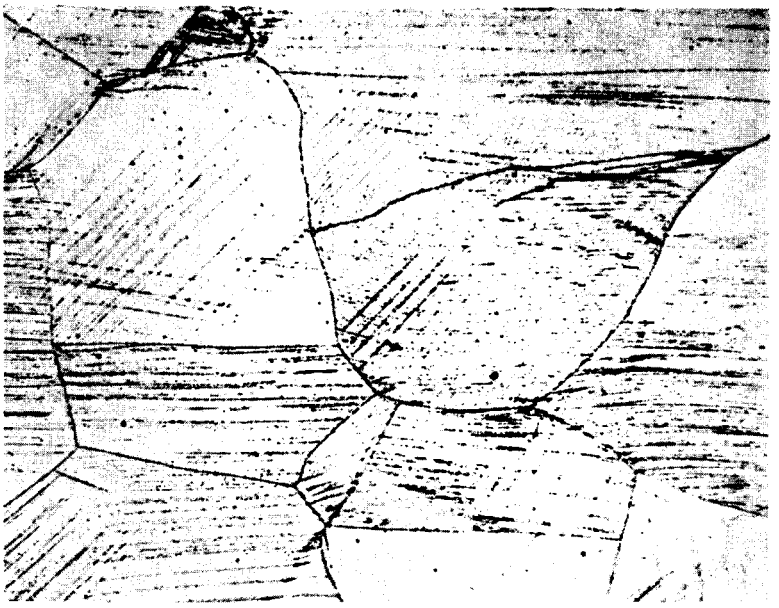

469-714 C 500X

FIGURE 7.14. At a Distance of Approximately 0.190 in. from the Weld Bead There Is No Effect of TIG Welding on the Structure of the Stabilized Type 316 SS.

D. EFFECTS OF FAST REACTOR IRRADIATION ON BIAXIAL STRESS-RUPTURE PROPERTIES OF TYPE 316 SS (7N72)

The objective of this program is to determine the effects of fast reactor irradiation on the biaxial stress-to-rupture properties of candidate fast reactor cladding materials. Biaxial stress-rupture tests have been performed on AISI Type 316 SS irradiated to a nominal fluence of $\sim 1 \times 10^{22}$ n/cm^2 (E > 0.1 MeV) in subassembly X-022 in EBR-II. Most of the irradiated samples tested were irradiated to a fluence of 0.8×10^{22} n/cm^2. Test temperatures were 1000, 1200, and 1400 °F. The remainder of the samples were irradiated to higher fluence (1×10^{22} n/cm^2) and will be tested at temperatures of 900, 1000, and 1200 °F.

Plots of stress versus rupture time for the various tests are shown in Figure 7.15, and plots of strain versus rupture

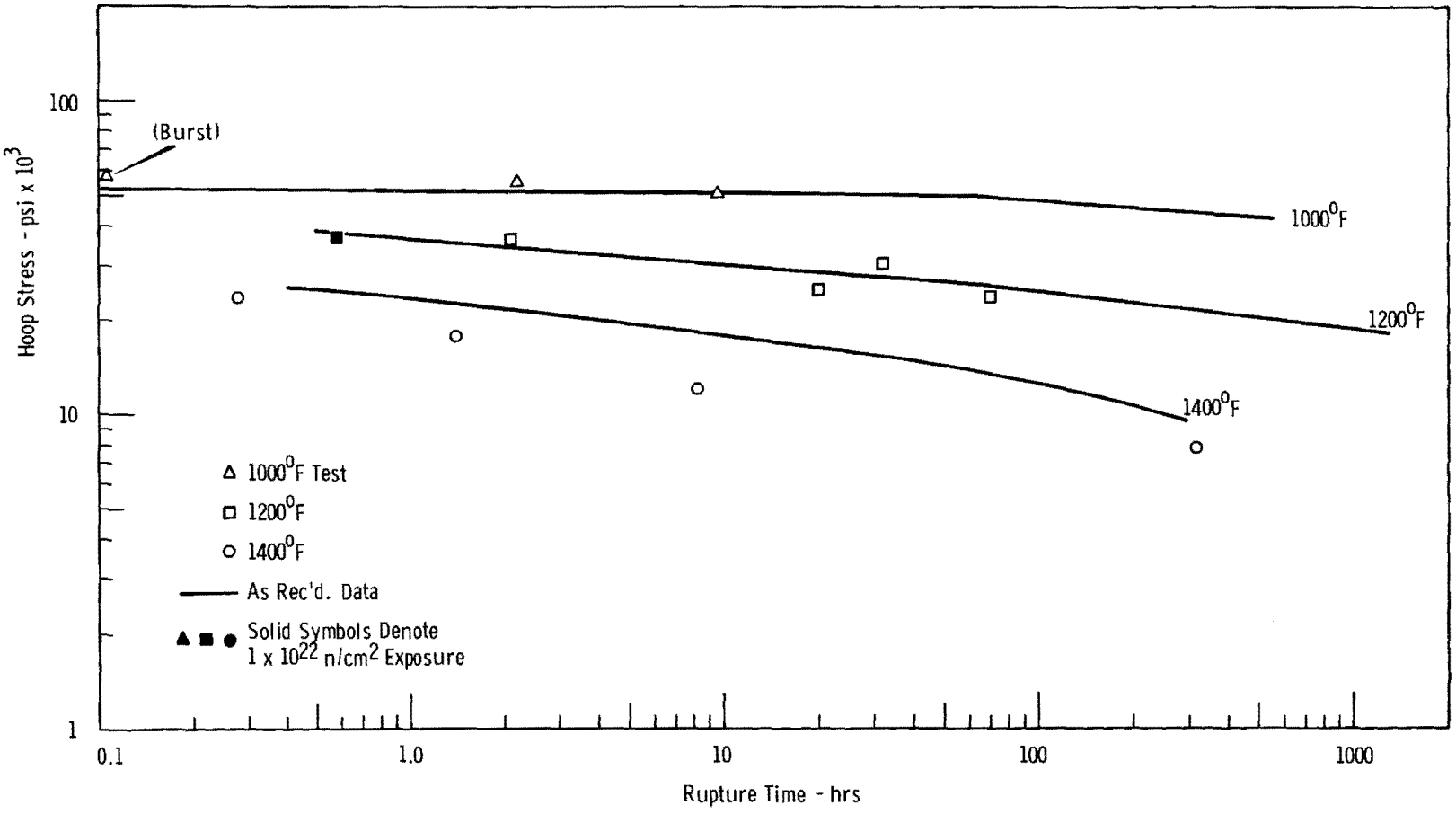

Neg 0693125-1

FIGURE 7.15. The Effect of Biaxial Stress and Temperature on the Rupture Life of AISI Type 316 SS Tested in Inert Gas.

time are shown in Figure 7.16. The data points show stress or strain and rupture time for as-irradiated tests while the solid lines represent control test results. Some irradiation hardening (strengthening) is evident at 1000 °F for the short rupture times shown. The as-irradiated test data are in fair agreement with the as-received test data to about a 10-hr rupture life. At 1200 °F the data fall in a scatter band around the curve formed by the as-received data. At 1400 °F marked decreases in rupture life are observed, the reduction being a factor of 7 to 10 less than the unirradiated values.

The failure behavior of the irradiated specimens is considerably different than for the controls. An illustration of typical bursts of irradiated and unirradiated specimens is shown in Figures 7.17 and 7.18. Both specimens were tested at 1400 °F in an argon atmosphere and had rupture times between 5 and 10 hours. It can be observed that the as-received specimen tears apart transversely, a section approximately the same length as the initial longitudinal split (see Figure 7.17), leaving the balance of the specimen undamaged from which the more precise diameter measurements can be made. The as-irradiated specimens do not show a tendency to tear in the transverse direction. Rather, the longitudinal split becomes more pronounced, often propagating the entire length of the specimen.

Because of the tendency of irradiated specimens to fail in a burst mode, opening more fully from end to end, a good evaluation of rupture strain usually cannot be made. However, where data are available, irradiation is seen to greatly reduce ductility, (see Figure 7.16). The lowest ductility in as-received material is at 1200 °F. This appears also to be the case for the irradiated material. Rupture strain at 1000 and 1400 °F test temperatures in the unirradiated and irradiated condition appears to be comparable.

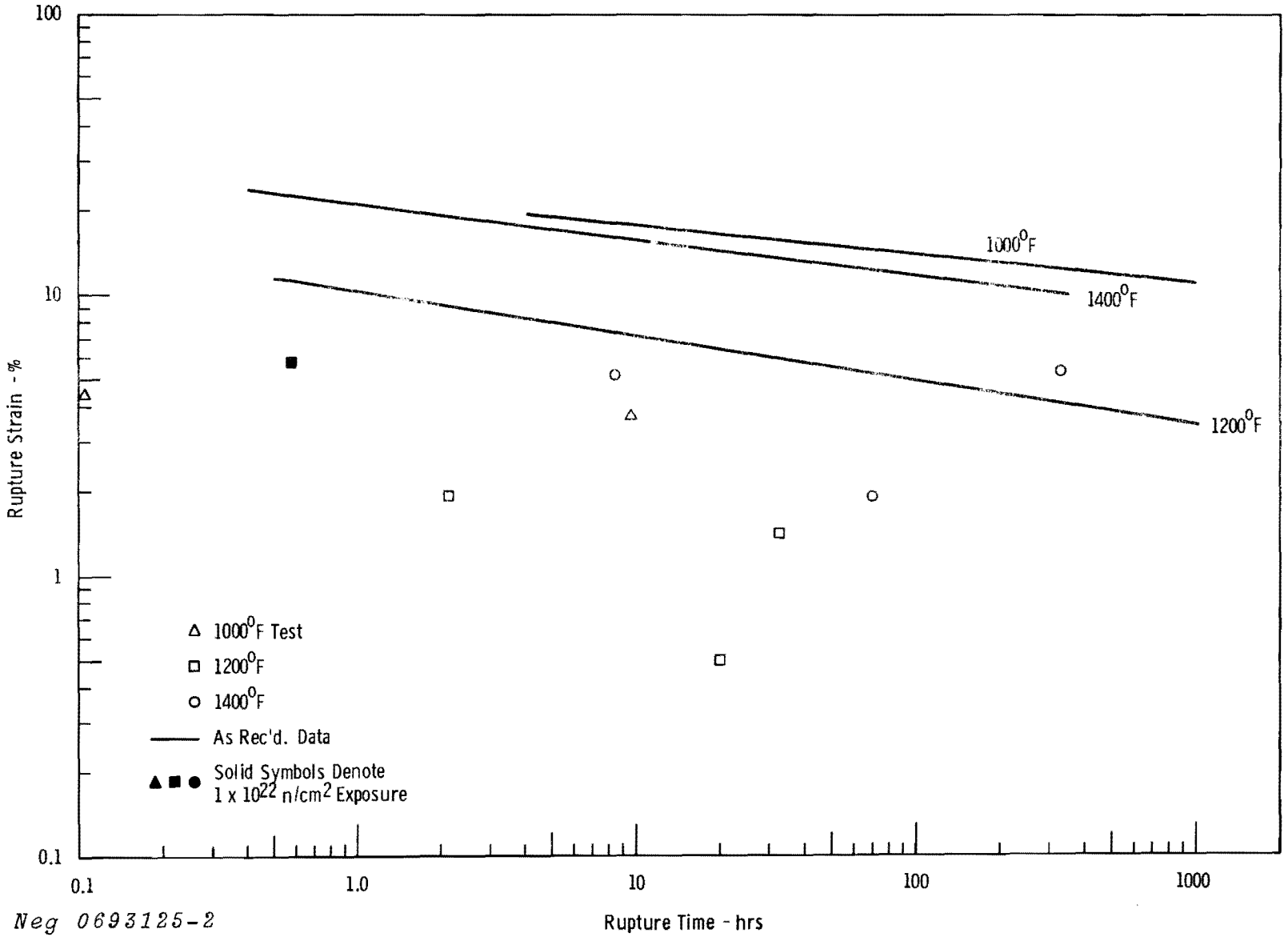

Neg 0693125-2

FIGURE 7.16. The Effect of Rupture Time and Temperature on the Ductility of AISI Type 316 SS Tested in Inert Gas.

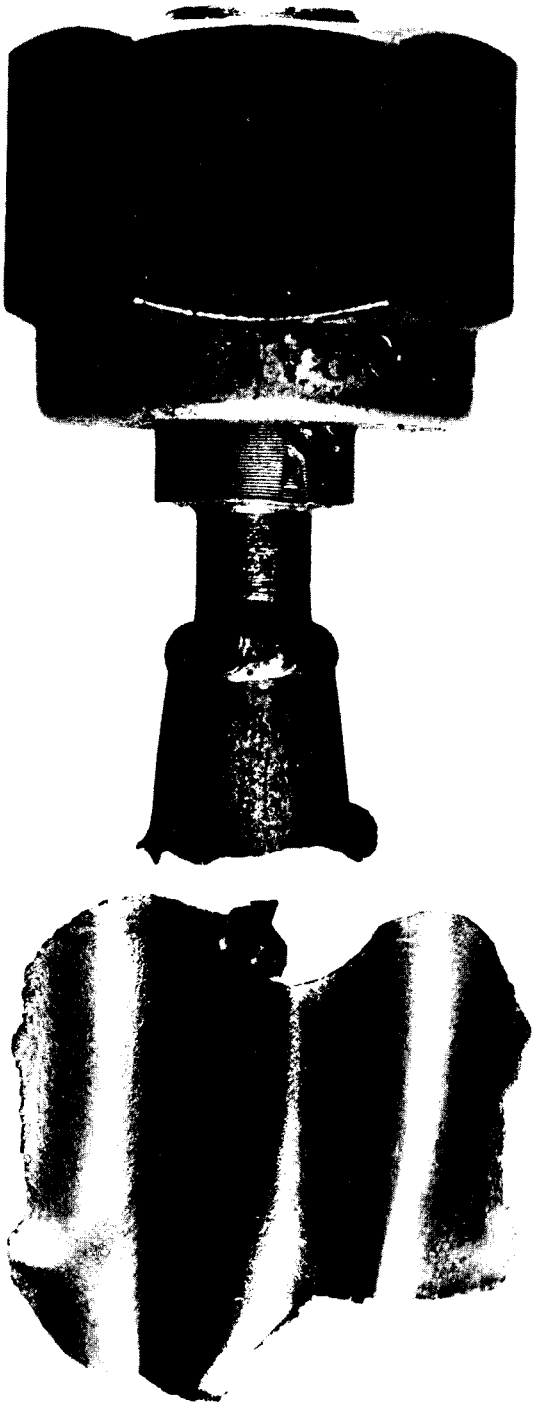

FIGURE 7.17. *A Typical Burst Failure for AISI Type 316 SS in the As-Received Condition. Test conditions were 1400 °F, 19,800 psi stress, rupture time 6.8 hours.*

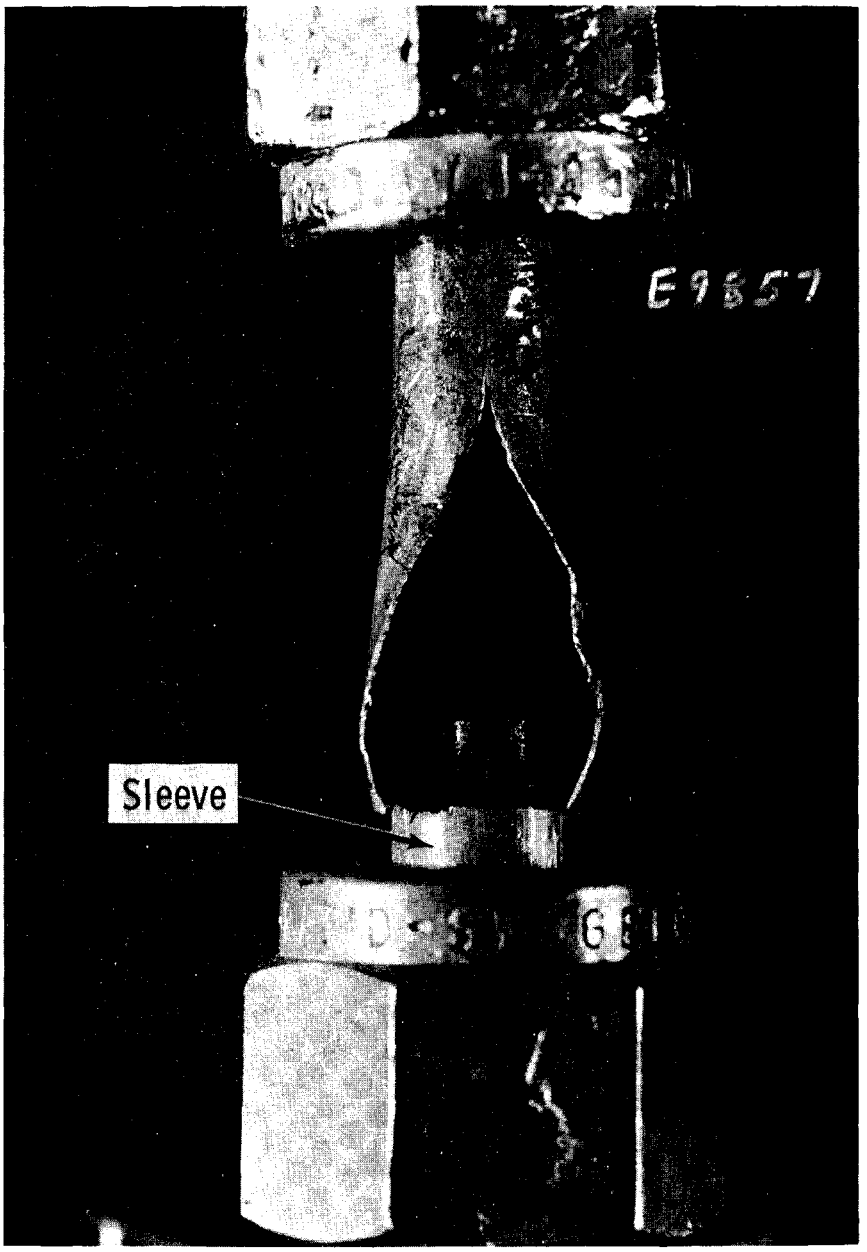

FIGURE 7.18. *A Typical Burst Failure for AISI Type 316 SS Irradiated to ∿1 × 10^{22} n/cm^2 (E > 0.1 MeV). Test conditions were 1400 °F, 12,000 psi stress, rupture time 8.2 hours.*

Time-to-rupture data from AISI Type 316 SS, both as-received and as-irradiated, tested in the Biaxial Stress Test Facility, have been re-plotted using the "Theta" parameter suggested by other investigators.[1,2] The master plot, shown in Figure 7.19, shows that biaxial stress-to-rupture data at various test temperatures can be related with the Theta parameter:

$$\log \sigma \log t_r \exp [-Q/RT]$$

where

σ = applied stress (psi),
t_r = time to rupture (hr),
Q = activation energy for creep (cal/mole),
T = absolute temperature (°K),
R = gas constant (cal/mole-degree).

It can be observed that by a value of Q = 95,000 cal/mole allows representation of all as-received data, by a single line. Excellent correlation is obtained between tests at various test temperatures.

As-irradiated stress-rupture data is also plotted on the Theta master plot. An excellent comparison can again be made between the various test temperatures showing the validity of the parameter.

At low Theta values, irradiation hardening is observed which results in an increase in stress-to-rupture. The increase in rupture stress is consistent with tensile results on AISI Type 316 SS from the same irradiation experiment. At high Theta values, the stress rupture life is decreased. This is probably the result of helium embrittlement dominating

1. *J. T. Venard, Stress-Rupture Properties of Type 304 Stainless Steel Tubing, ORNL-JM 535, June 1963.*
2. *R. L. Orr, O. D. Sherby, and J. E. Dorn, Am. Soc. Metals, Trans. Quart. 46, 113-28 (1954).*

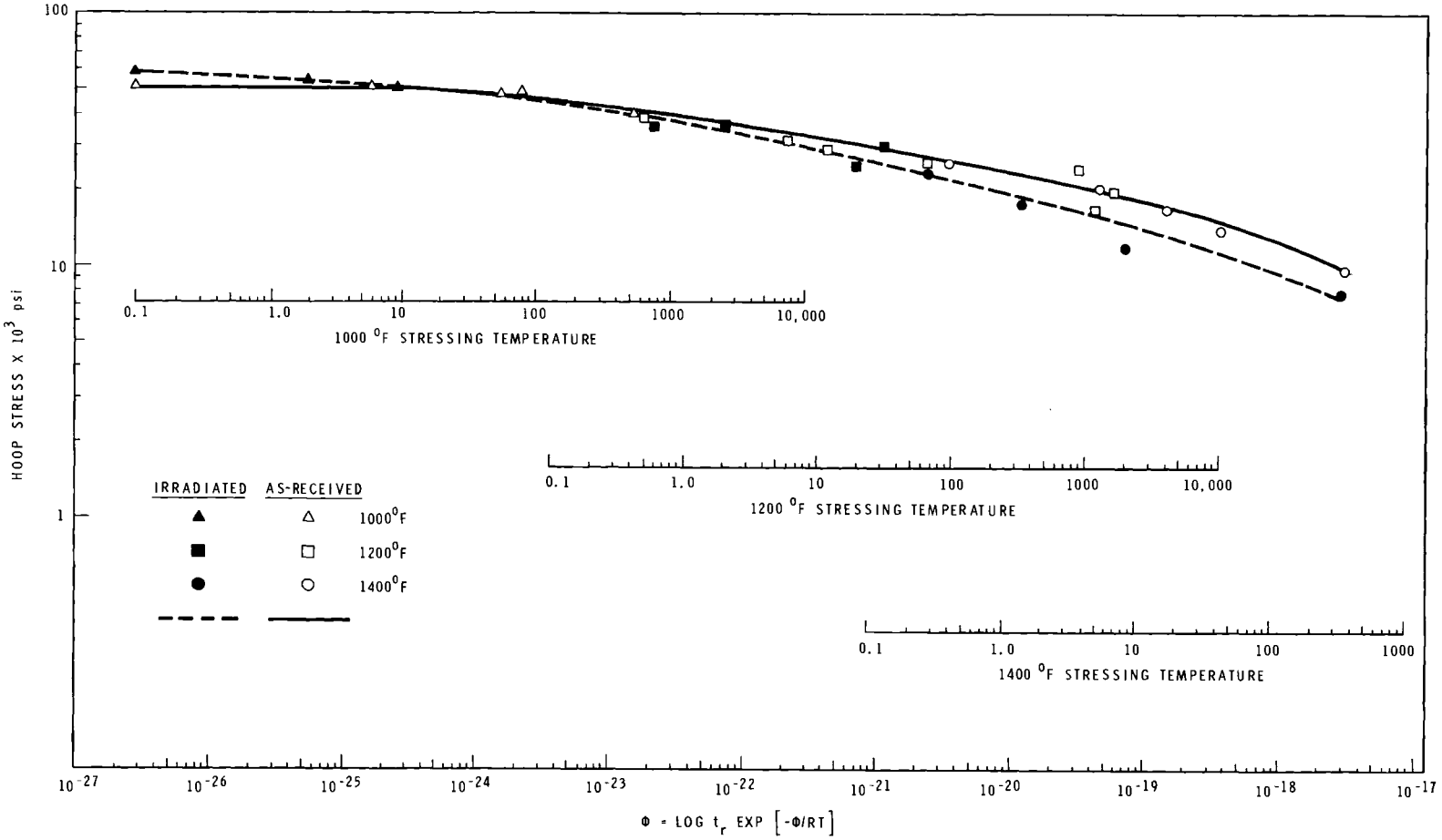

Neg 0693098

FIGURE 7.19. Theta Parameter Master Plot of Irradiated and As-Received AISI Type 316 SS Cladding Tested in Inert Atmosphere. (Exposure is ∿1 × 10^{22} n/cm^2 [E > 0.1 MeV] at 815 °F in EBR-II.)

irradiation hardening at the elevated temperature.[1] The fractures at high temperatures appear to be intergranular as expected from helium embrittlement processes. At intermediate Theta values, an even balance between irradiation hardening and helium embrittlement appears to exist.

During the coming months, attempts will be made to establish further the validity of using the Theta parameter for extrapolations by evaluating correlations of microstructural features by relating different tests via the Theta plot.

E. BEHAVIOR OF FUEL ELEMENTS (7N72)

1. Performance During Transients

A model to predict the failure of a FTR fuel pin during three types of transient conditions was developed. Preliminary analyses were made, using the model, to predict the time and axial position of failure during transient overpower excursions, and two types of loss-of-coolant accidents.

Two mechanisms are believed to initiate failure during an overpower excursion. The cladding can exceed its strain limit as a result of, (a) the expansion of the solid fuel when it becomes molten, or (b) fission gas pressure when gas is released from the molten fuel and is trapped in the central void. The time to failure from either cause was found to depend upon the assumed steady-state gas release. In the case of fuel melting, failure should occur near the axial midplane where the largest fraction of the fuel is molten. Failure caused by the release of gas to the central void should occur at a position corresponding to the top of the central void where the pressure is highest and the cladding temperature is highest and the cladding strength is lowest.

---

1. *R. S. Barnes, "Embrittlement of Stainless Steels and Nickel Base Alloys at High Temperature Induced by Neutron Irradiation" Nature Vol. 206, June 26, 1965, pp. 1307-1310.*

Calculations made for the loss of coolant accidents, i.e., flow coastdown and pipe rupture, predicted failure to occur as a result of high cladding temperature rather than high fuel temperature. The time to failure is dependent upon the steady-state gas release. Unlike the transient overpower excursion, where excessive pressure is predicted to occur from gas released during fuel melting; cladding failure during a loss-of-coolant accident is expected to occur because of the significant reductions in cladding strength at elevated temperatures. The internal pressure buildup of steady-state released fission gas is a function of the increasing coolant exit temperature (assuming perfect gas behavior). Failure was predicted to occur near the top of the pin when the cladding temperature reaches 1600 to 1800 °F.

2. Hybrid Computer Simulation of Fuel Performance

R. D. Leggett, R. L. Fish and C. R. Cole

The equations describing fission gas release, pressure buildup and three-zone sintering have been formulated and have been programmed onto the Hybrid Computer. Fuel melting and thermal flux radial power profiles are now being incorporated into the program.

The expected fuel restructuring and fission gas release were calculated for several pins of the PNL-1 series (UO_2–25 wt% PuO_2, Type 304 SS cladding, 0.250-in. OD × 0.016-in. wall, irradiated in EBR-II) using the two-zone "SINTER" code, assuming an in-reactor sintering temperature of 1700 °C, sintered fuel density of 98% of theoretical, and a gap coefficient of 1200 Btu ft^{-2} $°F^{-1}$ hr^{-1}. Table 7.III compares the calculated values with the observed values. Except for PNL-1-17, there is reasonable agreement between calculated and observed axial hole diameters and the percent of fission gas released. The agreement for the diameter of columnar grain growth is poor. These observations indicate that PNL-1-17

operated colder than our calculation predicts. The data from the pins in Table 7.III and other data that become available will be analyzed with the modified three-zone sintering model.

TABLE 7.III. Comparison of "SINTER" Calculations with Postirradiation Observations of Mixed Oxide Fuel Pins

Pin No.	s, % TD	Power, kW/ft	Burnup, MWd/tonneM	Hole Diam., in. $\times 10^3$		Col. Gr. Diam., in. $\times 10^3$		Fission Gas Release, %	
				Obs.	Calc.	Obs.	Calc.	Obs.	Calc.
PNL-1-3	87.6	8.8	8140	13	16	80	59	12	10
PNL-1-6	84.0	8.1	7850	18	20	80	54	11	9
PNL-1-17	85.6	9.2	8790	13	30	75	94	10	15
PNL-1-19*	83.8	9.5	9200	33	35	125	112	25	21

* *A gap coefficient of 1000 Btu ft^{-2} $°F^{-1}$ hr^{-1} was used because of the larger fuel-cladding gap in this pin.*

F. STANDARDIZATION OF ANALYTICAL PROCEDURES (7N71)

1. Analytical Chemistry Program

Certain impurity limits imposed on FFTF fuels from the neutronics standpoint are being reviewed. For reasons in the realm of physics it is recommended that the sum of the concentrations of samarium, europium, gadolinium and dysprosium be limited to 100 ppm. At the present time, the BNW Analytical Labs use a semi-quantitative spectrographic method for rare earths in nonnuclear materials. Adequacy of this method is being evaluated.

The potential Am interference with the Pu assay procedure is being studied. Preliminary results from LASL indicate that Am offers no interference in concentrations up to 1100 ppm. LASL is extending this work to include concentrations of Am to about 0.6%.

Offsite work on homogeneity reported last month included making some alpha-autoradiographs of both Phase I and Phase II

pellets (ME-21, PL-10). These autoradiographs illustrated noticeable differences in the total alpha activities of the two types of pellets. This effect resulted from the filter medium used to collimate the alpha particles. Later total alpha analysis of these pellets at BNW showed them to be essentially identical.

2. Raw Materials Analysis

Three contractors (Babcock and Wilcox, NUMEC, and United Nuclear) are participating in the program for prequalification as LMFBR fuel suppliers and all three have started processing the raw materials. Babcock and Wilcox and UNC have reported no problems on PuO_2 shipper-receiver assay differences, while NUMEC has reported a difference of 1.5 to 2%. This is currently being resolved through referee analysis by the National Bureau of Standards.

VIII. FUELS RECYCLE

A. FUEL SUPPLIER QUALITY ASSURANCE (7N70)

LMFBR fuel supplier prequalification contractors were visited by a BNW team to evaluate process and quality assurance procedures prior to start of fabrication. All vendors were sufficiently complete in their documentation to proceed with work up to crossblending of PuO_2 and UO_2.

B. BNW FUEL SUPPLIER PREQUALIFICATION QUALITY ASSURANCE SURVEY (7N70)

An informal prequalification quality assurance survey was made of NUMEC, United Nuclear, and Babcock and Wilcox as potential fuel suppliers.

C. PELLET FABRICATION TECHNOLOGY (7N73)

1. Special Pellet Shapes

A test group of pellets incorporating both a dish and a chamfer were pressed and sintered this month. The green pellets have a 45 degree chamfer, 0.015 in. to 0.020 in. on a side, and a dish $\sim$0.004 in. deep.

A second test group of annular pellets with a 0.060 in. green diameter axial hole were also fabricated this month. The annular pellets did not provide any unique fabrication problems, but the chamfered pellets required manual removal from the lower punch face after ejection to avoid scarring the fuel pellet end.

2. Statistical Analyses of Fuel Pellet Measurements

Since the last reporting period, a statistical analysis of sintered fuel pellet dimensions has been completed. Pellets used in this study represent approximately one-half of those pellets produced for the physics test pins. Table 8.I gives a statistical summary of the pellet measurements deemed most important from the standpoint of sintering to size.

TABLE 8.I. Statistical Analyses of Sintered Fuel Pellet Measurements[a]

Batch No.	Approx. Population	End Diameter (in.) D_1	Center Diameter (in.) D_2	End Diameter (in.) D_3	Taper[b] (in.)	Hourglass[c] (in.)	Percent	Theoretical Density
A-5-S18	1,270	0.19689	Not Taken	0.19527	0.00162	Not Taken	93.30	Ave
		0.00018		0.00030	0.00029		0.36	Std Dev
A-6-S18	2,420	0.19534	Not Taken	0.19432	0.00102	Not Taken	93.44	Ave
		0.00020		0.00024	0.00022		0.51	Std Dev
A-7-S20	560	0.19499	Not Taken	0.19400	0.00100	Not Taken	93.52	Ave
		0.00011		0.00012	0.00014		0.18	Std Dev
B-1-S19	1,255	0.19416	0.19245	0.19313	0.00103	0.00120	93.91	Ave
		0.00016	0.00042	0.00019	0.00024	0.00039	0.56	Std Dev
B-2-S19	1,750	0.19425	Not Taken	0.19307	0.00118	Not Taken	94.50	Ave
		0.00019		0.00018	0.00020		0.45	Std Dev
B-3-S20	1,875	0.19505	Not Taken	0.19375	0.00130	Not Taken	92.91	Ave
		0.00018		0.00027	0.00022		0.29	Std Dev
B-4-S21	1,620	0.19627	0.19442	0.19481	0.00146	0.00112	93.82	Ave
		0.00042	0.00051	0.00041	0.00040	0.00037	0.66	Std Dev
B-5-S21	1,610	0.19613	0.19428	0.19490	0.00123	0.00124	93.61	Ave
		0.00018	0.00024	0.00020	0.00021	0.00022	1.04	Std Dev[d]
B-6-S22	1,184	0.19782	0.19635	0.19656	0.00126	0.00084	91.60	Ave
		0.00063	0.00057	0.00065	0.00032	0.00035	0.83	Std Dev
B-7-S22	1,736	0.19603	0.19438	0.19503	0.00100	0.00115	92.58	Ave
		0.00010	0.00016	0.00019	0.00019	0.00017	0.36	Std Dev
C-1-S23	1,458	0.19585	0.19421	0.19484	0.00101	0.00113	93.85	Ave
		0.00025	0.00031	0.00022	0.00020	0.00027	0.37	Std Dev
C-2-S23	1,510	0.19609	0.19431	0.19499	0.00110	0.00123	93.55	Ave
		0.00013	0.00014	0.00010	0.00015	0.00012	0.31	Std Dev

(a) Based on sample sizes of 30.

(b) Taper $= D_1 - D_3$

(c) Hourglass $= \frac{D_1 + D_3}{2} - D_2$

(d) Large standard deviation, and correspondingly large tolerance interval for this batch was believed due to an incorrect pellet weight reading. After eliminating this pellet, the range of densities was 92.97 to 94.13 percent.

3. Evaluation of Pellet Impurities

Metallic impurities, carbon, fluorine, chlorine, and water content data from 28 development and irradiation test pellet batches were summarized to determine the following relationships:

a. Impurities in processed powder that are driven off during sintering.
b. Reliability of the chemical analyses of sintered pellets. (Determined by comparing chemical analyses of sintered pellets from the same batch but analyzed at different times.)
c. Reliability of chemical analyses of fuel powder lots by comparison of multiple analyses conducted on the same powder lot.
d. Reproducibility of fuel pellet impurity contents among sintering runs for pellets produced from the same powder lot.

The data are being analyzed to determine statistical significance. Preliminary data concerning possible impurity change through sintering is shown in Table 8.II.

TABLE 8.II. Effect of Sintering on Impurity Content

Impurity	Before Sintering (ppm)	After Sintering (ppm)
Al	470	470
Cu	60	18
Fe	72	54
Ni	<44	<16
P	<48	<43
C	340	<36
H_2O	3300	5

4. Effects of Milling on PuO_2 Sinterability

To determine the effect of grinding of PuO_2 powder, a small quantity of oxalate source plutonia was recalcined to 625 °C and subportions of both as-received and recalcined powder were then dry ball milled using Al_2O_3 media for 8 to 20 hours. Pellets were pressed at 40,000 psi and sintered at 1550 °C for two hours in helium bubbled through water (approximately 1500 ppm H_2O). Table 8.III on the following page shows the results obtained.

TABLE 8.III. Effect of Milling on the Sinterability of PuO_2

Treatment	B.E.T. Surface Area (M^2/gm)	Carbon (ppm)	Aluminum (ppm)	Green Density %TD	Sintered Density %TD
No Milling					
As Received	37.0	1125	10	48.6	91.0
625 °C Calcine	17.4	590	ND	55.9	92.8
8-hr Milling					
As Received	27.5	ND	10	49.8	88.9
625 °C Calcine	12.1	ND	ND	57.5	85.8
20-hr Milling					
As Received	24.0	ND	10	51.6	86.2
625 °C Calcine	10.0	ND	ND	58.5	85.1

ND Not determined

The foregoing table shows that milling reduced the B.E.T. surface area for both as received and calcined PuO_2. This effect is possibly a result of agglomeration. The difference in sintered densities also implies that the agglomerate condition has been changed. Scanning electron micrographs will be obtained to help explain the nature and state of particle agglomeration. In addition, particle size, and O/Pu ratios are being determined.

5. Pellet Fabrication for Test Pins for Irradiation in EBR-II

Recent changes in PNL-9, 10, and 11 specifications require a development effort to identify appropriate changes in the

fuel fabrication process. Currently, process conditions are standardized to produce fuel pellets in a 93 ± 2.0% TD density range and a right circular cylinder geometry. The newly specified fuel pellet geometry (3 ± 1.5 mil dish and 15 ± 5 mil land) will be accommodated by testing several punch sizes and configurations. Initially punches with a 17.5 mil land and a 3.5 mil dish with a 60 degree angle from land to dish are being fabricated. The specified fuel pellet density (90.5 ± 2.5% TD) will be obtained through modification of fuel processing conditions and operations.

The four approaches to changing fuel processing with the best potential for meeting revised density specifications are (a) adjusted powder activity, (b) volatile pore formers, (c) less efficient compaction lubricant, and (d) preslugging. Evaluation of these four approaches by changing the processing parameter is in progress using six experimental fuel batches. Two kilograms of fuel consisting of 65% ^{235}U enrichment in the EBR-II test composition of 75% UO_2 and 25% PuO_2 were prepared for the experimental batches.

D. FUEL PIN FABRICATION TECHNOLOGY (7N73)

1. Fabrication of 300 Fuel Pins for Criticality Studies

The fabrication of 300 physics test pins for criticality studies continued during August. Fuel pin processing and assembly has improved with added assembly experience. Overall yields and reject rates will be available after final inspection.

Pellet measurements are being made to determine the effect of radial and axial position within the furnace on O/M, sintered dimensions and density of the fuel pellets. These results will be presented next month.

2. Fabrication of Fuel Pins for PNL Test Subassemblies

Forty fuel pins for EBR-II instrumented subassembly PNL-17 were completed through final closure welding. Wire wrap and

instrumentation of these pins will be completed as soon as thermocouples arrive from the vendor.

Forty-five fuel pins for EBR-II subassembly PNL-8 were wire wrapped. Final measurements and inspection are in progress.

All components for fuel pins for EBR-II subassembly PNL-6 are ready for final cleaning and assembly operations.

3. Welding Development

a. Wire-End Cap Termination Weld Evaluation

The 3/32-in. fillet weld design (previously called "small weld") for attaching the wire wrap to the end cap is being evaluated. The procedure for fabricating and testing the weld samples has been outlined in *FFTF Fusion Welding*, A-0088-R, July 11, 1969.

A total of 22 welds were made. The wire, 0.056-in. diameter, 20% cold-worked, Type 316 SS, was welded at each end to a Type 316 SS rod, simulating the wire to end cap joint. Six welds were made by setting the current at low end of the tolerance limits to get the minimum acceptable penetration. Six welds were made with the current set at the high end of the tolerance limits to get maximum acceptable penetration. Ten welds were made using the nominal mid-range setting.

The completed welds were radiographed as required by A-0088-R. Two pictures were taken, one at 0 degrees (side view) and one at 90 degrees (top view). All welds were acceptable in the 90 degree direction. Three welds, one minimum penetration and two mid-range penetration, were marginal, having some fusion but thin penetration.

Tensile tests were made as an addition to the requirements of A-0088-R for comparison with previous tests. As expected, the fracture in all cases occurred in the heat-affected zone of the wire next to the weld. It logically follows that the

strongest joint would then be where there was the least annealing in the heat-affected zone. The results, Table 8.IV, show that this conclusion is valid as the average strength of the minimum penetration weld is highest while that of the maximum penetration is the lowest. The weld defects seen on radiographs had no effect on joint strength.

TABLE 8.IV. Average Weld Test Tensile Data and Results

Type of Penet.	Length (in.)	Width (in.)	Height (in.)	Current (amp)	Duration of Current (sec)	Fracture Location (joint)	Maximum Load (lb)	Strength (psi)
Min	0.102	0.100	0.079	7.2	10.3	-	225.0	91,400
Med	0.12	0.100	0.078	7.9	9.6	-	217.0	88,160
Max	0.14	0.116	0.077	8.6	7.0	-	213.7	86,800
Ave	0.122	0.104	0.078	7.72	9.0	-	218.3	88,630

b. Evaluation of Fuel Pin End Closure by Acoustic Emission

Welding of a batch of 45 bottom end welds in 0.230-in. diameter tubing was monitored by acoustic emission. Only 7% of these welds exceeded full-scale emission response while 82% produced insignificant response. This is a reduction in emission response over previous batches and may be a result of using vacuum melted Type 316 SS for this last batch of fuel pins. A difference in welding properties of the vacuum melted Type 316 SS was also indicated by the necessity of 14% higher arc current to obtain full penetration of the joint.

E. TEST AND EXPERIMENTAL FACILITIES (7N73)

1. Project Status

Project BCP-034 (Fuel Subassembly Fabrication Demonstration Facility) provides a facility for demonstration of fabrication methods to produce fast reactor fuel pin subassemblies. The overall project is 52% complete and on schedule.

Project BAP-022 (Plutonium Fuels Laboratory Addition - 308 Building) provides the special facilities required for initial storage, handling, testing, assembly and instrumentation of FFTF nonirradiated fuel. The design of this facility is in progress and approximately 20% complete.

2. Miscellaneous Equipment Status

The three Sunbeam outgassing furnace tank assemblies have been shipped by the vendor. One tank assembly has been received and is being assembled with other outgassing furnace system components.

3. Compressibility Measuring Fixtures

A simple fixture using a flow duct and other components is being fabricated for making compressibility measurements on the CCTL Mark I subassembly.

A more precise fixture to be used to measure compressibility of the CCTL Mark I and Mark II subassemblies is being designed. Fabrication of this fixture is scheduled to be complete by October 2, 1969.

4. Processing Equipment

Exit gas moisture monitors have been installed on both sintering furnaces in the pilot line. With both ingoing and outgoing moisture probes, more information and better control of the fuel pellet O/M ratio are expected.

New thermocouple fittings in the sintering furnaces permit routine determinations of the central vertical temperature profiles in each furnace.

A Thermac Series-6000 temperature-power controller and a Data-Trak control programmer were purchased. These solid-state units are being used to control the Hoskins resistance heated furnaces which are presently being used for calcining PuO_2 and for debinding green pellets. These units provide a more accurate

heating cycle than the manual controllers used in the past and automate the furnace run.

Requests for bids have been processed through Purchasing for the automatic X-ray film processor. Bids were to be in by the week of September 2.

Continuous process sintering furnace bid due dates were received up to August 5. Bids were received from Astro Industries of Santa Barbara, California, and Degussa, Inc. of West Germany. Bids are being reviewed.

The cleaning tanks to be installed in Room 231 are in the process of being fabricated and are 50% complete. Fabrication will be complete by September 3.

The wire wrap machine has been fabricated and is ready for installation.

A new furnace element was fabricated for the Scanning Electron Microscope hot stage incorporating electron beam heating. This element is being tested to 1600 °C.

F. LMFBR Fuel and Cladding Information Center (7N72)

Current activity has related to the preparation of data-input forms for the cladding fabrication section and storage of data for lots G and H of Type 316 SS purchased by Battelle-Northwest.

Work continued on the preparation of a format to store data available on fuel pins which are now being irradiated or being prepared for irradiation. This format will provide a method to put the data on card decks which later will be transferred to and stored on magnetic tape.

Data from 147 additional tensile tests were added to the REM File. Seventy-nine tests on stainless steel were added to Master File No. 1 to bring the total to 2,197 and 68 tests added to the stainless steel characterization studies Master File No. 6 bringing its total to 141.

IX. PHYSICS

A. CRITICAL EXPERIMENTS PROGRAM

1. Status of Phase B Critical Experiments (7N83)

Core and control ring edgeworth measurements and radial reaction rate traverses of ^{239}Pu (fission), ^{238}U (fission), and ^{10}B (capture) have been completed. Following the reaction rate traverses, the ZPPR was shut down for a projected three weeks of containment testing.

2. Analysis of 56B Critical Experiments (7N83)

Calculations have been made of axial and radial reactivity worth and reaction rate distributions for those materials which were measured in the Assembly 56B experiments. This work essentially concludes the analysis of the Phase B, Part III critical experiments.

The specific measurements which were analyzed were ^{10}B and ^{239}Pu reactivity worths, ^{239}Pu and ^{238}U fission rates and ^{10}B absorption rate. The analysis was made using the 2-D perturbation code PERT V with fluxes and adjoints from the diffusion code 2DB. All cross sections were the 26-group BNWL modified set.

The analytical techniques are different in group structure and in calculation theory (transport versus diffusion) from both the Assembly 48, 48A analysis[1] and the analyses of Assemblies 51[2] and 52.[3] Yet the results

---

1. *R. A. Bennett, S. L. DeMyer, Analysis of FTR Phase A Control Rod Experiments in ZPR III Assembly 48 and 48A, BNWL-967, Battelle-Northwest, Richland, Washington, April 1969.*
2. *W. R. Young, R. A. Bennett, Analysis of Phase B Critical Experiments, Part 1, ZPR III Assembly 51, BNWL-1138, Battelle-Northwest, Richland, Washington, July 1969 (Draft Issue).*
3. *W. R. Young, R. A. Bennett, Analysis of Phase B Critical Experiments, Part 2, ZPR III Assemblies 52a, b, c, d, e, and f. BNWL-1139, Battelle-Northwest, Richland, Washington, July 1969 (Draft Issue).*

compare with experiment in a similar manner in all of the above. A generalized comparison of calculation and experiment would include:

a. The calculated worth of ^{239}Pu is too large near the core center and in the radial reflector but agrees closely with the experiment at the core-reflector boundary and in the axial reflector.
b. The calculated ^{10}B reaction rates, when normalized to the experiment, are too low at the core reflector interface and too high in the radial reflector but agreement is good elsewhere.
c. The calculated ^{238}U fission rates are in good agreement with the experiment.
d. The calculated ^{10}B worth and ^{239}Pu reaction rates are in fair agreement with the experiment except in the region of the core reflector interface.

The consistent problem of lack of agreement between calculation and experiment has been studied. Although the reason for disagreement has not been found, it has been concluded that the disagreement was not caused by collapsing of energy groups nor the model used in the calculation of the fluxes.

3. Analysis of FTR-1 Experiments on ZPPR (7N83)

The experimental program in FTR-1 on ZPPR has been completed and the results reported by ANL.[1,2] The program consisted of (1) measuring the critical mass and core drawer edgeworths; (2) loading the configuration of ZPR-III/FTR-1 and measuring the subcriticality of this loading; and (3) loading an approximate two-drawer thick B_4C ring just outside a radius

1. *Argonne National Laboratory FFTF Monthly Informal Technical Progress Report, May 1969.*
2. *Argonne National Laboratory FFTF Monthly Informal Technical Progress Report, June 1969.*

precalculated to be the critical radius of FTR-2 (∿58 cm) and measuring the degree of subcriticality.

The reference loading of FTR-1 contains 362.84 kg fissile mass and is 141.46 Ih supercritical. The multiplication constant of the equivalent cylinder was calculated to be 0.981 using the two-dimensional diffusion theory code, 2DB in R-Z geometry with a 13 group cross section set. An X-Y calculation of the as-built system yielded a k_{eff} of 0.977. Both of these eigenvalues are subject to a transport and heterogeneity correction of about 1.7 ΔK. Thus, the corrected R-Z k_{eff} is 0.998 and the X-Y k_{eff} is 0.994 with corresponding c/e values of 0.997 and 0.993.

Measurements of the worth of core drawers relative to reflector material were made for several drawers along the core periphery and the worths of two of these drawers have been calculated in 2DB X-Y mode. The worths of drawers 130-32 and 134-29 were computed to be 21.5 Ih (42.3 Ih/kg) and 53.0 Ih (52.4 Ih/kg), respectively. The corresponding c/e values were 1.15 and 1.07.

When ZPR-III/FTR-1 critical configuration was rebuilt on ZPPR, the reactivity was measured to be $3.29 subcritical. The subcriticality of this loading is induced by the larger void fraction in the drawers in the ZPPR. An X-Y calculation of the configuration indicated a subcriticality of $3.79 (c/e 1.15).

As the first part of the transition from FTR-1 to FTR-2, the B_4C ring characterizing FTR-2 was loaded and the subcriticality of the system measured. The degree of subcriticality was calculated (using an X-Y model) to be $7.68. The experimental result has not been reported by ANL at this time.

B. FTR EVALUATION

1. FTR Stability Analysis (7N83)

The updating of prior preliminary stability analyses for the FTR split-conical core is continuing. The procedure presently utilized for the analysis is a standard lumped feedback path model involving a linearized set of matrix equations describing the neutronics and feedback mechanisms. The approach is novel, however, in the description of the reactor via more than a single node so that such effects as the spatial dependent sodium void coefficient could be adequately treated.

The resulting feedback function for the FTR reference core is shown in Figure 9.1 along with EBR-II experimental data. The reference concept is shown to be stable. Of the parametric studies made, the only situation discovered leading to unstable operation is that for a purely hypothetical zero Doppler coefficient and a positive tube expansion coefficient. This case is also shown along with the case for a Doppler coefficient equal to one percent of the reference value. In the latter case, the reactor is again stable.

C. CODES AND COMPUTATION METHODS

1. Coupling of MELT-II and VENUS Codes (7N83)

An early version of VENUS, a two-dimensional Lagrangian coordinate neutronics-hydrodynamic code, has been obtained from Argonne. Of the numerous modifications made to the code, perhaps the most significant was that of interfacing it directly to the MELT-II code. This substantially enhances the capabilities to analyze core disruptive accidents. Other significant code additions include a new neutron kinetics package and a much more flexible equation of state routine, both for sodium-in and sodium-out conditions.

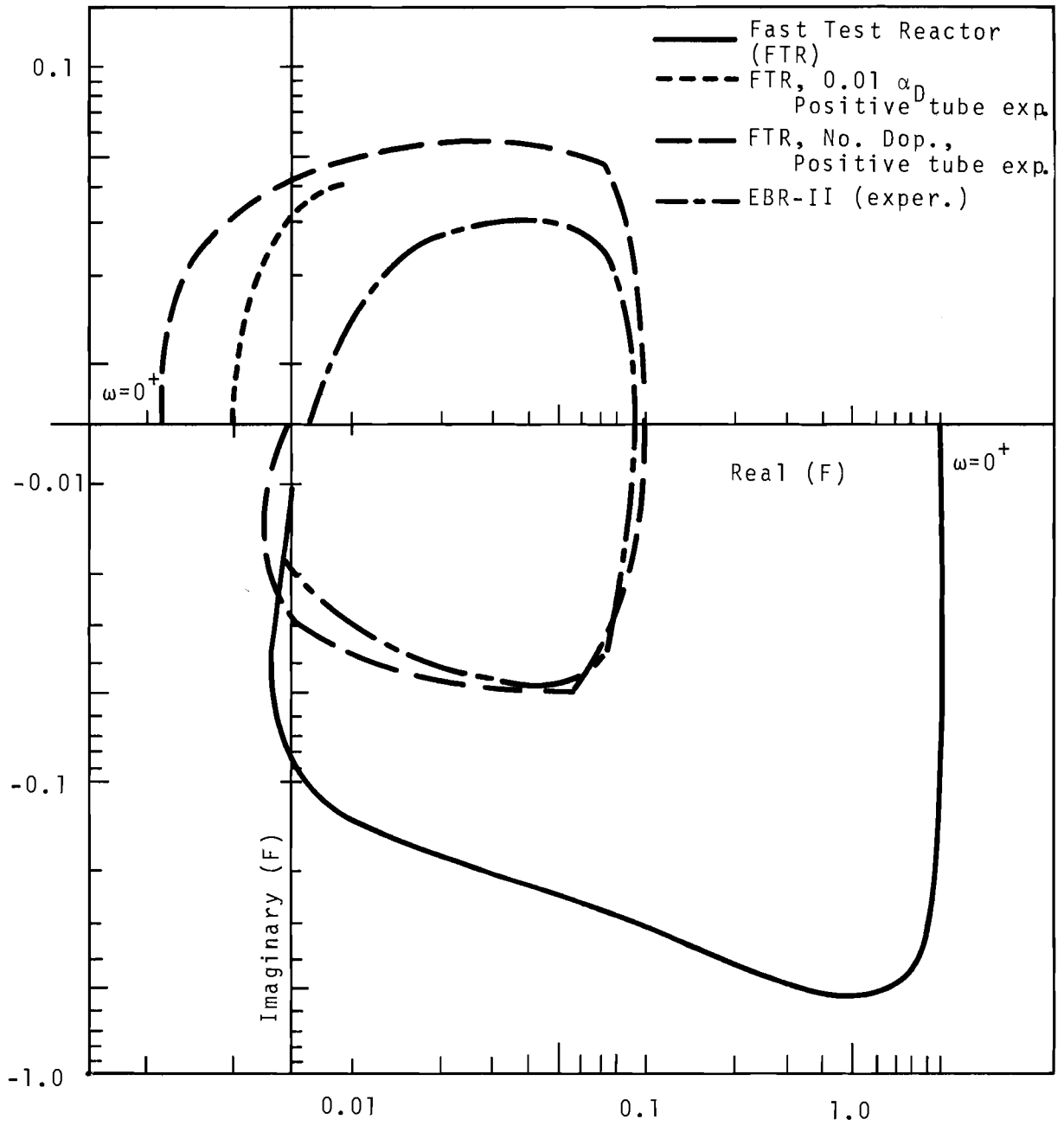

FIGURE 9.1. Phase Plane Plot of Feedback Functions

2. ETOX (7N83-7C00)

The ETOX code, which generates group average cross-section constants from the ENDF/B library to be used as input into fast reactor codes, is currently being modified in the resolved region. This improvement will give greater accuracy for the infinitely dilute cross-section of NA-23 isotope.

Improvements have been introduced in the calculation of the inelastic scattering matrix for general isotopes.

X. SAFETY

A. ANALYSIS OF PLANT PROTECTION SYSTEM

1. Reliability Analysis (7N82)

An analysis was made to establish an approximate testing interval for the PPS. Based on the computed unavailability results, the recommended initial test interval is approximately once per week for the PPS. It was further concluded that the major contribution to subsystem unavailability is the instrument sensors and signal conditioning electronics. Unavailability values for "nominal" failure rate data and the recommended weekly test interval range from 10^{-4} to 10^{-6}. The high values of this range are for the neutron flux instrumentation. Thus, it is required that the low-level neutron monitors will be backed up by the intermediate level neutron monitors, and these in turn will be backed up by the power level neutron monitors.

2. Fault Tree Analysis (7N82)

New fault trees have been developed for accidents which lead to sodium boiling and fuel melting with the reactor at power. These fault trees combine initiating faults and plant protection system failures and can be used to determine the probability of the top event occurring. This work supplements and extends the PPS system reliability analysis.

B. CORE MELTDOWN STUDIES

1. Containment Transients (7N82)

The CONSDM code has been modified to compute temperature and pressure transients following the unlikely occurrence of a hypothetical core meltdown accident. Transients are computed for two spaces, one representing the reactor cavity and the other the three heat transport cells. Cooling capability in the cavity floor and walls is included in the model. In the HTS cells, heat absorption in the structural concrete masses is computed.

Two basic cases have been analyzed with the code. The first case assumes the presence of a NaK sink in the reactor cavity floor and walls maintained at 400 °F. The walls are insulated with 4 in. of low-conductivity (k = 0.076 B/hr-ft °F @600 °F) material, and the floor contains an insulating slab of urania. The second case assumes a similar configuration in the cavity walls, but assumes no cooling of the cavity floor. In both cases, all sodium above the inlet nozzles in the inlet plenum is assumed to be expelled into the HTS cells by the DBA. That is, some 410,000 lb of reactor vessel sodium at the mixed mean temperature of 1038 °F forms a pool, about 2 ft deep on the floor of each cell and occupies some 8,030 ft^3 of the volume of the cells. Sodium from the inlet plenum below the inlet nozzles (50,650 lb) is assumed to drain into the reactor cavity. This sodium, initially at 900 °F, increases in temperature to about 1060 °F and forms a pool, about 1 ft deep, on the cavity floor, occupying some 1000 ft^3 of the cavity volume.

Leakage from the inner barrier to the outer barrier was computed from the design leak tightness requirement of 10 Vol% leakage per 24 hr at 30 psig and 100 °F.

Results from the first case, cooling in walls and floor, show an initial pressure peak of about 50 psig in the cavity, followed by a secondary peak in the cavity and cells of 10.6 psig occurring 0.9 hr after the start of the incident. In 118 hr, pressure is at 1.7 psig. For the case of cooling in the cavity walls only, the secondary pressure peak is 16.7 psig occurring at about the same time as the previous case. The calculations were carried out for 58 hours; at that time pressure in the cavity and cells was 8.4 psig.

2. Fuel Flow After Meltdown (7N84)

An estimation of the profile of the fuel core and structural material behavior after a core meltdown, is being made with special emphasis on the downward progress of molten material and on the heat transfer into the concrete and soil. The objective is to determine the transient size, shape, penetration and thermal history of any molten pool and the distribution of heat flux in the system.

The problem is very complex, with the interaction of the oxide fuel and steel with the concrete being strongly influenced by the amount of heat being transferred upward. At this point in the analysis the following qualitative statements can tentatively be made about the problem.

The first reaction of the molten fuel with the concrete, composed of CaO, Al_2O_3, SiO_2, Fe_2O_3, and H_2O, will be vaporization of the water, which could occur with explosive force.

When the water is removed the concrete will melt in the range 1200 to 1400 °C. This process will tend to freeze the structural steel into a separate phase, which has a higher melting point than the concrete. Whether the water will oxidize part of this iron is difficult to determine, since the free energies of formation are nearly equal.

The fuel and fission product oxides have a high solubility in the concrete. Assuming perfect convective mixing of the liquid should allow an estimation of the melting point of the mixture from available phase diagrams as a function of penetration of fuel into the concrete and the penetration depth at which the iron freezes.

Geometrically, an attempt is contemplated to bracket the true behavior of the system between the solutions of two one-dimensional advancing liquid boundaries - uniform floor loading of fuel resulting in an advancing slab and point floor

loading resulting in an enlarging hemispherical pool. The assumptions that the molten mass will provide its own frozen wall and that the iron will freeze would need to be tested experimentally.

C. SODIUM FIRES STUDIES (7N82)

Transient heat transfer calculations for non-nuclear sodium pool fires associated with the main containment vessel have been obtained with the SOFIRE computer code.[1] Two cases were analyzed, as shown in Table 10.I. Results are summarized as follows:

1. Heat transport system pipe failure. Fourteen days after reactor shutdown the shield plugs may be removed for access to an HTS cell. An HTS pipe failure may spill sodium on the cell floor and pool burning in air would continue until all sodium was consumed. Assuming no venting and no leakage from the sphere, a peak pressure of 5.7 psig is attained. See Figure 10.1.

2. Closed loop tube failure. During reactor shutdown the machinery dome and reactor top head personnel shield may be partially or completely removed. A closed loop tube failure with circulation pumps running may expel sodium coolant in a pool in the top head recess. Pool burning would continue until all sodium was consumed. Assuming no venting and no leakage from the sphere a peak pressure of 4.4 psig is attained. See Figure 10.2.

---

1. *SOFIRE code developed by Atomics International for USAEC under contract AT(11-1)-GEN-8; Technical Progress Report for Unclassified AEC Project, NAA-SR-12010, July 1966.*

TABLE 10.I. SOFIRE Code Results for Sodium Pool Fires Associated with the Main Containment Vessel

Description	Symbol	Units	Accident Location 1. HTS Cell Initial	1. HTS Cell Final	2. Top Head Recess Initial	2. Top Head Recess Final
Atmospheric temperature	T_o	°F	80		80	
Area venting to sphere	A_H	ft^2	100		635	
Time from start of accident	T	hours	0	14.2	0	3.3
Cell air temperature	T_1	°F	80	725	80	410
Sphere air temperature	T_2	°F	80	440	80	270
Cell and sphere pressure	P	psig	0	5.7	0	4.4
Sphere steel temperature	T_3	°F	80	400	80	190
Sphere surface temperature	T_4	°F	80	107	80	85
Sodium pool surface temperature	T_{s1}	°F	500	1270	500	1410
Sodium pool center temperature	T_{s2}	°F	500	1255	500	1390
Cell wall concrete center temperature	T_{w2}	°F	100	103	200	200
Cell floor slab no. 1 - 0.1 ft thick	T_{c1}	°F	100	1200	500	1270
Cell floor slab no. 2 - 0.5 ft thick	T_{c2}	°F	100	890	500	620
Cell floor slab no. 3 - 4.4 ft thick	T_{c3}	°F	100	110	500	500
Heat flow to cell wall	Q_1	$B/hr\text{-}ft^2$	0	220	-130	330
Heat flow from sphere surface	Q_2	$B/hr\text{-}ft^2$	0	80	0	105
Mass of sodium in pool	W_{Na}	Tons	50	0	10	0

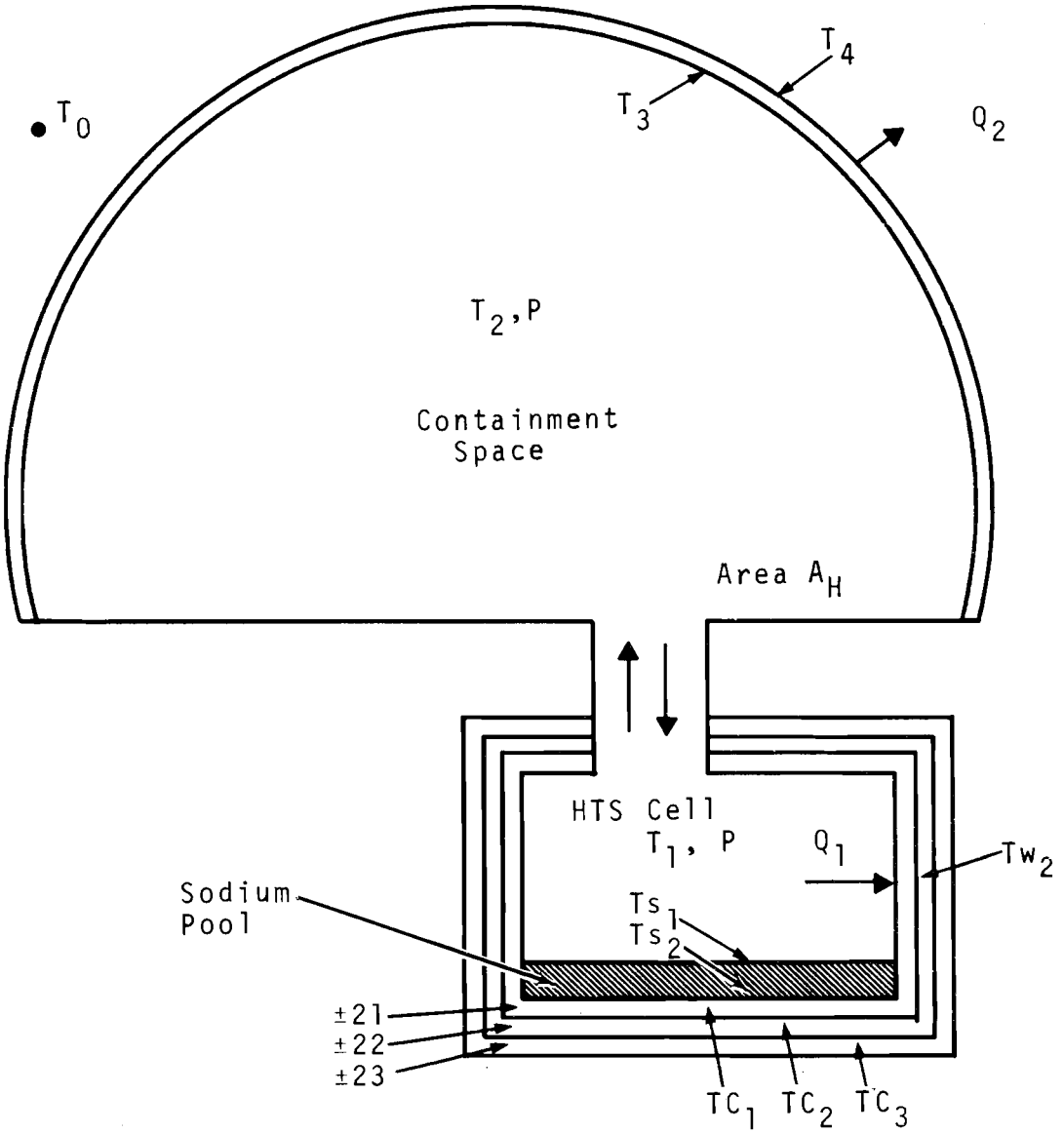

FIGURE 10.1. *Model for Non-nuclear Pool Fire, Primary Sodium Pipe Rupture in HTS Cell with Shield Plugs Removed to Containment Sphere.*

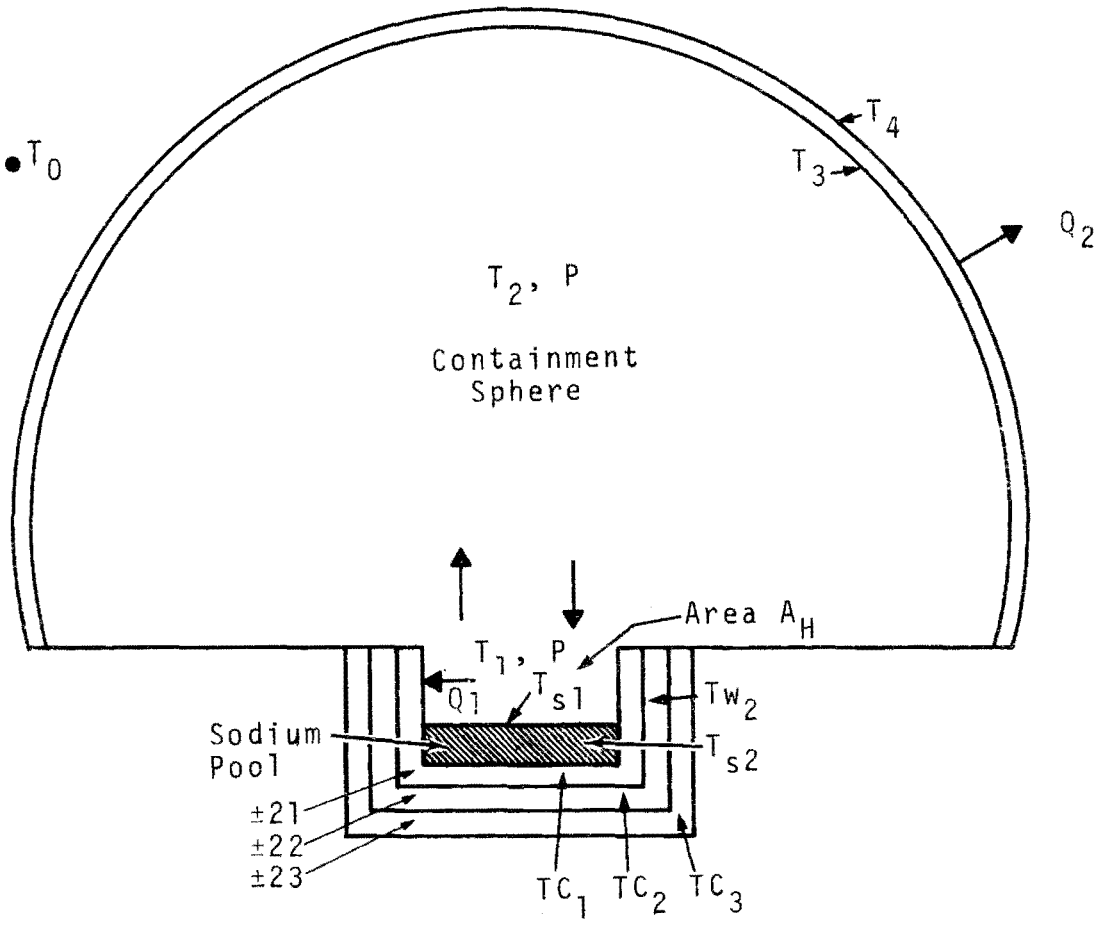

FIGURE 10.2. *Model for Non-nuclear Pool Fire, Closed Loop Failure in Reactor Top Head Recess with Machinery Dome Removed.*

In the case of the HTS cell the larger cell wall mass and surface area are more effective in removing heat from the sodium pool and sodium flame. In addition, the smaller vent area through shield plug openings is effective in restricting the flow of hot gases up into the sphere. The result is that the peak pressure is not much greater than for the closed loop case, even though the amount of the sodium spill is much larger.

D. DESIGN BASIS ACCIDENT STUDIES

1. Shock Loading in FFTF Vessel Cover (7N82)

Shock loading in the FFTF vessel cover was calculated assuming that one-half of the DBA energy of 1000 MW-sec would be carried in a shock wave similarly to TNT explosives in water. This would be equivalent to detonation of 500 lb of TNT in the core region. Results showed that for an unrestrained cover, the maximum height the cover would be lifted by the explosion would be 2.4 feet. The energy received by the cover represents about 0.18% of the DBA energy. This contrasts with 4.6% of the DBA energy received from propellent type loading. Therefore, the TNT type shock wave represents a much less efficient mechanism for accelerating the vessel cover.

2. Post DBA Pressures and Temperatures (7N82)

A program which calculates long term pressure and temperatures within the reactor cavity, equipment cells, and containment sphere for a "sodium out" accident has been completed. The model is shown in Figure 10.3 and briefly described below. This model includes the outer containment barrier as well as the inner barrier. However, it is only applicable to a limiting accident case (the dry case) wherein all sodium is assumed to have been expelled from the reactor cavity. That is, the model does not include the capability to treat contribution of sodium vapor pressure to total containment pressure.

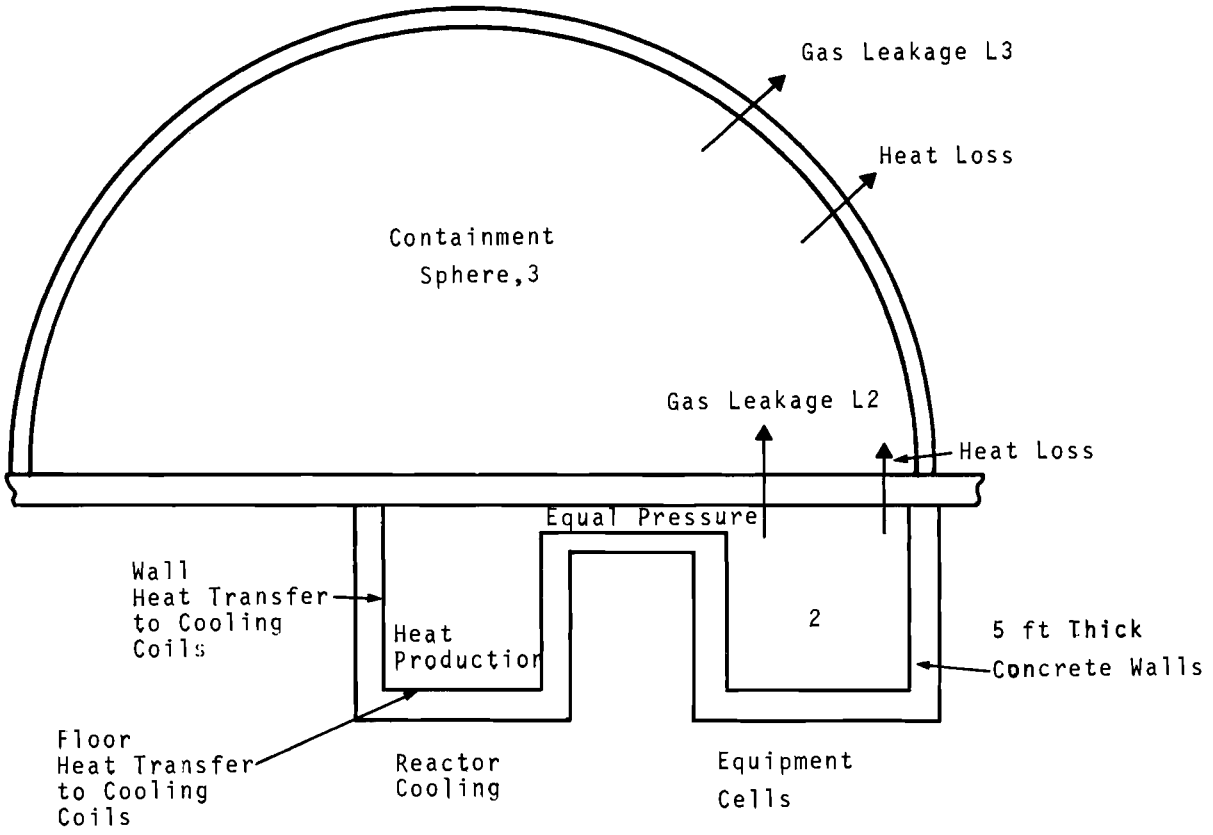

[Not to Scale]

FIGURE 10.3. Pictorial Computer Model Dry DBA

The reactor cavity (Cell No. 1) is connected to the equipment cells (Cell No. 2) by a free passage, so both are at the same pressure. The reactor fuel decay heat is liberated in Cell No. 1, which is transferred through the wall, floor and to the internal metal structures. Both Cells No. 1 and No. 2 have fission gas decay heat proportioned according to the gas mass distribution. Cell No. 2 has concrete walls which allow non-linear temperature distributions during transients. The leakage of gases from Cells No. 1 and No. 2 to the reactor sphere (Cell No. 3) has been calculated based upon 10% of the gas mass per day for a design pressure difference of 30 psi. Cell No. 3 is heated by conduction through the roof of Cell No. 2 and by fission products which leak from Cells No. 1 and No. 2. Cell No. 3 also loses gas to the atmosphere at a rate of 1% of the gas mass per day based on a design pressure of 15 psig.

The program has been applied with and without cooling in the reactor cavity floor. However, only the results without cooling are presented here because the resultant pressures and leakage rates were similar. There is an initial pressure peak of 20 psia within 1/2 hr caused by fission gas heating in the equipment cells, but then the concrete begins to absorb heat faster than it is being produced and both temperature and pressure in cell No. 2 drops off. The temperature of the reactor cavity continues to increase for 200 hr and reaches 2030 °F. The pressure does not increase because the equipment cells have a much larger volume and their decreasing temperature is the dominant factor.

The gas leakage rates are shown in Figure 10.4. The leakage from the equipment cells reaches a maximum of 17.5 lb/hr within 1 hr and then slowly decreases. The containment sphere leak rate builds up much more slowly as it is heated by conduction and fission gas release. It reaches a maximum about 200 hr after the accident. The initial leak rate of 3 lb/hr was caused by a mismatch of pressure of 0.05 in. Hg. It was left in the results to illustrate the possible effect of atmospheric changes.

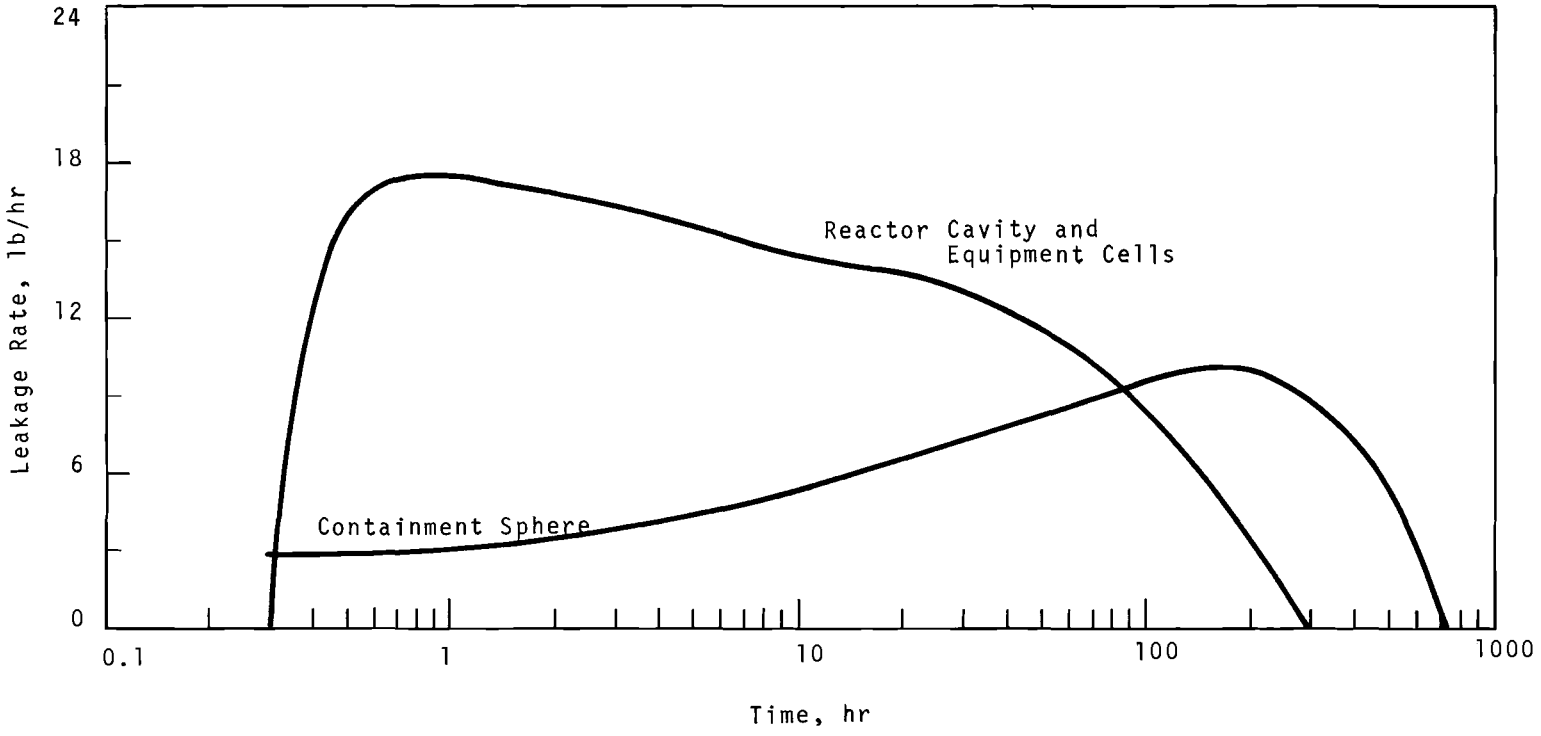

FIGURE 10.4. Gas Leakage History from Equipment Cells and Containment Sphere (No Cooling in Reactor Cavity Floor)

DISTRIBUTION

OFFSITE

No. of Copies

31 AEC Division of Reactor Development and Technology*

M. Shaw, Director, RDT
Asst Dir for Nuclear Safety
Analysis & Evaluation Br, RDT:NS
Environmental & Sanitary Engrg Br, RDT:NS
Research & Development Br, RDT:NS
Asst Dir for Plant Engrg, RDT
Facilities Br, RDT:PE
Components Br, RDT:PE
Instrumentation & Control Br, RDT:PE
Liquid Metal Systems Br, RDT:PE
Asst Dir for Program Analysis, RDT
Asst Dir for Project Mgmt, RDT
Liquid Metals Project Br, RDT:PM
FFTF Project Manager, RDT:PM (3)
ASST Dir for Reactor Engrg, RDT
Control Mechanisms Br, RDT:RE
Core Design Br, RDT:RE (2)
Fuel Engineering Br, RDT:RE
Fuel Handling Br, RDT:RE
Reactor Vessels Br, RDT:RE
Asst Dir for Reactor Tech, RDT
Coolant Chemistry Br, RDT:RT
Fuel Recycle Br, RDT:RT
Fuels & Materials Br, RDT:RT
Reactor Physics Br, RDT:RT
Special Technology Br, RDT:RT
Asst Dir for Engrg Standards, RDT
EBR-II Project Manager, RDT:PM

1 AEC Idaho Operations Office*
Nuclear Technology Division

C. W. Bills, Director

1 AEC San Francisco Operations Office*
Director, Reactor Division

4 AEC Site Representatives*

Argonne National Laboratory
Atomics International
Atomic Power Development Assoc.
General Electric Co.

---

* Distribution by FFTF

No. of Copies	
5	Bechtel Corporation* J. J. Teachnor, Project Administrator, FFTF
10	Westinghouse Electric Corp* Atomic Power Division Advanced Reactor Systems J. C. R. Kelly
1	AEC Chicago Patent Group G. H. Lee
1	AEC Division of Technical Information Extention
3	Argonne National Laboratory R. A. Jaross LMFBR Program Office N. J. Swanson
1	Atomic Power Development Associates Document Librarian
7	Atomics International FFTF Program Office (5) Liquid Metal Information Center - J. J. Droher (2)
2	Babcock & Wilcox Co. Atomic Energy Division S. H. Esleeck G. B. Garton
1	BNW Representative N. A. Hill (ZPR III)
1	Combustion Engineering 1000 MWe Follow-on Study W. P. Staker, Project Manager
5	General Electric Co. Advanced Products Operation Karl Cohen (3) Bertram Wolfe Nuclear Systems Programs D. H. Ahmann

* Distribution by FFTF

No. of Copies

2 Gulf General Atomic Inc.
General Atomic Div

D. Coburn

1 Idaho Nuclear Corporation

D. R. DeBoisblanc

1 Oak Ridge National Laboratory

W. O. Harms

1 Stanford University
Nuclear Division
Division of Mechanical Engrg

R. Sher

1 United Nuclear Corporation
Research and Engineering Center

R. F. DeAngelis

ONSITE-HANFORD

1 AEC Chicago Patent Group

R. K. Sharp (Richland)

3 Battelle Memorial Institute

105 Battelle-Northwest

F. W. Albaugh
G. J. Alkire
S. O. Arneson
J. M. Batch
A. L. Bement, Jr.
R. A. Bennett
T. K. Bierlein
L. D. Blackburn
C. L. Boyd
R. L. Brown
W. L. Bunch
C. A. Burgess
J. J. Cadwell
A. C. Callen
C. M. Cantrell
J. R. Carrell
T. D. Chikalla
T. T. Claudson
P. D. Cohn
J. H. Cox
G. M. Dalen
J. M. Davidson
F. G. Dawson
D. R. de Halas
A. W. DeMerschman
D. R. Doman
G. E. Driver
K. Drumheller
R. V. Dulin
J. F. Erben
T. W. Evans
P. L. Farnsworth
L. M. Finch
J. C. Fox
E. E. Garrett
W. L. Hampson

Battelle-Northwest (contd)

J. E. Hanson
K. M. Harmon
H. Harty
R. A. Harvey
B. R. Hayward
R. E. Heineman
J. W. Helm
R. J. Hennig
G. M. Hesson
J. J. Holmes
H. G. Johnson
E. M. Johnston
J. N. Judy
F. J. Kempf
D. D. Lanning
G. A. Last
D. C. Lehfeldt
H. D. Lenkersdorfer
C. W. Lindenmeier
W. W. Little, Jr.
C. E. Love
B. Mann
D. Marinos
C. A. Munro
R. E. Nightingale
L. T. Pedersen
G. S. Petersen
R. E. Peterson
H. G. Powers
W. D. Richmond
W. E. Roake
R. L. Roske
F. H. Shadel
D. W. Shannon
F. R. Shober
D. E. Simpson
C. R. F. Smith
D. D. Stepnewski
G. H. Strong
C. D. Swanson
J. W. Thornton
J. C. Tobin
K. G. Toyoda
J. C. Tverberg
C. E. Vogel
M. Vogel
R. C. Walker
E. T. Webber
J. H. Westsik
J. F. Wett
R. G. Wheeler
F. J. Williams
N. G. Wittenbrock
T. W. Withers
M. R. Wood
F. W. Woodfield
D. C. Worlton
H. H. Yoshikawa
H. S. Pringle
Technical Information (5)
Technical Publications (3)
Legal-703 Bldg.
Legal-ROB, 221-A

4 AEC RDT Site Representatives*

P. G. Holsted
T. A. Nemzek

2 AEC Richland Operations Office*

J. M. Shivley

1 Bechtel Corporation*

M. O. Rothwell

* Distribution by FFTF

No. of Copies

1 Westinghouse Electric Corp.*

R. Strzelecki (Richland)

22 Battelle-Northwest*

E. R. Astley
J. C. Cochran
D. L. Condotta
E. A. Evans
F. C. Gronemeyer
P. L. Hofmann
W. B. McDonald
J. S. McMahon
R. J. Squires
FFTF Files (10)
FFTF TPO Files (List "M") (3)

* Distribution by FFTF